BIBLIOGRAPHY

- Ahovan ZA, Esmaeili Z, Eftekhari BS, Khosravimelal S, Alehosseini M, Orive G, Dolatshahi-Pirouz A, Chauhan NP, Janmey PA, Hashemi A, Kundu SC. (2022). Antibacterial smart hydrogels: New hope for infectious wound management. Materials Today Bio, 17, 100499.
- Ahsan, W., Alam, S., Javed, S., Alhazmi, H. A., Albratty, M., Najmi, A., & Sultan, M. H. (2022). Study of drug release kinetics of rosuvastatin calcium immediate-release tablets marketed in Saudi Arabia. Dissolution Technologies, 29.
- Albahri, G., Badran, A., Hijazi, A., Daou, A., Baydoun, E., Nasser, M., & Merah, O. (2023). The therapeutic wound healing bioactivities of various medicinal plants. Life, 13(2), 317.
- Aleksandrova, Y. I., Shurpik, D. N., Nazmutdinova, V. A., Mostovaya, O. A., Subakaeva, E. V., Sokolova, E. A., Zelenikhin, P.V. & Stoikov, I. I. (2023). Toward pathogenic biofilm suppressors: Synthesis of amino derivatives of pillar [5] arene and supramolecular assembly with DNA. Pharmaceutics, 15(2), 476.
- Alhumaid, N. K., Alajmi, A. M., Alosaimi, N. F., Alotaibi, M., Almangour, T. A., Nassar, M. S., Memish, Z.A., Binjomah, A.Z., Al-Jedai, A., Almutairi, A.S., Algarni, S., & Tawfik, E. A. (2024). Epidemiology of reportable bacterial infectious diseases in Saudi Arabia. Infectious Diseases and Therapy, 13(4), 667-684.
- Alshememry, A. K., Kalam, M. A., Shahid, M., Ali, R., Alhudaithi, S. S., Alshumaimeri, N. A., BinHudhud, Z.A., Aldaham, A.A., Binkhathlan, Z. & Almomen, A. A. (2024). Delafloxacin-Loaded Poly (d, l-lactide-co-glycolide) nanoparticles for topical ocular use: *In vitro* characterization and antimicrobial activity. ACS omega.

- Altamimi, M., Syed, S. A., Tuzun, B., Alhazani, M. R., Alnemer, O., & Bari, A. (2023). Synthesis, biological evaluation, and molecular docking of isatin hybrids as anti-cancer and anti-microbial agents. Journal of Enzyme Inhibition and Medicinal Chemistry, 39(1).
- Althaher, A. R., & Alwahsh, M. (2023). An overview of ATP synthase, inhibitors, and their toxicity. Heliyon, 9
- Alvarez-Martínez, F. J., Barrajón-Catalán, E., Herranz-López, M., &Micol, V. (2021). Antibacterial plant compounds, extracts and essential oils: An updated review on their effects and putative mechanisms of action. Phytomedicine, 90, 153626.
- Anusha, K., Anand, A., Babu, K. S., & Tiwari, A. K. (2022). Bombax ceiba calyces regulate carbohydrate and lipid digesting enzyme's actions, display insulin sensitizing and antioxidant activities *in vitro*: A nutritional and phytochemicals examination, Indian Journal of Traditional Knowledge. 21, 323-331.
- Arthur, D. (2024). Supramolecular prodrug systems for controlled drug release and bioactivation. Journal of Chemical and Pharmaceutical Research, 16(2), 31-32.
- Asghar, A. A., Akhlaq, M., Jalil, A., Azad, A. K., Asghar, J., Adeel, M., Albadrani, G.M., Al-Doaiss, A.A., Kamel, M., Altyar, A.E. & Abdel-Daim, M. M. (2022). Formulation of ciprofloxacin-loaded oral self-emulsifying drug delivery system to improve the pharmacokinetics and antibacterial activity. Frontiers in Pharmacology, 13, 967106.
- Atacan, K., Güy, N., Semerci, A. B., Yemisci, E., Kursunlu, A. N., & Ozmen, M. (2023). Antibacterial and catalytic applications of two water-soluble pillar [5] arene derivatives. Journal of Molecular Structure, 1289, 135905.
- Augusco, M. A. C., Sarri, D. A., Panontin, J. F., Rodrigues, M. A. M., Fernandes, R. D. M. N., Silva, J. F. M. D., Cardoso, C.A., & Scapin, E. (2023). Extracts from the leaf of *Couroupita guianensis* (Aubl.): Phytochemical, toxicological analysis and evaluation of antioxidant and antimicrobial activities against oral microorganisms. Plants, 12(12), 2327.

- Azevedo, M. M., Lisboa, C., Cobrado, L., Pina-Vaz, C., & Rodrigues, A. (2020). Hard-to-heal wounds, biofilm and wound healing: An intricate interrelationship. British Journal of Nursing, 29(5), S6-S13.
- Baker, R. E., Mahmud, A. S., Miller, I. F., Rajeev, M., Rasambainarivo, F., Rice, B. L., Takahashi, S., Tatem, A. J., Wagner, C. E., Wang, L.-F., Wesolowski, A & Metcalf, C. J. E. (2022). Infectious disease in an era of global change. Nature Reviews Microbiology, 20(4), 193-205.
- Bandy, A., Wani, F. A., Mohammed, A. H., Dar, U. F., Dar, M. R., &Tantry, B. A. (2022). Bacteriological profile of wound infections and antimicrobial resistance in selected Gram-negative bacteria. African Health Sciences, 22(4), 576-586.
- Barroso, C. B., Seki, L. M., Esteves, W. T., Nascimento, M. C., & Echevarria, A. (2024). Evaluation of the antibacterial activity of isatin against *Campylobacter jejuni* and *Campylobacter coli* strains. Applied Microbiology, 4(1), 486-495.
- Bbosa, G. S., Mwebaza, N., Odda, J., Kyegombe, D. B., & Ntale, M. (2014). Antibiotics/antibacterial drug use, their marketing and promotion during the post-antibiotic golden age and their role in emergence of bacterial resistance. Health, 2014.
- Belachew, T. F., Asrade, S., Geta, M., & Fentahun, E. (2020). In vivo evaluation of wound healing and anti-inflammatory activity of 80% methanol crude flower extract of *Hagenia abyssinica* (Bruce) JF Gmel in mice. Evidence-Based Complementary and Alternative Medicine, 2020(1), 9645792.
- Bellio, P., Fagnani, L., Nazzicone, L., & Celenza, G. (2021). New and simplified method for drug combination studies by checkerboard assay. MethodsX, 8, 101543.

- Beltran-Torres, M., Sugich-Miranda, R., Santacruz-Ortega, H., Lopez-Gastelum, K. A., Ayala-Zavala, J. F., Rocha-Alonzo, F., Velazquez-Contreras, E.F. & Vazquez-Armenta, F. J. (2022). Synthesis and characterization of bismuth (III) complex with an EDTA-based phenylene ligand and its potential as anti-virulence agent. Peer Journal of Inorganic Chemistry, 4, e4.
- Bhardwaj, P., & Thakur, S. (2022). In vitro anticancer activity of medicinal plants of Himalayan region. Indian Journal of Traditional Knowledge (IJTK), 21(2), 269-275.
- Boinski, T., & Szumna, A. (2012). A facile, moisture-insensitive method for synthesis of pillar [5] arenes—the solvent templation by halogen bonds. Tetrahedron, 68(46), 9419-9422
- Bojarska, J., Remko, M., Breza, M., Madura, I. D., Kaczmarek, K., Zabrocki, J., & Wolf, W. M. (2020). A supramolecular approach to structure-based design with a focus on synthons hierarchy in ornithine-derived ligands: Review, synthesis, experimental and *in silico* studies. Molecules, 25(5), 1135.
- Bolla, S. R., Al-Subaie, A. M., Al-Jindan, R. Y., Balakrishna, J. P., Ravi, P. K., Veeraraghavan, V. P., Pillai, A.A., Gollapalli, S.S.R., Joseph, J.P. & Surapaneni, K. M. (2019). *In vitro* wound healing potency of methanolic leaf extract of *Aristolochia saccata* is possibly mediated by its stimulatory effect on collagen-1 expression. Heliyon, 5(5), e01648.
- Boominathan, M., & Arunachalam, M. (2020). Formation of supramolecular polymer network and single-chain polymer nanoparticles via host–guest complexation from pillar [5] arene pendant polymer. ACS Applied Polymer Materials, 2(11), 4368-4372.
- Boominathan, M., Kiruthika, J., & Arunachalam, M. (2019). Construction of anion-responsive crosslinked polypseudorotaxane based on molecular recognition of pillar [5] arene. Journal of Polymer Science Part A: Polymer Chemistry, 57(14), 1508-1515.

- Breijyeh, Z., & Karaman, R. (2024). Antibacterial activity of medicinal plants and their role in wound healing. Future Journal of Pharmaceutical Sciences, 10(1), 68.
- Bruna, T., Maldonado-Bravo, F., Jara, P., & Caro, N. (2021). Silver nanoparticles and their antibacterial applications. International Journal of Molecular Sciences, 22(13), 7202.
- Burkhanbayeva, T., Guslyakov, A. N., Tarikhov, F. F., Pavlov, D. I., Erkasov, R. S., Bakibaev, A. A., Potapov, A.S., Yanovsky, V.A.&Malkov, V. S. (2024). Synthesis and study of a novel supramolecular host–complex based on cucurbit [6] uril and 1, 4-bis (2-hydroxyethyl) piperazine dihydrochloride. Journal of Saudi Chemical Society, 28(2), 101819.
- Butkiewicz, H., Hyziuk, P., Kosiorek, S., Sashuk, V., Zimnicka, M. M., & Danylyuk, O. (2024). Carboxylated pillar [5] arene cavity accommodates organic cations in the host-guest complexes. Tetrahedron, 162, 134117.
- Cai, Y. M., Hutchin, A., Craddock, J., Walsh, M. A., Webb, J. S., & Tews, I. (2020). Differential impact on motility and biofilm dispersal of closely related phosphodiesterases in *Pseudomonas aeruginosa*. Scientific Reports, 10(1), 6232.
- Cai, Y., Fu, X., Zhou, Y., Lei, L., Wang, J., Zeng, W., & Yang, Z. (2023). A hydrogel system for drug loading toward the synergistic application of reductive/heat-sensitive drugs. Journal of Controlled Release, 362, 409-424.
- Cavallo, I., Sivori, F., Mastrofrancesco, A., Abril, E., Pontone, M., Di Domenico, E. G., & Pimpinelli, F. (2024). Bacterial biofilm in chronic wounds and possible therapeutic approaches. Biology, 13, 109.
- Chandra, F., Dutta, T., & Koner, A. L. (2020). Supramolecular encapsulation of a neurotransmitter serotonin by cucurbit [7] uril. Frontiers in Chemistry, 8, 582757.

- Chaudhary, P., Janmeda, P., Docea, A. O., Yeskaliyeva, B., Abdull Razis, A. F., Modu, B., Calina, D.,& Sharifi-Rad, J. (2023). Oxidative stress, free radicals and antioxidants: Potential crosstalk in the pathophysiology of human diseases. Frontiers in Chemistry, 11, 1158198.
- Cheke, R. S., Patil, V. M., Firke, S. D., Ambhore, J. P., Ansari, I. A., Patel, H. M., Shinde, S.D., Pasupuleti, V.R., Hassan, M.I., Adnan, M., Kadri, A., & Snoussi, M. (2022). Therapeutic outcomes of isatin and its derivatives against multiple diseases: Recent developments in drug discovery. Pharmaceuticals, 15(3), 272.
- Chelkeba, L., &Melaku, T. (2022). Epidemiology of Staphylococci species and their antimicrobial-resistance among patients with wound infection in Ethiopia: A systematic review and meta-analysis. Journal of Global Antimicrobial Resistance, 29, 483-498.
- Chen, J., Leung, F. K. C., Stuart, M. C., Kajitani, T., Fukushima, T., Van Der Giessen, E., & Feringa, B. L. (2018). Artificial muscle-like function from hierarchical supramolecular assembly of photoresponsive molecular motors. Nature Chemistry, 10(2), 132-138.
- CLSI (2012), Methods for dilution antimicrobial susceptibility tests for bacteria that grow aerobically approved standard, CLSI document M07–A9, (9th ed.) Clinical and laboratory standards Institute, 950 West Valley Road, Suite 2500, Wayne, Pennsylvania 19087, USA.
- Coates, A. R. M., Hu, Y., Holt, J., & Yeh, P. (2020). Antibiotic combination therapy against resistant bacterial infections: Synergy, rejuvenation and resistance reduction. Expert Review of Anti-Infective Therapy, 18
- Costa, R. A., Ortega, D. B., Fulgêncio, D. L., Costa, F. S., Araújo, T. F., & Barreto, C. C. (2019). Checkerboard testing method indicates synergic effect of pelgipeptins against multidrug resistant *Klebsiella pneumoniae*. Biotechnology Research and Innovation, 3(1), 187-191

- Dai, Y., Yu, W., Cheng, Y., Zhou, Y., Zou, J., Meng, Y., Chen, F., & Yao, Y. (2025). Recent developments in pillar[5]arene-based nanomaterials for cancer therapy. Chemical Communications. Advance Article.
- Darvishi, S., Tavakoli, S., Kharaziha, M., Girault, H. H., Kaminski, C. F., &Mela, I. (2022). Advances in the sensing and treatment of wound biofilms. Angewandte Chemie, 134(13), e202112218.
- Das, U. K., & Velpandian, T. (2019). 9 Fluoroquinolones and Other Antibacterials. Contemporary Perspectives on Ophthalmology, 10e, 87.
- De Gaudio, A. R., Rinaldi, S., & Adembri, C. (2011). Systemic antibiotics. In H. van Saene, L. Silvestri, M. de la Cal, & A. Gullo (Eds.), Infection control in the intensive care unit 67-97, Springer, Milano.
- Dehbashi, S., Tahmasebi, H., Alikhani, M. Y., Vidal, J. E., Seifalian, A., &Arabestani, M. R. (2024). The healing effect of *Pseudomonas* Quinolone Signal (PQS) with co-infection of *Staphylococcus aureus* and *Pseudomonas aeruginosa*: A preclinical animal co-infection model. Journal of Infection and Public Health, 17(2), 329-338.
- Demidova-Rice, T. N., Hamblin, M. R., & Herman, I. M. (2012). Acute and impaired wound healing: Pathophysiology and current methods for drug delivery, part 1: Normal and chronic wounds: Biology, causes, and approaches to care. Advances in Skin & Wound Care, 25(7), 304-314.
- Diban, F., Di Lodovico, S., Di Fermo, P., D'Ercole, S., D'Arcangelo, S., Di Giulio, M., & Cellini, L. (2023). Biofilms in chronic wound infections: innovative antimicrobial approaches using the in vitro Lubbock chronic wound biofilm model. International Journal of Molecular Sciences, 24(2), 1004.
- Ding, X., Tang, Q., Xu, Z., Xu, Y., Zhang, H., Zheng, D., Wang,S., Tan, Q., Maitz,J., Maitz, P.K., Yin,S., Wang,Y., & Chen, J. (2022). Challenges and innovations in treating chronic and acute wound infections: from basic science to clinical practice. Burns & Trauma, 10, tkac014.

- Donlan, R. M. (2002). Biofilms: Microbial life on surfaces. Emerging Infectious Diseases, 8, 881–890.
- Drago, L. (2019). Chloramphenicol resurrected: A journey from antibiotic resistance in eye infections to biofilm and ocular microbiota. Microorganisms, 7(9), 278.
- Drapeau, C. M. J., Grilli, E., & Petrosillo, N. (2010). Rifampicin combined regimens for Gram-negative infections: Data from the literature. International Journal of Antimicrobial Agents, 35(1), 39-44.
- Du, X., Ma, M., Zhang, Y., Yu, X., Chen, L., Zhang, H., Meng, Z., Jia, X., Chen, J., Meng, Q. & Li, C. (2023). Synthesis of cationic biphen [4, 5] arenes as biofilm disruptors. Angewandte Chemie, 135(21), e202301857.
- Duan, Q., Zhang, Q., Shi, J., Zhang, B., Zhou, L., Sang, S., & Xue, J. (2022). Synergistic effect of drug delivery system combining DOX and V9302 on gastric cancer cells. Chemistry Select, 7(33), e202202187.
- Eggers, M. (2019). Infectious disease management and control with povidone iodine. Infectious Diseases and Therapy, 8, 581-593.
- El-Sherbeni, S. A., & Negm, W. A. (2023). The wound healing effect of botanicals and pure natural substances used in *in vivo* models. Inflammopharmacology, 31(2), 755-772.
- El-Sheshtawy, H. S., Chatterjee, S., Assaf, K. I., Shinde, M. N., Nau, W. M., & Mohanty, J. (2018). A supramolecular approach for enhanced antibacterial activity and extended shelf-life of fluoroquinolone drugs with cucurbit [7] uril. Scientific Reports, 8(1), 13925.
- Epand, R. M., Walker, C., Epand, R. F., & Magarvey, N. A. (2016). Molecular mechanisms of membrane targeting antibiotics. Biochimica et Biophysica Acta (BBA) - Biomembranes, 1858(5), 980-987.

- Eshboev, F., Mamadalieva, N., Nazarov, P. A., Hussain, H., Katanaev, V., Egamberdieva, D., & Azimova, S. (2024). Antimicrobial action mechanisms of natural compounds isolated from endophytic microorganisms. Antibiotics, 13(3), 271.
- Esposito, S., Blasi, F., Curtis, N., Kaplan, S., Lazzarotto, T., Meschiari, M., Mussini,C., Peghin, M., Rodrigo, C., Vena, A., Principi, N., & Bassetti, M. (2023a). New antibiotics for *Staphylococcus aureus* infection: An update from the world association of infectious diseases and immunological disorders (WAidid) and the Italian society of anti-infective therapy (SITA). Antibiotics, 12(4), 742.
- Esposito, T., Pisanti, S., Martinelli, R., Celano, R., Mencherini, T., Re, T., & Aquino, R. P. (2023b). *Couroupita guianensis* bark decoction: From amazonian medicine to the UHPLC-HRMS chemical profile and its role in inflammation processes and re-epithelialization. Journal of Ethnopharmacology, 313, 116579.
- Finbloom, J. A., Raghavan, P., Kwon, M., Kharbikar, B. N., Yu, M. A., & Desai, T. A. (2023). Codelivery of synergistic antimicrobials with polyelectrolyte nanocomplexes to treat bacterial biofilms and lung infections. Science Advances, 9(3), eade8039.
- Flemming, H. C., Wingender, J., Szewzyk, U., Steinberg, P., Rice, S. A., & Kjelleberg, S. (2016). Biofilms: An emergent form of bacterial life. Nature Reviews Microbiology, 14(9), 563-575.
- Flores-Holguín, N., Frau, J., &Glossman-Mitnik, D. (2021). In silico pharmacokinetics, ADMET study and conceptual DFT analysis of two plant cyclopeptides isolated from rosaceae as a computational Peptidology approach. Frontiers in Chemistry, 9, 708364.
- Flynn, J., Ryan, A., & Hudson, S. P. (2022). Synergistic antimicrobial interactions of nisin A with biopolymers and solubilising agents for oral drug delivery. European Journal of Pharmaceutics and Biopharmaceutics, 171, 29-38.

- Franklin, T. J., & Snow, G. A. (1989). Inhibitors of protein synthesis. In Biochemistry of Antimicrobial Action (pp. 112-136). Springer.
- Frimayanti, N., Yaeghoobi, M., Namavar, H., Ikhtiarudin, I., & Afzali, M. (2020). *In silico* studies and biological evaluation of chalcone-based 1, 5-benzothiazepines as new potential H1N1 neuraminidase inhibitors. Journal of Applied Pharmaceutical Science, 10(10), 086-094.
- Gehrke, A. K. E., Giai, C., & Gómez, M. I. (2023). *Staphylococcus aureus* adaptation to the skin in health and persistent/recurrent infections. Antibiotics, 12(10), 1520.
- Gilbert, H. A. (2020). Florence Nightingale's Environmental Theory and its influence on contemporary infection control. Collegian, 27(6), 626-633.
- Goel, N., Hashmi, Z., Khan, N., Ahmad, R., & Khan, W. H. (2023). Recent strategies to combat multidrug resistance. In Non-Traditional Approaches to Combat Antimicrobial Drug Resistance (pp. 1-27). Singapore: Springer Nature Singapore.
- Goudarzi, M., Navidinia, M., Khadembashi, N., & Rasouli, R. (2021). Biofilm matrix formation in humans: Clinical significance, diagnostic techniques, and therapeutic drugs. Archives of Clinical Infectious Diseases, 16, e107919.
- Guo, H. (2019). Isatin derivatives and their anti-bacterial activities. European Journal of Medicinal Chemistry, 164, 678-688.
- Guo, H., Zhang, R., Han, Y., Wang, J., & Yan, C. (2020). A p-tert-Butyldihomooxacalix [4] arene based soft gel for sustained drug release in water. Frontiers in chemistry, 8, 33.
- Guo, S., & Dipietro, L. A. (2010). Factors affecting wound healing. Journal of Dental Research, 89, 219-229

- Guo, S., Huang, Q., Chen, Y., Wei, J., Zheng, J., Wang, L., Wang, Y. & Wang, R. (2021). Synthesis and bioactivity of guanidinium-functionalized pillar [5] arene as a biofilm disruptor. Angewandte Chemie International Edition, 60(2), 618-623.
- Haji, S. H., Ali, F. A., & Aka, S. T. H. (2022). Synergistic antibacterial activity of silver nanoparticles biosynthesized by carbapenem-resistant Gram-negative *Bacilli*. Scientific Reports, 12(1), 15254.
- Han, C., Zhang, Z., Yu, G., & Huang, F. (2012). Syntheses of a pillar [4] arene [1] quinone and a difunctionalized pillar[5]arene by partial oxidation. Chemical Communications, 48(79), 9876-9878.
- Han, C., Zhao, D., Li, H., Wang, H., Huang, X., & Sun, D. (2018). Effective binding of neutral dinitriles by pillar[4] arene[1] quinone both in solution and in solid State. Chemistry Select, 3(1), 11-14.
- Han, C., Zhao, D., Lü, Z., Zhan, F., Zhang, L., Dong, S., & Jin, L. (2019). Synthesis of a difunctionalized pillar[5]arene with hydroxyl and amino groups at A1/A2 positions. European Journal of Organic Chemistry,(14), 2508-2512.
- Han, G., & Ceilley, R. (2017). Chronic wound healing: A review of current management and treatments. Advances in Therapy, 34, 599-610.
- Hao, Y., Zhang, F., Mo, S., Zhao, J., Wang, X., Zhao, Y., & Zhang, L. (2021). Biomedical applications of supramolecular materials in the controllable delivery of steroids. Frontiers in Molecular Biosciences, 8, 700712.
- Hemmati, J., Chiani, M., Asghari, B., Roshanaei, G., Soleimani Asl, S., Shafiei, M., & Arabestani, M. R. (2024). Antibacterial and antibiofilm potentials of vancomycin-loaded niosomal drug delivery system against methicillin-resistant *Staphylococcus aureus* (MRSA) infections. BMC Biotechnology, 24(1), 47.

- Heredia, N. S., Vizuete, K., Flores-Calero, M., Pazmiño V, K., Pilaquinga, F., Kumar, B., & Debut, A. (2022). Comparative statistical analysis of the release kinetics models for nanoprecipitated drug delivery systems based on poly (lactic-co-glycolic acid). PLoS One, 17(3), e0264825.
- Hope, D., Ampaire, L., Oyet, C., Muwanguzi, E., Twizerimana, H., & Apecu, R. O. (2019). Antimicrobial resistance in pathogenic aerobic bacteria causing surgical site infections in Mbarara regional referral hospital, Southwestern Uganda. Scientific Reports, 9(1), 17299.
- Hu, X. Y., Gao, J., Chen, F. Y., & Guo, D. S. (2020). A host-guest drug delivery nanosystem for supramolecular chemotherapy. Journal of Controlled Release, 324
- Huang, X., Wu, S., Ke, X., Li, X., & Du, X. (2017). Phosphonated pillar [5] arene-valved mesoporous silica drug delivery systems. ACS Applied Materials & Interfaces, 9(23), 19638-19645.
- Idrees, M., Sawant, S., Karodia, N., & Rahman, A. (2021). Staphylococcus aureus biofilm: Morphology, genetics, pathogenesis and treatment strategies. International Journal of Environmental Research and Public Health, 18(14), 7602.
- Igarashi, M., & Miyazawa, T. (2001). The growth inhibitory effect of conjugated linoleic acid on a human hepatoma cell line, HepG2, is induced by a change in fatty acid metabolism, but not the facilitation of lipid peroxidation in the cells. Biochimica et Biophysica Acta (BBA)-Molecular and Cell Biology of Lipids, 1530(2-3), 162-171.
- Ikuta, K. S., Swetschinski, L. R., Aguilar, G. R., Sharara, F., Mestrovic, T., Gray, A. P., Weaver N.D., Wool, E.E., Han,C., Hayoon, A.G., Aali, A., Dhingra, S. (2022). Global mortality associated with 33 bacterial pathogens in 2019: A systematic analysis for the global burden of disease study 2019. The Lancet, 400(10369), 2221-2248.

- Israyilova, A., Peykova, T. Z., Kittleson, B., Sprowl, P. C., Mohammed, T. O., & Quave, C. (2024). From plant to patient: A historical perspective and review of selected medicinal plants in dermatology. JID Innovations, 5(1), 100321.
- Jamal, M., Ahmad, W., Andleeb, S., Jalil, F., Imran, M., Nawaz, M. A., Hussain, T., Ali, M., Rafiq, M., & Kamil, M. A. (2018). Bacterial biofilm and associated infections. Journal of the Chinese Medical Association, 81, 7–11.
- Jiang, Y., Pan, X., Chang, J., Niu, W., Hou, W., Kuai, H., Zhao, Z., Liu, J., Wang, M.,& Tan, W. (2018). Supramolecularly engineered circular bivalent aptamer for enhanced functional protein delivery. Journal of the American Chemical Society, 140(22), 6780-6784.
- Jin, X., Zhu, L., Xue, B., Zhu, X., & Yan, D. (2019). Supramolecular nanoscale drug-delivery system with ordered structure. National Science Review, 6(6), 1128-1137.
- Johnson, A. C., Buchanan, E. P., & Khechoyan, D. Y. (2022). Wound infection: A review of qualitative and quantitative assessment modalities. Journal of Plastic, Reconstructive & Aesthetic Surgery, 75(4), 1287-1296.
- Jonkergouw, C., Beyeh, N. K., Osmekhina, E., Leskinen, K., Taimoory, S. M., Fedorov, D., Anaya-Plaza, E., Kostiainen, M.A., Trant, J.F., Ras, R.H. & Linder, M. B. (2023). Repurposing host-guest chemistry to sequester virulence and eradicate biofilms in multidrug resistant *Pseudomonas aeruginosa* and *Acinetobacter baumannii*. Nature Communications, 14(1), 2141.
- Juvekar, M., Juvekar, A., Kulkarni, M., Wakade, A., Ambaye, R., & Wankhede, S. (2009). Phytochemical and pharmacological studies on the leaves of *Couroupita guianensis* Aubl. Planta Medica, 75, PJ168.
- Kaiser, P., Wächter, J., & Windbergs, M. (2021). Therapy of infected wounds: Overcoming clinical challenges by advanced drug delivery systems. Drug Delivery and Translational Research, 11, 1545-1567.

- Kaizerman-Kane, D., Hadar, M., Joseph, R., Logviniuk, D., Zafrani, Y., Fridman, M., & Cohen, Y. (2021). Design guidelines for cationic pillar [n] arenes that prevent biofilm formation by gram-positive pathogens. ACS Infectious Diseases, 7(3), 579-585.
- Karygianni, L., Ren, Z., Koo, H., & Thurnheer, T. (2020). Biofilm matrixome: Extracellular components in structured microbial communities. Trends in Microbiology, 28, 668-681.
- Kasinathan, I., Uma, S., Elumalai, K., & Kavitha Manivannan, M. R. (2024). Traditionally used medicinal plants for wound healing in Thiruvallur District, Tamil Nadu, India. International Journal of Current Pharmaceutical Research, 16(4), 1-6.
- Kavitha, D., Madhumitha, M., Ramya R. & Kumarappan, C. (2024). Dynamic protective potential of *Couroupita guianensis*. Aubl against reactive free radicals: An approach of stimulated in vitro model. Indian Journal of Traditional Knowledge (IJTK), 23(5), 441-451.
- Kavitha, D., Nandhini, G., & Padma, P. R. (2013). In vitro evaluation of isatin from *Couroupita guianensis* Aubl against the clinical isolates of bacteria and fungi. International Journal of Pharmaceutical Sciences Review and Research, 23(2), 228-230.
- Khalid, F., Poulose, C., Farah, D. F. M., Mahmood, A., Elsheikh, A., & Khojah, O. T. (2024). Prevalence and antimicrobial susceptibility patterns of wound and pus bacterial pathogens at a tertiary care hospital in central Riyadh, Saudi Arabia. Microbiology Research, 15(4), 2015-2034.
- Khezerlou, A., & Jafari, S. M. (2020). Nanoencapsulated bioactive components for active food packaging. Handbook of Food Nanotechnology. 493-532. Academic Press.
- Kim, D., Kim, Y., & Lim, S. (2022). Effects of swimming environment on bacterial motility. Physics of Fluids, 34(3), 031907.

- Kiruthika, J., & Arunachalam, M. (2022). Pillar[5]arene-based cross-linked polymer for the rapid adsorption of iodine from water and vapor phases. Polymer, 259, 125322.
- Kiruthika, J., Boominathan, M., Srividhya, S., Ajitha, V., & Arunachalam, M. (2021). Pillar [4] arene[1]quinone-based pseudo [3] rotaxanes by cooperative Host-Guest binding. Supramolecular Chemistry, 33(7), 390-399.
- Kiruthika, J., Srividhya, S., & Arunachalam, M. (2020). Anion-responsive pseudo[3]rotaxane from a difunctionalized pillar[4]arene[1]quinone and a bis-imidazolium cation. Organic Letters, 22(20), 7831-7836.
- Kowalska-Krochmal, B., & Dudek-Wicher, R. (2021). The minimum inhibitory concentration of antibiotics: Methods, interpretation, clinical relevance. Pathogens, 10(2), 165.
- Kulayta, K., Zerdo, Z., Seid, M., Dubale, A., Manilal, A., Kebede, T., Alahmadi,R.M., Raman,G., & Akbar, I. (2024). Biofilm formation and antibiogram profile of bacteria from infected wounds in a general hospital in Southern Ethiopia. Scientific Reports, 14(1), 26359.
- Kumar, R., Mishra, A., Gautam, P., Feroz, Z., Vijayaraghavalu, S., Likos, E. M., Shukla, G. C., & Kumar, M. (2022). Metabolic pathways, enzymes, and metabolites: Opportunities in cancer therapy. Cancers (Basel).
- Lahiri, H., & Basu, K. (2024). Supramolecular sensing platforms: techniques for *in vitro* biosensing. ChemEngineering, 8(4), 66.
- Lalonde, K. M., Black, C., & Lam, J. C. (2022). Principles of empiric antimicrobial usage and dosing: Lessons learned. Clinical Case Reports, 10, e05594.
- Las Heras, K., Igartua, M., Santos-Vizcaino, E., & Hernandez, R. M. (2020). Chronic wounds: Current status, available strategies and emerging therapeutic solutions. Journal of Controlled Release, 328, 532-550.

- Latif, M. S., Nawaz, A., Asmari, M., Uddin, J., Ullah, H., & Ahmad, S. (2022). Formulation development and in vitro/in vivo characterization of methotrexate-loaded nanoemulsion gel formulations for enhanced topical delivery. Gels, 9(1), 3.
- Li, Q., Zhu, H., & Huang, F. (2020). Pillararene-based supramolecular functional materials. Trends in Chemistry, 2.
- Li, S., Kuok, K. I., Ji, X., Xu, A., Yin, H., Zheng, J., Tan, H. & Wang, R. (2020). Supramolecular modulation of antibacterial activity of ambroxol by cucurbit [7] uril. ChemPlusChem, 85(4), 679-683.
- Li, X., Zuo, S., Wang, B., Zhang, K., & Wang, Y. (2022). Antimicrobial mechanisms and clinical application prospects of antimicrobial peptides. Molecules, 27(9), 2675.
- Li, Y., Vrana, N. E., Letellier, B., Lavalle, P., & Guilbaud-Chéreau, C. (2024). The use of supramolecular systems in biomedical applications for antimicrobial properties, biocompatibility, and drug delivery. Biomedical Materials. 19(4).
- Lin, M., Liu, Y., Gao, J., Wang, D., Xia, D., Liang, C., Li, N. & Xu, R. (2022). Synergistic effect of co-delivering ciprofloxacin and tetracycline hydrochloride for promoted wound healing by utilizing coaxial PCL/gelatin nanofiber membrane. International Journal of Molecular Sciences, 23(3), 1895.
- Lipsky, B. A., Dryden, M., Gottrup, F., Nathwani, D., Seaton, R. A., & Stryja, J. (2016). Antimicrobial stewardship in wound care: A position paper from the British society for antimicrobial chemotherapy and European wound management association. Journal of Antimicrobial Chemotherapy, 71(11), 3026-3035.
- Liu, C. C., & Lin, M. H. (2023). Hitchhiking motility of Staphylococcus aureus involves the interaction between its wall teichoic acids and lipopolysaccharide of *Pseudomonas aeruginosa*. Frontiers in Microbiology, 13, 1068251.

- Liu, C., Yang, Z., Song, X., Qian, Y., Huo, H., He, J., Zhang, J., Zhang, Z., Shi, M., Pang, J. & Tian, W. (2022). Light controlled drug-based supramolecular polymer self-assemblies for efficient antibacterial manipulation. Supramolecular Materials, 1, 100014.
- Liu, H., Wang, L., & Yao, C. (2023). Optimization of Antibacterial Activity and Biosafety through Ultrashort Peptide/Cyclodextrin Inclusion Complexes. International Journal of Molecular Sciences, 24(19), 14801.
- Liu, L., Zhou, Q., He, Q., Duan, W., & Huang, Y. (2021). A pH-responsive supramolecular drug delivery system constructed by cationic pillar[5]arene for enhancing antitumor activity. Frontiers in Chemistry, 9, 661143.
- Liu, M., Lu, J., Müller, P., Turnbull, L., Burke, C. M., Schlothauer, R. C., Carter, D. A., Whitchurch, C. B., & Harry, E. J. (2015). Antibiotic-specific differences in the response of *Staphylococcus aureus* to treatment with antimicrobials combined with manuka honey. Frontiers in Microbiology, 5
- Liu, W. B., Gao, R. T., Zhou, L., Liu, N., Chen, Z., & Wu, Z. Q. (2022). Combination of vancomycin and guanidinium-functionalized helical polymers for synergistic antibacterial activity and biofilm ablation. Chemical Science, 13(35), 10375-10382.
- Liu, Y. F., Ni, P. W., Huang, Y., & Xie, T. (2022). Therapeutic strategies for chronic wound infection. Chinese Journal of Traumatology, 25(01), 11-16.
- Liu, Y., Shi, D., Li, B., Jin, Y., Ling, D., & Li, F. (2024). Supramolecular macrocyclic artificial ion channels for biomedical applications. Fundamental Research. https://doi.org/10.1016/j.fmre.2024.06.012
- Logambal, S., Thilagavathi, T., Chandrasekar, M., Inmozhi, C., Kedi, P. B. E., Bassyouni, F. A., Uthrakumar, R., Muthukumaran, A., Naveenkumar, S., & Kaviyarasu, K. (2023). Synthesis and antimicrobial activity of silver nanoparticles: incorporated *Couroupita guianensis* flower petal extract for biomedical applications. Journal of King Saud University-Science, 35(1), 102455.

- Losito, A. R., Raffaelli, F., Del Giacomo, P., &Tumbarello, M. (2022). New drugs for the treatment of *Pseudomonas aeruginosa* infections with limited treatment options: A narrative review. Antibiotics, 11(5), 579
- Lowry, O. H., Rosebrough, N. J., Farr, A. L., & Randall, R. J. (1951). Protein measurement with the Folin phenol reagent. Journal of Biological Chemistry. 193(1), 265-275.
- Ludwig, T. G., & Goldberg, H. J. (1956). The anthrone method for the determination of carbohydrates in foods and in oral rinsing. Journal of Dental Research, 35(1), 90-94.
- Luotonen, O. I., Osmekhina, E., Anaya-Plaza, E., Kaabel, S., Harmat, A. L., Sammalkorpi, M., Jonkergouw, C., Linder, M.B. & Kostiainen, M. A. (2024). Resolving host-guest interactions between pillararenes and homoserine lactones to restrain bacterial quorum sensing. Cell Reports Physical Science, 5(7), 102089.
- Ma, M., Chen, J., Zhang, Y., Du, X., Chen, L., Yu, X., Zhou, Z., Liu, Y. & Meng, Q. (2022). Host–guest synergistic enhancement of antibacterial effect by a supramolecular strategy. Organic & Biomolecular Chemistry, 20(48), 9625-9628.
- Ma, X., & Zhao, Y. (2015). Biomedical applications of supramolecular systems based on host–guest interactions. Chemical Reviews, 115(15), 7794-7839.
- Maikawa, C. L., d'Aquino, A. I., Vuong, E. T., Su, B., Zou, L., Chen, P. C., Nguyen, L.T., Autzen, A.A., Mann, J.L., Webber, M.J. & Appel, E. A. (2021). Affinity-directed dynamics of host–guest motifs for pharmacokinetic modulation via supramolecular PEGylation. Biomacromolecules, 22(8), 3565-3573.
- Majumdar, D., Philip, J. E., Dubey, A., Tufail, A., & Roy, S. (2023). Synthesis, spectroscopic findings, SEM/EDX, DFT, and single-crystal structure of Hg/Pb/Cu–SCN complexes: In silico ADMET profiling and promising antibacterial activities. Heliyon, 9(5).

- Manna, S., Ghosh, A. K., & Mandal, S. M. (2019). Curd-peptide based novel hydrogel inhibits biofilm formation, quorum sensing, swimming mortility of multi-antibiotic resistant clinical isolates and accelerates wound healing activity. Frontiers in Microbiology, 10, 951,1-9.
- Masson-Meyers, D. S., Andrade, T. A., Caetano, G. F., Guimaraes, F. R., Leite, M. N., Leite, S. N., & Frade, M. A. C. (2020). Experimental models and methods for cutaneous wound healing assessment. International Journal of Experimental Pathology, 101(1-2), 21-37.
- Medvedev, A., Buneeva, O., & Glover, V. (2007). Biological targets for isatin and its analogues: Implications for therapy. Biologics, 1(2), 151-162. PMID: 19707325.
- Metcalf, D. G., & Bowler, P. G. (2020). Clinical impact of an anti-biofilm hydrofiber dressing in hard-to-heal wounds previously managed with traditional antimicrobial products and systemic antibiotics. Burns & Trauma, 8, tkaa004.
- Monk, E. J., Jones, T. P., Bongomin, F., Kibone, W., Nsubuga, Y., Ssewante, N., Muleya, I., Nsenga, L., Rao, V.B., & van Zandvoort, K. (2024). Antimicrobial resistance in bacterial wound, skin, soft tissue and surgical site infections in Central, Eastern, Southern and Western Africa: A systematic review and meta-analysis. PLOS Global Public Health, 4(4), e0003077.
- Mota, F. A., Pereira, S. A., Araujo, A. R., Passos, M. L., & Saraiva, M. L. M. (2021). Biomarkers in the diagnosis of wounds infection: An analytical perspective. TrAC Trends in Analytical Chemistry, 143, 116405.
- Munyeshyaka, E., Cyuzuzo, P., Yadufashije, C., & Karemera, J. (2021). Contribution of medical wards contamination to wound infection among patients attending Ruhengeri Referral Hospital. International Journal of Microbiology, 2021(1), 7838763.

- Mussini, A., Uriati, E., Hally, C., Nonell, S., Bianchini, P., Diaspro, A., Pongolini, S., Delcanale, P., Abbruzzetti, S. & Viappiani, C. (2022). Versatile supramolecular complex for targeted antimicrobial photodynamic inactivation. Bioconjugate Chemistry, 33(4), 666-676.
- Muteeb, G., Rehman, M. T., Shahwan, M., & Aatif, M. (2023). Origin of antibiotics and antibiotic resistance, and their impacts on drug development: A narrative review. Pharmaceuticals, 16(11), 1615.
- Muthulakshmi, V., Kumar, C. D., & Sundrarajan, M. (2022). Biological applications of green synthesized lanthanum oxide nanoparticles via *Couroupita guianensis* Abul leaves extract. Analytical Biochemistry, 638, 114482.
- Nazir, A., Abbas, M., Kainat, F., Iqbal, D. N., Aslam, F., Kamal, A., Mohammed, O.A., Zafar, K., Alrashidi, A.A., Alshawwa, S.Z. & Iqbal, M. (2024). Efficient drug delivery potential and antimicrobial activity of biocompatible hydrogels of dextrin/Na-alginate/PVA. Heliyon, 10(9), e29854.
- Negut, I., Grumezescu, V., & Grumezescu, A. M. (2018). Treatment strategies for infected wounds. Molecules, 23(9), 2392.
- Ogoshi, T., Hamada, Y., Sueto, R., Sakata, Y., Akine, S., Moeljadi, A. M. P., Hirao, H., Kakuta, T., Yamagishi, T.A., & Mizuno, M. (2019). Host–guest complexation using pillar [5] arene crystals: Crystal-structure dependent uptake, release, and molecular dynamics of an alkane guest. Chemistry–A European Journal, 25(10), 2497-2502.
- Ogoshi, T., Yamagishi, T. A., & Nakamoto, Y. (2016). Pillar-shaped macrocyclic hosts pillar [n] arenes: New key players for supramolecular chemistry. Chemical Reviews, 116(14), 7937-8002.
- Ohtani, S., Kato, K., Fa, S., & Ogoshi, T. (2022). Host–guest chemistry based on solid-state pillar [n] arenes. Coordination Chemistry Reviews, 462, 214503.

- Okur, M. E., Karantas, I. D., Şenyiğit, Z., Okur, N. Ü., & Siafaka, P. I. (2020). Recent trends on wound management: New therapeutic choices based on polymeric carriers. Asian Journal of Pharmaceutical Sciences, 15(6), 661-684.
- Packiavathy, I. A. S. V., Priya, S., Pandian, S. K., & Ravi, A. V. (2014). Inhibition of biofilm development of uropathogens by curcumin–an anti-quorum sensing agent from *Curcuma longa*. Food Chemistry, 148, 453-460.
- Pakravan, P., Kashanian, S., Khodaei, M. M., & Harding, F. J. (2013). Biochemical and pharmacological characterization of isatin and its derivatives: From structure to activity. Pharmacological Reports, 65(2), 313-335.
- Panigrahi, S. D., Klebba, K. C., Rodriguez, E. N., Mayhan, C. M., Kotagiri, N., & Kumari, H. (2024). Enhancing antibacterial efficacy through macrocyclic host complexation of fluoroquinolone antibiotics for overcoming resistance. Scientific Reports, 14(1), 24637.
- Paswan, S. K., & Saini, T. (2021). Comparative evaluation of *in vitro* drug release methods employed for nanoparticle drug release studies. Clinical Trials, 14, 17.
- Pathak, D., & Mazumder, A. (2024). A critical overview of challenging roles of medicinal plants in improvement of wound healing technology. DARU Journal of Pharmaceutical Sciences, 32, 379-419.
- Patra, J. K., Das, G., Fraceto, L. F., Campos, E. V. R., Rodriguez-Torres, M. D. P., Acosta-Torres, L. S., Diaz-Torres, L.A., Grillo, R., Swamy, M.K., Sharma, S., Habtemariam, S.,& Shin, H. S. (2018). Nano based drug delivery systems: Recent developments and future prospects. Journal of Nanobiotechnology, 16, 1-33.
- Ping, G., Wang, Y., Shen, L., Wang, Y., Hu, X., Chen, J., Hu B, Cui L, Meng Q.,& Li, C. (2017). Highly efficient complexation of sanguinarine alkaloid by carboxylatopillar [6] arene: pKa shift, increased solubility and enhanced antibacterial activity. Chemical Communications, 53(53), 7381-7384.

- Pires, D. E., Blundell, T. L., &Ascher, D. B. (2015). pkCSM: predicting small-molecule pharmacokinetic and toxicity properties using graph-based signatures. Journal of Medicinal Chemistry, 58(9), 4066-4072.
- Puca, V., Marulli, R. Z., Grande, R., Vitale, I., Niro, A., Molinaro, G., Prezioso,S., Muraro,R.,& Di Giovanni, P. (2021). Microbial species isolated from infected wounds and antimicrobial resistance analysis: Data emerging from a three-years retrospective study. Antibiotics, 10(10), 1162.
- Qin, S., Xiao, W., Zhou, C., Pu, Q., Deng, X., Lan, L., Liang, H., Song, X.,& Wu, M. (2022). *Pseudomonas aeruginosa*: pathogenesis, virulence factors, antibiotic resistance, interaction with host, technology advances and emerging therapeutics. Signal Transduction and Targeted Therapy, 7(1), 199.
- Ramesh, M. M., Shankar, N. S., & Venkatappa, A. H. (2024). Driving/critical factors considered during extraction to obtain bioactive enriched extracts. Pharmacognosy Reviews, 18(35),68-81.
- Razdan, K., Garcia-Lara, J., Sinha, V. R., & Singh, K. K. (2022). Pharmaceutical strategies for the treatment of bacterial biofilms in chronic wounds. Drug Discovery Today, 27(8), 2137-2150.
- Reygaert, W. C. (2018). An overview of the antimicrobial resistance mechanisms of bacteria. AIMS Microbiology, 4(3), 482-501.
- Roska, T. P., Mudjahid, M., Marzaman, A. N. F., Datu, N. N. P., & Permana, A. D. (2022). Development of chloramphenicol wound dressing protein-based microparticles in chitosan hydrogel system for improved effectiveness of dermal wound therapy. Biomaterials Advances, 143, 213175.
- Ruan, Y. R., Li, W. Z., Ye, Y. Y., Luo, J., Xu, S. Y., Xiao, J., Lin, X.W., Liu, S., Wang, X.Q. & Wang, W. (2023). Supramolecularly assisted chlorhexidine-bacterial membrane interaction with enhanced antibacterial activity and reduced side effects. Journal of Colloid and Interface Science, 641, 146-154.

- Rubio-Canalejas, A., Baelo, A., Herbera, S., Blanco-Cabra, N., Vukomanovic, M., & Torrents, E. (2022). 3D spatial organization and improved antibiotic treatment of a *Pseudomonas aeruginosa*–*Staphylococcus aureus* wound biofilm by nanoparticle enzyme delivery. Frontiers in Microbiology, 13, 959156.
- Sanya, D. R. A., Onésime, D., Vizzarro, G., & Jacquier, N. (2023). Recent advances in therapeutic targets identification and development of treatment strategies towards *Pseudomonas aeruginosa* infections. BMC Microbiology, 23(1), 86.
- Sarkar, B., Das, K., Saha, T., Prasad, E., & Gardas, R. L. (2021). Insights into the formations of host–guest complexes based on the Benzimidazolium based ionic liquids− β-Cyclodextrin systems. ACS Physical Chemistry Au, 2(1), 3-15.
- Sathe, N., Beech, P., Croft, L., Suphioglu, C., Kapat, A., & Athan, E. (2023). Pseudomonas aeruginosa: Infections and novel approaches to treatment “Knowing the Enemy” the threat of *Pseudomonas aeruginosa* and exploring novel approaches to treatment. Infectious Medicine, 2(3), 178-194.
- Sathiyajith, C., Shaikh, R. R., Han, Q., Zhang, Y., Meguellati, K., & Yang, Y. (2017). Biological and related applications of pillar[n]arenes. Chemical Communications, 46(4), 6600-6620.
- Satpathy, S., Sen, S. K., Pattanaik, S., & Raut, S. (2016). Review on bacterial biofilm: An universal cause of contamination. Biocatalysis and Agricultural Biotechnology, 7, 56-66.
- Shanmugam, B., & Srinivasan, U. M. (2024). Formulation and characterization of antibiotic drug loaded aquasome for the topical application. Future Science OA, 10(1), 2367849.
- Sheba, L. A., & Anuradha, V. (2019). An updated review on *Couroupita guianensis* Aubl: a sacred plant of India with myriad medicinal properties. Journal of Herbmed Pharmacology, 9(1), 1-11.

- Sheba, L. A., Anuradha, V., Ali, M. S., & Yogananth, N. (2023). Wound healing potential of *Couroupita guianensis* Aubl. fruit pulp investigated on excision wound model. Applied Biochemistry and Biotechnology, 195(11), 6516-6536.
- Shi, T. H., Ohtani, S., Kato, K., Fa, S., & Ogoshi, T. (2023). Host–guest behavior of pillar [n] arene-based supramolecular assemblies. Trends in Chemistry, 5(7), 537-550.
- Shukla, S. (2015). Studying antimicrobial-induced morphostructural damage of bacteria by Scanning Electron Microscope. Bangladesh Journal of Pharmacology, 10(4), 870-874.
- Shurpik, D. N., Aleksandrova, Y. I., Mostovaya, O. A., Nazmutdinova, V. A., Tazieva, R. E., Murzakhanov, F. F., Gafurov, M.R., Zelenikhin, P.V., Subakaeva, E.V., Sokolova, E.A. & Stoikov, I. I. (2022). Self-healing thiolated pillar[5]arene films containing moxifloxacin suppress the development of bacterial biofilms. Nanomaterials, 12(9), 1604.
- Shurpik, D. N., Aleksandrova, Y. I., Mostovaya, O. A., Nazmutdinova, V. A., Zelenikhin, P. V., Subakaeva, E. V., Mukhametzyanov, T.A., Cragg, P.J. & Stoikov, I. I. (2021). Water-soluble pillar[5]arene sulfo-derivatives self-assemble into biocompatible nanosystems to stabilize therapeutic proteins. Bioorganic Chemistry, 117, 105415.
- Shwetha, R., Roopashree, T. S., Das, K., Prashanth, N., & Kumar, R. (2020). HPTLC fingerprinting of various extracts of *Couroupita guianensis* flowers for establishment of *in vitro* antimalarial activity through isolated compound. Annals of Phytomedicine, 9(1), 133-140.
- Silver, L. L. (2003). Novel inhibitors of bacterial cell wall synthesis. Current Opinion in Microbiology, 6(5), 431-438.
- Soni, J., Sinha, S., & Pandey, R. (2024). Understanding bacterial pathogenicity: A closer look at the journey of harmful microbes. Frontiers in Microbiology, 15, 1370818.

- Strutt, N. L., Forgan, R. S., Spruell, J. M., Botros, Y. Y., & Stoddart, J. F. (2011). Monofunctionalized pillar [5] arene as a host for alkanediamines. Journal of the American Chemical Society, 133(15), 5668-5671.
- Strutt, N.L., Zhang, H., Schneebeli, S.T. & Stoddart, J.F. (2014), Amino-Functionalized Pillar[5]arene. Chemistry A European Journal, 20, 10996-11004.
- Subakaeva, E., Zelenikhin, P., Sokolova, E., Pergat, A., Aleksandrova, Y., Shurpik, D., & Stoikov, I. (2023). The Synthesis and antibacterial properties of pillar [5] arene with streptocide fragments. Pharmaceutics, 15(12), 2660.
- Sumathi, S., & Anuradha, R. (2017). *Couroupita guianensis* Aubl: An updated review of its phytochemistry and pharmacology. Asian Journal of Pharmacy and Pharmacology, 3(1), 1-8.
- Sun, H., Huang, S. Y., Jeyakkumar, P., Cai, G. X., Fang, B., & Zhou, C. H. (2021). Natural berberine-derived azolyl ethanols as new structural antibacterial agents against drug-resistant *Escherichia coli*. Journal of Medicinal Chemistry, 65(1), 436-459.
- Talapko, J., Meštrović, T., Juzbašić, M., Tomas, M., Erić, S., HorvatAleksijević, L., Bekić, S., Schwarz, D., Matić, S., Neuberg, M. & Škrlec, I. (2022). Antimicrobial peptides—Mechanisms of action, antimicrobial effects and clinical applications. Antibiotics, 11(10), 1417
- Te Dorsthorst, D. T., Verweij, P. E., Meis, J. F., Punt, N. C., & Mouton, J. W. (2002). Comparison of fractional inhibitory concentration index with response surface modeling for characterization of *in vitro* interaction of antifungals against itraconazole-susceptible and-resistant *Aspergillus fumigatus* isolates. Antimicrobial agents and chemotherapy, 46(3), 702-707.
- Timotius, D., Kusumastuti, Y., Imani, N. A. C., Putri, N. R. E., Rahayu, S. S., Wirawan, S. K., & Ikawati, M. (2020). Kinetics of drug release profile from maleic anhydride-grafted-chitosan film. Materials Research Express, 7(4), 046403.

- Tomar, M. K., Pahwa, S., Tyagi, L. K., Gupta, C., Maan, P., & Sethi, V. A. (2022). Formulation, characterization, and antibacterial study of microsponge-loaded gel of clarithromycin for topical drug delivery. Drug Delivery Letters, 12(2), 122-134.
- Tosun, M., Uysal, A., Kursunlu, A. N., & Guler, E. (2024). A new family of macrocyclic antibiotics based-on Pillar [5] arene concluding multi quinoline moieties. Tetrahedron, 151, 133812.
- Tripathi, R. R., & Sonawane, R. P. (2013). An extraction of the isatin from the *Couroupita guianesis* (cannon ball tree) and a novel synthesis of the N, N'-(2-oxo-3'H-spiro [indoline-3, 2'-[1, 3, 4] thiadiazole]-3', 5'-diyl] diacetamide from the Isatin. International Letters of Chemistry, Physics and Astronomy, 10(2), 119-125
- Truszkowska, M., Stengel, D., Schmidt, M. R., Marx, F., Coraca-Huber, D., & Bernkop-Schnürch, A. (2024). Synergistic antimicrobial effect of daptomycin and ethyl lauroyl arginate containing self-emulsifying drug delivery system against bacterial infections. Journal of Drug Delivery Science and Technology, 102, 106324.
- Uberoi, A., McCready-Vangi, A., & Grice, E. A. (2024). The wound microbiota: microbial mechanisms of impaired wound healing and infection. Nature Reviews Microbiology, 1-15.
- Uddin, T. M., Chakraborty, A. J., Khusro, A., Zidan, B. R. M., Mitra, S., Emran, T. B., Dhama, K., Ripon, M.K.H., Gajdács,M., Sahibzada, M.U.K., Hossain, & Koirala, N. (2021). Antibiotic resistance in microbes: History, mechanisms, therapeutic strategies and future prospects. Journal of Infection and Public Health, 14(12), 1750-1766.
- Urnukhsaikhan, E., Bold, B. E., Gunbileg, A., Sukhbaatar, N., & Mishig-Ochir, T. (2021). Antibacterial activity and characteristics of silver nanoparticles biosynthesized from *Carduus crispus*. Scientific Reports, 11(1), 21047.

- Van Andel, T., & Carvalheiro, L. G. (2013). Why urban citizens in developing countries use traditional medicines: The case of Suriname. Evidence-Based Complementary and Alternative Medicine, 2013, Article 687197
- Vetrivel, A., Ramasamy, M., Vetrivel, P., Natchimuthu, S., Arunachalam, S., Kim, G. S., & Murugesan, R. (2021). *Pseudomonas aeruginosa* biofilm formation and its control. Biologics, 1(3), 312-336.
- Wang, H., Liu, H., Wang, M., Hou, J., Li, Y., Wang, Y., & Zhao, Y. (2024b). Cucurbituril-based supramolecular host–guest complexes: Single-crystal structures and dual-state fluorescence enhancement. Chemical Science, 15(2), 458-465.
- Wang, H., Wang, Y., Xu, W., Zhang, H., Lv, J., Wang, X., Zheng, Z., Zhao, Y., Yu, L., Yuan, Q. & Gao, L. (2023b). Host–guest-interaction enhanced nitric oxide photo-generation within a pillar [5] arene cavity for antibacterial gas therapy. ACS Applied Materials & Interfaces, 15(47), 54266-54279.
- Wang, H., Yan, Y. Q., Yi, Y., Wei, Z. Y., Chen, H., Xu, J. F., Wang, H., Zhao, Y. & Zhang, X. (2020). Supramolecular peptide therapeutics: Host–guest interaction-assisted systemic delivery of anticancer peptides. CCS Chemistry, 2(6), 739-748.
- Wang, J., Battini, N., Ansari, M. F., & Zhou, C. H. (2021). Synthesis and biological evaluation of quinazolonethiazoles as new potential conquerors towards *Pseudomonas aeruginosa*. Chinese Journal of Chemistry, 39(5), 1093-1103.
- Wang, S., Li, W., Wang, Z., Yang, W., Li, E., Xia, X., Yan, F., & Chiu, S. (2024a). Emerging and reemerging infectious diseases: Global trends and new strategies for their prevention and control. Signal Transduction and Targeted Therapy, 9(1), 223.
- Wang, Y., Zhang, L., Yuan, X., & Wang, D. (2023a). Treatment with paeoniflorin increases lifespan of *Pseudomonas aeruginosa* infected *Caenorhabditis elegans* by inhibiting bacterial accumulation in intestinal lumen and biofilm formation. Frontiers in Pharmacology, 14, 1114219.

- Webber, M. J., & Langer, R. (2017). Drug delivery by supramolecular design. Chemical Society Reviews, 46
- Weber, D. J., Rutala, W. A., Anderson, D. J., & Sickbert-Bennett, E. E. (2023). Biofilms on medical instruments and surfaces: Do they interfere with instrument reprocessing and surface disinfection. American Journal of Infection Control, 51(11, Supplement), A114-A119.
- Williamson, D. A., Carter, G. P., & Howden, B. P. (2017). Current and emerging topical antibacterials and antiseptics: Agents, action, and resistance patterns. Clinical Microbiology Reviews, 30, 827-860.
- Wolcott, R. D., Rumbaugh, K. P., James, G., Schultz, G., Phillips, P., Yang, Q., Watters, C., Stewart, P. S., & Dowd, S. E. (2010). Biofilm maturity studies indicate sharp debridement opens a time-dependent therapeutic window. Journal of Wound Care, 19(8), 320-328.
- Wong, V. W. Y., Huang, Y., Wei, W. I., Wong, S. Y. S., & Kwok, K. O. (2022). Approaches to multidrug-resistant organism prevention and control in long-term care facilities for older people: A systematic review and meta-analysis. Antimicrobial Resistance & Infection Control, 11(1), 7.
- Woo, K., Dowsett, C., Costa, B., Ebohon, S., Woodmansey, E. J., & Malone, M. (2021). Efficacy of topical cadexomer iodine treatment in chronic wounds: Systematic review and meta-analysis of comparative clinical trials. International Wound Journal, 18, 586-597.
- World Health Organization. (2016). Global guidelines for the prevention of surgical site infection. World Health Organization.
- Wörner, J., Moelleken, M., Dissemond, J., & Pein-Hackelbusch, M. (2023). Supporting wound infection diagnosis: Advancements and challenges with electronic noses. Frontiers in Sensors, 4, 1250756.
- Wu, Y. K., Cheng, N. C., & Cheng, C. M. (2019). Biofilms in chronic wounds: pathogenesis and diagnosis. Trends in biotechnology, 37(5), 505-517.

- Xie, X., Gao, B., Ma, Z., Liu, J., Zhang, J., Liang, J., Chen, Z., Wu, L. & Li, W. (2021). Host–guest interaction driven peptide assembly into photoresponsive two-dimensional nanosheets with switchable antibacterial activity. CCS Chemistry, 3(7), 1949-1962.
- Xing Ma and Yanli Zhao (2015). Biomedical applications of supramolecular systems based on host-guest interactions. Chemical Reviews, 115(15), Article 7794-7839.
- Yaacoub, S., Truppa, C., Pedersen, T. I., Abdo, H., & Rossi, R. (2022). Antibiotic resistance among bacteria isolated from war-wounded patients at the weapon traumatology training center of the international committee of the redcross from 2016 to 2019: A secondary analysis of WHONET surveillance data. BMC Infectious Diseases, 22(1), 257.
- Yang, H., Zhao, D., Wang, S., Yang, L., Huang, J., Zhang, Z., & Li, S. (2023). A study on the antibacterial activity and antimicrobial resistance of pyridinium cationic pillar[5]arene against *Staphylococcus aureus* and *Escherichia coli*. International Microbiology, 26(1), 59-68.
- Yang, W., Zhang, W., Chen, J., & Zhou, J. (2024a). Mono-functionalized pillar[n]arenes: Syntheses, host–guest properties and applications. Chinese Chemical Letters, 35(1), 108740.
- Yang, Y., Li, P., Feng, H., Zeng, R., Li, S., & Zhang, Q. (2024b). Macrocycle-Based Supramolecular Drug Delivery Systems: A Concise Review. Molecules, 29(16), 3828.
- Yassin, A., Huralska, M., Pogue, J. M., Dixit, D., Sawyer, R. G., & Kaye, K. S. (2023). State of the management of infections caused by multidrug-resistant gram-negative organisms. Clinical Infectious Diseases, 77(9), e46-e56.

- Zakharova, L. Y., Maganova, F. I., Sinyashin, K. O., Gaynanova, G. A., Mirgorodskaya, A. B., Vasilieva, E. A., & Sinyashin, O. G. (2023). Supramolecular strategy for the design of nanocarriers for drugs and natural bioactives: current state of the art (a review). Russian Journal of General Chemistry, 93(7), 1867-1899.
- Zakhour, J., Sharara, S. L., Hindy, J. R., Haddad, S. F., & Kanj, S. S. (2022). Antimicrobial treatment of *Pseudomonas aeruginosa* severe sepsis. Antibiotics, 11(10), 1432.
- Zegadło, K., Gieroń, M., Żarnowiec, P., Durlik-Popińska, K., Kręcisz, B., Kaca, W., & Czerwonka, G. (2023). Bacterial motility and its role in skin and wound infections. International Journal of Molecular Sciences, 24(2), 1707.
- Zhang, G.-F., Liu, X., Zhang, S., Pan, B., & Liu, M.L. (2018). Ciprofloxacin derivatives and their antibacterial activities. European Journal of Medicinal Chemistry, 146, 599-612.
- Zhang, M., Feng, H., Gao, Y., Gao, X., & Ji, Z. (2023). Effect of topical antibiotics on the prevention and management of wound infections: A meta-analysis. International Wound Journal, 20(10), 4015-4022.
- Zhang, Y., Ma, M., Chen, L., Du, X., Meng, Z., Zhang, H., Zheng, Z., Chen, J. & Meng, Q. (2022). A Biocompatible Liquid Pillar [n] arene-Based Drug Reservoir for Topical Drug Delivery. Pharmaceutics, 14(12), 2621.
- Zhao, A., Sun, J., & Liu, Y. (2023). Understanding bacterial biofilms: From definition to treatment strategies. Frontiers in Cellular and Infection Microbiology, 13, 1137947.
- Zhou, C., Wang, Q., Jin, L., Wang, R., Yin, Y., Sun, S., Zhang, J. & Wang, H. (2020). *In vitro* synergistic activity of antimicrobial combinations against BLA KPC and bla NDM-Producing *Enterobacterales* with BLA IMP or mcr genes. Frontiers in Microbiology, 11, 533209.

- Zhou, L., Chen, Y., Yang, J., Duan, Y., Gong, H., Ye, H., Hong, Y., Liu, M., Hao, G., Du, F. & Wang, P. (2024). An Eco-friendly β-cyclodextrin/Stilbene-Integrated supramolecular material Realizes the effective treatment of bacterial diseases via enhancing the biofilm eradication and Agrochemical bioavailability. Chemical Engineering Journal, 500, 157282.
- Zhu, Y., Escorihuela, J., Wang, H., Sue, A. C. H., & Zuilhof, H. (2023). Tunable supramolecular Ag+-host interactions in pillar[n]arene[m]quinones and ensuing specific binding to 1-alkynes. Molecules, 28(20), 7009.
- Zuilhof, H., Sue, A. C. H., & Escorihuela, J. (2021). On the stability and formation of pillar [n] arenes: A DFT study. The Journal of Organic Chemistry, 86(21), 14956-14963.
- Zyryanov, G. V., Kopchuk, D. S., Kovalev, I. S., Santra, S., Majee, A., & Ranu, B. C. (2023). Pillar arenes as promising carriers for drug delivery. International Journal of Molecular Sciences, 24(6), 5167.

Appendices

APPENDICES

Appendix 1

Evaluation of pharmacokinetic profile of selected hosts and guests by pkCSM

(http://biosig.unimelb.edu.au/pkcsm/prediction#)

Principle

The pharmacokinetic properties of any compound are crucial in developing them into as lead compounds or drugs. pkCSM is a web tool that can be widely used to determine the pharmacokinetic parameters (Absorption, Distribution, Metabolism, Excretion and Toxicity) of small molecules using SMILES (Simplified Molecular Input Line Entry Specification) of the particular compound.

Water Solubility

The water solubility of a compound (logS) reflects the solubility of the molecule in water at 25ºC. Lipid- soluble drugs are less well absorbed than water-soluble ones, especially when they are enteral. This model is built using experimental water solubility measurements of 1,708 molecules.

Results Interpretation

The predicted water solubility of a compound is given as the logarithm of the molar concentration (log mol/L).

Caco-2 Permeability

The Caco-2 cell line is composed of human epithelial colorectal adenocarcinoma cells. The Caco-2 monolayer of cells is widely used as an in vitro model of the human intestinal mucosa to predict the absorption of orally administered drugs. This model is based on 674 drug like molecules with Caco-2 permeability values and predicts the logarithm of the apparent permeability coefficient (log Papp; log cm/s).

Results Interpretation

A compound is considered to have a high Caco-2 permeability if it has a Papp > 8 x 10-6 cm/s. For the pkCSM predictive model, high Caco-2 permeability would translate in predicted values > 0.90.

Intestinal Absorption (Human)

The Intestine is normally the primary site for absorption of a drug from an orally administered solution. This method is built to predict the proportion of compounds that were absorbed through the human small intestine.

Results Interpretation

For a given compound it predicts the percentage that will be absorbed through the human intestine. A molecule with an absorbance of less than 30% is considered to be poorly absorbed.

Skin Permeability

Skin permeability is a significant consideration for many consumer products efficacy, and of interest for the development of transdermal drug delivery. This predictor was built using 211 compounds whose in vitro human skin permeability has been measured

Results Interpretation

It predicts whether if given compound is likely to be skin permeable, expressed as the skin permeability constant logKp (cm/h). A compound is considered to have a relatively low skin permeability if it has a logKp > -2.5.

P-glycoprotein substrate

The P-glycoprotein is an ATP-binding cassette (ABC) transporter. It functions as a biological barrier by extruding toxins and xenobiotics out of cells. P-glycoprotein transport screening is performed using transgenic mdr knockout mice and *in vitro* cell systems. This model was built using 332 compounds that have been characterised for their ability to be transported by Pgp.

Results Interpretation

The model predicts whether a given compound is likely to be a substrate of Pgp or not.

P-glycoprotein I and II inhibitors

Modulation of P-glycoprotein mediated transport has significant pharmacokinetic implications for Pgp substrates, which may either be exploited for specific therapeutic advantages or result in contraindications. This predictive models were built using 1,273 and 1,275 compounds that have been characterised for their ability to inhibit P-glycoprotein I and P-glycoprotein II transport, respectively.

Results Interpretation

The predictor will determine whether a given compound is likely to be a P-glycoprotein I/II inhibitor.

VDss (Human)

The steady state volume of distribution (VDss) is the theoretical volume that the total dose of a drug would need to be uniformly distributed to give the same concentration as in blood plasma. The higher the VD is, the more of a drug is distributed in tissue rather than plasma. It can be affected by renal failure and dehydration. This predictive model was built using the calculated steady state volume of distribution (VDss) in humans from 670 drugs. The predicted logarithm of VDss of a given compound is given as the log L/kg.

Results Interpretation

VDss is considered low if below 0.71 L/kg (log VDss < -0.15) and high if above 2.81 L/kg (log VDss > 0.45).

Fraction Unbound (Human)

Most drugs in plasma will exist in equilibrium between either an unbound state or bound to serum proteins. The efficacy of a given drug may be affected by the degree to which it binds proteins within blood, as the more that is bound the

less efficiently it can traverse cellular membranes or diffuse. This predictive model was built using the measured free proportion of 552 compounds in human blood (Fu).

Results Interpretation

For a given compound, the predicted fraction that would be unbound in plasma will be calculated.

Blood Brain Barrier permeability

The brain is protected from exogenous compounds by the blood-brain barrier (BBB). The ability of a drug to cross into the brain is an important parameter to consider, that helps to reduce side effects and toxicities or to improve the efficacy of drugs whose pharmacological activity is within the brain. Blood-brain permeability is measured *in vivo* in animal models as logBB, the logarithmic ratio of brain to plasma drug concentrations. This predictive model was built using 320 compounds whose logBB has been experimentally measured.

Results Interpretation

For a given compound, a logBB > 0.3 is considered as readily cross the blood-brain barrier while molecules with logBB < −1 are considered as poorly distributed to the brain.

CNS permeability

Measuring blood brain permeability is difficult with confounding factors. The blood-brain permeability- surface area product (logPS) is a more direct measurement. It is obtained from in situ brain perfusions with the compound directly injected into the carotid artery. This lacks the systemic distribution effects which may distort brain penetration. This predictive model was built using 153 compounds whose logPS has been experimentally measured.

Results Interpretation

Compounds with a logPS > -2 are considered to penetrate the Central Nervous System (CNS), while those with logPS < -3 are considered as unable to penetrate the CNS.

CYP2D6/CYP3A4 substrate

The cytochrome P450's are responsible for metabolism of many drugs. However, inhibitors of the P450's can dramatically alter the pharmacokinetics of these drugs. It is therefore important to assess whether a given compound is likely to be a cytochrome P450 substrate. The two main isoforms responsible for drug metabolism are 2D6 and 3A4. These models were built using 671 compounds whose metabolism by each cytochrome P450 isoform has been measured.

Results Interpretation

The predictor will assess whether a given molecule is likely to be metabolised by either P450.

Cytochrome P450 inhibitors

Cytochrome P450 is an important detoxification enzyme in the body, mainly found in the liver. It oxidises xenobiotics to facilitate their excretion. Many drugs are deactivated by the cytochrome P450's, and some can be activated by it. Inhibitors of this enzyme, such as grapefruit juice, can affect drug metabolism and are contraindicated. It is therefore important to assess a compound's ability to inhibit the cytochrome P450. Models for different isoforms were built (CYP1A2/CYP2C19/CYP2C9/CYP2D6/CYP3A4) using from over 14000 to 18000 compounds whose ability to inhibit the cytochrome P450 has been determined. A compound is considered to be a cytochrome P450 inhibitor if the concentration leads to 50% inhibition and is less than 10 uM.

Results Interpretation

The predictors will assess whether a given molecule is likely going to be a cytochrome P450 inhibitor, for a given isoform.

Total Clearance

Drug clearance is measured by the proportionality constant CLtot, and occurs primarily as a combination of hepatic clearance (metabolism in the liver and biliary clearance) and renal clearance (excretion via the kidneys). It is related to bioavailability, and is important for determining dosing rates to achieve steady-

state concentrations. This predictor was built using the total clearance data for 398 compounds.

Results Interpretation

The predicted total clearance log(CLtot) of a given compound is given in log(ml/min/kg).

Renal OCT2 substrate

Organic Cation Transporter 2 is a renal uptake transporter that plays an important role in disposition and renal clearance of drugs and endogenous compounds. OCT2 substrates also have the potential for adverse interactions with coadministered OCT2 inhibitors. Assessing a candidate's potential to be transported by OCT2 provides useful information regarding not only its clearance but potential contraindications. This model was built using 906 compounds whose transport by OCT2 has been experimentally measured.

Results Interpretation

The predictor will assess whether a given molecule is likely to be an OCT2 substrate.

AMES toxicity

The Ames test is a widely employed method to assess a compounds mutagenic potential using bacteria. A positive test indicates that the compound is mutagenic and therefore may act as a carcinogen. This predictive model was built on the results of over 8,000 compounds Ames tests.

Results Interpretation

It predicts whether a given compound is likely to be Ames positive and hence mutagenic.

Maximum Tolerated Dose (Human)

The maximum recommended tolerated dose (MRTD) provides an estimate of the toxic dose threshold of chemicals in humans. The model is trained using 1222 experimental data points from human clinical trials and predicts the logarithm

of the MRTD (log mg/kg/day). This will help guide the maximum recommended starting dose for pharmaceuticals in phase I clinical trials, which are currently based on extrapolations from animal data.

Results Interpretation

For a given compound, a MRTD of less than or equal to 0.477 log(mg/kg/day) is considered low, and high if greater than 0.477 log(mg/kg/day).

hERG I and II Inhibitors

Inhibition of the potassium channels encoded by hERG (human ether-a-go-go gene) are the principal causes for the development of acquire long QT syndrome - leading to fatal ventricular arrhythmia. Inhibition of hERG channels has resulted in the withdrawal of many substances from the pharmaceutical market. These predictors were built using hERG I and II inhibition information for 368 and 806 compounds, respectively.

Results Interpretation

The predictor will determine if a given compound is likely to be a hERG I/II inhibitor.

Oral Rat Acute Toxicity (LD50)

It is important to consider the toxic potency of a potential compound. The lethal dosage values (LD50) are a standard measurement of acute toxicity used to assess the relative toxicity of different molecules. The LD50 is the amount of a compound given all at once that causes the death of 50% of a group of test animals.

Results Interpretation

The model was built on over 10000 compounds tested in rats and predicts the LD50 (in mol/kg).

Oral Rat Chronic Toxicity

Exposure to low-moderate doses of chemicals over long periods of time is of significant concern in many treatment strategies. Chronic studies aim to identify the lowest dose of a compound that results in an observed adverse effect (LOAEL), and the highest dose at which no adverse effects are observed (NOAEL). This predictor was built using the LOAEL results from 445 compounds.

Results Interpretation

For a given compound, the predicted log Lowest Observed Adverse Effect (LOAEL) in log(mg/kg_bw/day) will be generated. The LOAEL results need to be interpreted relative to the bioactive concentration and treatment lengths required.

Hepatotoxicity

Drug-induced liver injury is a major safety concern for drug development and a significant cause of drug attrition. This predictor was built using the liver associated side effects of 531 compounds observed in humans. A compound was identified as hepatotoxic if it had at least one pathological or physiological liver event which is strongly associated with disrupted normal function of the liver.

Results Interpretation

It predicts whether a given compound is likely to be associated with disrupted normal function of the liver.

Skin Sensitisation

Skin sensitisation is a potential adverse effect for dermally applied products. The evaluation of whether a compound, that may encountered the skin, can induce allergic contact dermatitis is an important safety concern. This predictor was built using 254 compounds which have been evaluated for their ability to induce skin sensitisation.

Results Interpretation

It predicts whether a given compound is likely to be associated with skin sensitisation.

T. Pryiformis toxicity

T. Pyriformis is a protozoa bacterium, with its toxicity often used as a toxic endpoint. This method was built using the concentration of 1,571 compounds required to inhibit 50% of growth (IGC50).

Results Interpretation

For a given compound, the pIGC50 (negative logarithm of the concentration required to inhibit 50% growth in log ug/L) is predicted, with a value > -0.5 log ug/L is considered as toxic.

Minnow toxicity

The lethal concentration values (LC50) represent the concentration of a molecule necessary to cause the death of 50% of the Flathead Minnows. This predictive model was built on LC50 measurements for 554 compounds.

Results Interpretation

For a given compound, a log LC50 will be predicted. LC50 values below 0.5 mM (log LC50 < -0.3) are regarded as high acute toxicity.

Appendix 2

Characterization of host-guest complexation by ^{1}H NMR spectroscopy

Host-guest complexation between P[5]A and isatin

The NMR titration experiments were conducted as follows:

Preparation of Solutions: A stock solution of decamethoxypillar[5]arene (P[5]A) was prepared in a deuterated solvent $CDCl_3$. The concentration of P[5]A was adjusted to 8 mM by dissolving 3 mg of P[5]A in 0.5 ml of $CDCl_3$. A stock solution of 81.6 mM isatin was prepared in deuterated acetone by dissolving 6 mg of isatin in 0.5 ml of acetone-d_6.

Titration with Isatin: Various equivalents of Isatin were added to the P[5]A stock solution. The molar ratio of P[5]A to Isatin ranged from 0.2 to 2.0. Each addition of Isatin was carefully measured to achieve the desired ratio. After adding each aliquot of isatin, the sample was carefully shaken to ensure thorough mixing and homogenization of the host and guest molecules. The sample was shaken carefully after each addition and ^{1}H-NMR spectra were recorded at 25°C.

Host-guest complexation between BEA and isatin

The ^{1}H NMR titration experiment was performed as follows:

Preparation of isatin Solution: 6 mg of isatin was accurately weighed and dissolved in 0.5 mL of deuterated acetone (acetone-d_6) in a vial. This resulted in the preparation of an 81 mM solution of isatin.

Preparation of BEA Solution: Separately, 2 mg of BEA was accurately weighed and dissolved in 0.5 mL of acetone-d_6 in a separate NMR tube. This led to the preparation of a 4.8 mM solution of BEA.

NMR Titration with isatin: The ^{1}H NMR titration experiments were conducted by sequentially adding 10 µL aliquots of the 81 mM isatin solution to a 4.8 mM solution of BEA in the NMR tube. Each addition of isatin introduced incremental changes in the concentration of the guest molecule. After the addition of each aliquot of isatin, the sample was carefully shaken to ensure thorough mixing and

homogenization of the host (BEA) and guest (isatin) molecules. This ensured that the host-guest complexes formed uniformly throughout the solution. ^{1}H-NMR spectra were recorded at a constant temperature of 25°C after each addition of isatin. These spectra provided information about the chemical shifts and peak intensities of the resonances, allowing for the monitoring of host-guest interactions and the formation of inclusion complexes.

Appendix 3

Assessment of binding constant of synthesized pillar[n]arenes-isatin inclusion complexes by the WINEQNMR2 program

Binding constants were estimated from the ^{1}H NMR titration experiments using the WINEQNMR2 program. In the WinEQNMR2 computer program, observed chemical shift values and the concentrations of host and guest molecules of every titration experiment were entered. In addition, data of expected binding stoichiometry, limiting chemical shifts and estimates of binding constants were given in the program for refinement. The given parameters were refined by non-linear least square analysis until the best fit was observed between the calculated and observed chemical shift values. The accuracy of the results was analyzed by the plots of observed chemical shifts versus the concentration of guests. The input values were varied until the best-fit is obtained for the stability constants, and their errors converged.

The fitplot generated from the WINEQNMR2 program is derived based on the experimental data obtained from the ^{1}H NMR titration experiments. The WINEQNMR2 program takes as input the experimental ^{1}H NMR titration data, which includes the chemical shifts of the host and guest resonances at different molar ratios or concentrations. The user specifies the appropriate binding model or equilibrium model to fit the experimental data. This model may include different types of host-guest interactions, such as 1:1 stoichiometry, 1:2 stoichiometry, or other more complex binding equilibria. The program fits the selected model to the experimental data by estimating the parameters associated with the binding equilibrium, such as the association constant (K) and the stoichiometry of the complex. Using the input data and the specified model, the program performs curve fitting to generate theoretical binding curves or isotherms. These curves represent the expected changes in the chemical shifts of the host and guest resonances as a function of the molar ratio or concentration of the host and guest.

The fitplot is then generated based on the results of the curve fitting process. It typically consists of overlaid experimental data points (such as

chemical shifts) and the corresponding theoretical curves obtained from the fitted model. The fitplot allows for visual comparison between the experimental data and the model predictions, enabling the assessment of the goodness-of-fit and the validity of the chosen binding model.

The fitplot is analyzed to evaluate the quality of the fit and to extract relevant parameters, such as the association constant and stoichiometry of the host-guest complex. Any discrepancies between the experimental data and the theoretical curves may indicate limitations of the selected model or experimental factors that need to be considered.

Appendix 4

Determination of host-guest chemistry in the synthesized pillar[n]arenes-isatin inclusion complexes by UV-visible spectroscopy

Host-guest complexation between P[5]A and isatin

The UV-visible titration experiment was performed as follows:

Preparation of Solutions: A series of solutions containing decamethoxypillar[5]arene (P[5]A) and isatin were prepared in dimethyl sulfoxide (DMSO). The concentrations of both P[5]A and isatin were set to 1×10^{-4} M each. This ensured a constant total concentration of the host-guest components in the solution.

UV-visible Spectroscopy Setup: The instrument was configured to scan the wavelength range of interest, typically in the UV-visible region. This allowed for the detection of electronic transitions and absorbance changes, which are indicative of host-guest complexation.

Investigation of Host-Guest Complexation: Varying concentrations of isatin were added to the solution of P[5]A in DMSO. The volume ratio of the host (P[5]A) solution to the guest (isatin) solution ranged from 0.5:4.5 to 4.5:0.5. Importantly, the total concentration of both P[5]A and isatin was kept constant at 1×10^{-4} M throughout the experiment.

Spectroscopic Analysis: UV-visible spectra were recorded for each solution after the addition of isatin. Changes in absorbance and electronic transitions were monitored as indicators of host-guest complexation.

Data Interpretation: The obtained spectra were analyzed to assess the occurrence and extent of host-guest complexation. Changes in absorbance intensities and spectral features were correlated with the formation of inclusion complexes between P[5]A and isatin.

Host-guest complexation between BEA and isatin

The UV-visible titration experiment was conducted as follows:

Preparation of BEA Solution: A solution of BEA at a concentration of 1×10^{-4} M was prepared in dimethyl sulfoxide (DMSO). This solution served as the host for the isatin guest during the titration experiment.

Titration with Isatin: Aliquots of isatin were added to the 1×10^{-4} M BEA solution, with varying equivalents ranging from 0.2 to 5. Each addition introduced incremental changes in the concentration of the isatin guest while maintaining a constant concentration of BEA.

UV-visible Spectroscopy: After each addition of isatin to the BEA solution, UV-visible spectra were recorded using a spectrophotometer. These spectra captured the absorption patterns and absorbance changes corresponding to the host-guest complexation between BEA and isatin.

Analysis of UV-visible Data: The UV-visible spectra data were analyzed to determine the changes in absorbance and peak shifts upon complex formation. The interaction between BEA and isatin was assessed based on the observed spectral changes, including shifts in absorbance peaks and changes in absorbance intensities.

Appendix 5

Antibacterial efficacy of pillar[5]arene-isatin inclusion complexes by Agar well diffusion method

(CLSI, 2012)

Principle

Agar plates are inoculated with a standardized inoculum of the bacteria and an antimicrobial disk/well is placed on the inoculated agar plate. The well/disk contains the standardized known amount of an antimicrobial agent, which diffuses into the agar when in contact with the agar surface. The plate is incubated under standardized conditions following Clinical and Laboratory Standards Institute (CLSI) guidelines. During incubation, the antimicrobial agent diffuses into the agar and inhibits the growth of the bacteria, producing a “zone of inhibition” around the disk. Following incubation, the diameter of this zone is measured and the results are interpreted as resistant, intermediate, or susceptible using standard guidelines.

Materials

- ✓ Bacterial strains (*Staphylococcus aureus*, *Bacillus subtilis* and *Pseudomonas aeruginosa*, *Klebsiella pneumoniae*, *Escherichia coli*, *Salmonella paratyphi* A)
- ✓ Nutrient agar
- ✓ Sterile saline solution

Procedure

Standardization of the bacterial inoculums

The inoculum standardization is an essential step for the accurate performance of the assay. Initially, the bacterial colonies (~ 4 to 5 colonies) from well-grown nutrient agar plates were carefully taken with the help of a sterile swab or loop. Then, the colonies were dispensed into the sterile saline solution. The turbidity of the bacteria inoculated solution was adjusted with 0.5 McFarland standard. In general, 0.5 McFarland is equal to ~10^8 CFU/mL.

Inoculation of Mueller-Hinton plate with bacterial inoculums and pillar[5]arene-isatin inclusion complexes

A sterile cotton swab was dipped into the standardized bacterial inoculums and it was introduced to the sterile media by swabbing method. Swabbing the culture on the media was performed several times by rotating the plates 60º each time to ensure uniformity. Homogeneous plating is an important parameter to yield reliable results. Followed by, ~6 mm wells were punched on the agar surface and 20 mM stock solutions of isatin, pillar[n]arenes, pillar[5]arene-isatin inclusion complexes and chloramphenicol (standard antibiotic) were added into the respective wells. The plates were incubated at 37ºC for 24 hours to observe the antimicrobial potential of the selected compounds in terms of zone of inhibition (diameter in mm).

Appendix 6

Determination of time kill kinetics of selected compounds against *Staphylococcus aureus* and *Pseudomonas aeruginosa*

Principle

The fundamental principle behind the time-kill kinetic study is to determine the rate at which a compound kills microorganisms based on survival data collected at sufficient exposure times. This allows for the plotting of a graph that models the population decline over time to the point of extinction.

Materials required

1. Luria Bertani (LB) agar

Yeast extract	-	5g
Tryptone	-	5g
Sodium chloride	-	5g
Agar	-	10g

Dissolved all the components in 1liter of distilled water and the final pH was adjusted to 7.2

2. Luria Bertani (LB) broth

Tryptone	-	10g
Sodium chloride	-	5g

Dissolved all the components in 1liter of distilled water and the final pH was adjusted to 7.2

Procedure

10 µl of overnight culture of selected bacterial pathogens were added to 1ml of culture medium to attain 1:100 dilution. Then, the culture was allowed to obtain the logarithmic stage cultures by keeping them in the shaker cum incubator. Then, the MICs of isatin, pillar[5]arene and pillar[5]arene-isatin inclusion

complexes were added to the log-phase cultures of bacteria. The treated and the control groups of bacterial pathogens were incubated at 37ºC with shaking. After that, 100µl of culture at different time intervals (0, 60, 120 and 180 minutes) from the treated and control tubes were plated on LB agar plates. The plates were incubated at 37ºC for 16-24 hours and then colonies were counted. The log CFU/ml value was calculated to plot the graph.

Appendix 7

Determination of cellular leakage of bacterial cell wall components (protein) treated with pillar[5]arene-isatin inclusion complexes by Lowry's method

(Lowry *et al.*, 1951)

Principle

The intensity of the blue colour developed by the reduction of phosphomolybdic and phosphotungstic components in the Folin-Ciocalteau reagent by the amino acids tyrosine and tryptophan present in the protein and the colour developed by the Biuret reaction of the protein with alkaline cupric tartarate are measured spectrophotometrically at 670nm.

Reagents

1. Solution A: 1% Copper Sulphate
2. Solution B: 2% Sodium Potassium Tartarate
3. Solution C: 2% Sodium Carbonate in 0.1N Sodium Hydroxide
4. Solution D: Mixed just before use, 1ml of solution A, 1ml of solution B and 100ml of solution C.
5. Solution E: Folin-Ciocalteau reagent (Mixed equal volumes of commercially available reagent and distilled water just prior to use). Stored and protected from light.
6. Standard BSA:
    a) Stock solution: A stock solution containing 50mg BSA in 50ml was prepared. 1ml of this solution contains 1mg of protein.
    b) Working standard: Diluted the stock solution in the ratio 1:10 for use as working standard.1 ml of this solution contains 100 µg of protein.

Procedure

The working standard solution (0.2 to 1.0ml) of BSA and the supernatant of treated and untreated *Staphylococcus aureus* and *Pseudomonas aeruginosa* were

taken into clean dry test tubes. The tubes were then made up to 1ml with 0.1N sodium hydroxide and shaken well to treat the protein with alkali. Then, 3 ml solution D was added, mixed well and incubated at 37°C for 3 minutes. Followed by, 0.3 ml solution E was added, mixed well and incubated at 37°C for 3 minutes again. The blue color developed was read at 670 nm against the reagent blank. The regression was performed to calculate the amount of protein released from the cell walls of treated and untreated bacteria.

Appendix 8

Determination of cellular leakage of bacterial cell wall components (glucose) treated with pillar[5]arene-isatin inclusion complexes by Anthrone method

(Ludwig and Goldberg, 1956)

Principle

Carbohydrates are dehydrated by conc.H_2SO_4 to form furfural. Active form of the reagent is anthranol, the enol tautomer of anthrone, which reacts by condensing with the carbohydrate furfural derivative to give a green colour in dilute and a blue colour in concentrated solutions, which is determined colorimetrically. The blue - green solution shows absorption maximum at 620 nm.

Reagents

1. Anthrone reagent: Dissolve 200mg anthrone in 100ml of ice- cold 95% Sulphuric acid. Prepare fresh before use.
2. Standard Glucose: Stock- Dissolve 100mg in 100ml distilled water. 1.0ml of this solution contains 1.0 mg of glucose.
3. Working Standard: 10ml of stock diluted to 100ml with distilled water. Store refrigerated after adding a few drops of toluene. 1.0ml of this solution contains 100µg of glucose.

Procedure

The working standard glucose solution ranging from 0.2 to 1.0 ml was pipetted out in a dry test tube. Similarly, the supernatant of treated and untreated bacterial pathogens was also taken into another clean & dry test tube. All the tubes were made up of 1 ml of distilled water. Following by, 4ml of anthrone reagent was added to all the tubes and heated for 8 minutes in a boiling water bath and allowed them to cool rapidly. The developed dark green colour was read at 630 nm against the reagent blank. The regression was performed to calculate the amount of glucose released from the cell walls of treated and untreated bacterial pathogens.

Appendix 9

Morphological characterization of pillar[5]arene-isatin inclusion complexes treated and untreated bacterial pathogens by SEM

(Shukla, 2015)

Principle

The scanning electron microscopy (SEM) method was used to examine the morphostructural changes in bacterial cells induced by antimicrobial compounds. The SEM-based visual approach has referred to the study of bacterial cells and their physiological consequences that have been affected by antibacterial agents permitting the observation of characteristic morphological defects of cell wall and biofilm communities and providing valuable insights into processes involved in bacterial cell death. This experiment visualized various step-by-step techniques used in the slide preparation of bacterial cells treated with specific antimicrobial agents. It is used for analyzing morphological alterations such as an increase of cell wall roughness, cell disruption, biofilm inhibition, cell swelling and lysed cell formation due to loss of intracellular material using SEM analysis when compared with untreated normal cells as a control. The SEM approach used in this visual experiment may analyze the antimicrobial effect of any commercially known or new compounds in a very conducive manner.

Reagents

- Bacterial culture broth (*Staphylococcus aureus* and *Pseudomonas aeruginosa*)
- Phosphate buffer solution 0.05 M (pH 7.4)
- Glutaraldehyde (2.5%)
- Ethanol (50%, 70%, 80%, 90%, 95% and 100%)

Procedure

Preparation of bacterial cell culture

Initially, inoculated 100 µl of bacterial stock cultures such as *Staphylococcus aureus* and *Pseudomonas aeruginosa* (approximately 10^7 CFU/mL) into the sterile nutrient broth (100 mL) under a laminar air flow hood. Then, the inoculated broth was incubated at 37ºC for 16-18 hours. Followed by, the pillar[5]arene-isatin inclusion complexes was added to the culture medium. Then, transfer 900 µl of bacterial culture in Eppendorf tubes for sample treatment as well as for control. Both the treated and untreated bacterial cultures were centrifuged at 3,000-4,000 rpm for 5 minutes. The supernatant was discarded and the pellet was washed using 1 mL of phosphate buffer solution 0.05 M (pH 7.4). The process of washing was repeated with the same buffer. Finally, the pellets of both treated and untreated bacterial cultures were collected separately.

Slide preparation for morphological analysis

The cultures were made as smear on the glass slided using micropipette tip ends. 2.5% glutaraldehyde was used as the fixative solution and placed at 4ºC overnight. The smear was washed with phosphate-buffered solution (0.05 M) for 1 min. Followed by, the smear was rehydrated and dehydrated using the gradient of ethanol 50%, 70%, 80%, 90%, 95% and 100% for each about 10 minutes. The slides were stored at -20ºC in the refrigerator.

Scanning electron microscopic instrumentation and analysis

The prepared slides were dried using liquid and gas CO_2 at temperatures ranging from 20-40ºC. After drying, the slides were mounted on a 10 or 25-mm copper cell. The slides on the coating machine (Hitachi W-1030) were placed to make a platinum coating on the slide. The coated slides were subjected to the field emission–scanning electron microscope. The images were observed by setting photo speed, contrast/ brightness and image size.

Appendix 10

Crystal violet method for the determination of biofilms inhibition and eradication profiles of selected compounds in *Staphylococcus aureus* and *Pseudomonas aeruginosa*

Principle

Biofilms are surface-attached microbial communities wherein microbial cells are embedded in self-produced extracellular polymeric substances. Biofilms cause severe problems in clinical as well as industrial settings. A bacterial biofilm is grown on the bottom of a microtiter plate which is stained using the crystal violet dye. The dye is retained by the biofilm, and the amount of biofilm can be estimated by measuring the absorbance of the dye at 540 nm.

Materials

- ✓ Tryptic soy broth
- ✓ Bacterial strains (*Staphylococcus aureus* and *Pseudomonas aeruginosa*)
- ✓ 0.1% Crystal violet dye
- ✓ Phosphate buffered saline
- ✓ Ethanol

Procedure

Initially, the bacterial inoculums (*Staphylococcus aureus* and *Pseudomonas aeruginosa*) were incubated with sub-inhibitory concentrations of isatin, pillar[5]arene and pillar[5]arene-isatin inclusion complexes. After incubation of *Staphylococcus aureus* and *Pseudomonas aeruginosa* with the different sub-MICs of selected compounds, supernatants in terms of planktonic cells were carefully removed. Then, it was rinsed thrice with phosphate-buffered saline (PBS) and 200 µl of methanol was added to fix the biofilm for 15 minutes. Following, 200 µl of crystal violet (CV) solution (0.1%) was added and maintained for 5 min. The CV solution was removed, and each well was gently washed with distilled water multiple times. Then, 200µl of ethanol was added and incubated for 30 minutes.

The absorbance value was read at 495 nm using a microplate reader. The percentage of biofilm inhibition and eradication was calculated using the formula as follows:

% Biofilm inhibition/eradication = 100−(OD_{570} sample/ OD_{570} control × 100)

OD_{570} sample = OD value of bacteria treated with the compounds

OD_{570} control = OD value of untreated bacteria

Appendix 11

Validation of drug release mechanisms using mathematical models

Zero order model

According to the principles of pharmacokinetics, drug release from the dosage form can be represented by the equation: $C_{-} = C_0 + K_0 t$; Where, C_t – the amount of drug released at time t; C_0 - initial concentration of drug at time t=0; K_0- zero-order rate constant. Thus, zero-order kinetics defines the process of constant drug release from a drug delivery system. Hence to study the drug release kinetics data obtained from *in vitro* dissolution study was plotted against time i.e., cumulative drug release vs. time. Hence the slope of the above plot gives the zero-order rate constant and the correlation coefficient of the above plot will give information on whether the drug release follows zero-order kinetics or not.

First order model

First-order kinetics of drug release profile can be represented by the following equation: DC/dt=-K1C. Where K1 is the first order rate constant, expressed in time-1 or per hour. Hence it can be defined as that in first order process, the rate is directly proportional to the concentration of the drug undergoing reaction i.e., the greater the concentration faster the reaction. Hence, it follows linear kinetics. After rearranging and integrating the equation, log C=log C_0 -K_1 t/2.303, where, K_1 – first-order rate equation expressed in time-1 or per hour, C_0 is the initial concentration of the drug, C is the percent of drug remaining at time t Hence to study the drug release kinetics data obtained from in vitro dissolution study is plotted against time i.e., log % of drug remaining vs. time and the slope of the plot gives the first order rate constant. The correlation coefficient of the plot will give information on whether the drug release follows first-order kinetics or not.

Higuchi model

The release of a drug from a drug delivery system (DDS) involves both dissolution and diffusion. Several mathematical equations models describe drug dissolution and/or release from DDS. In the modern era of controlled-release oral

formulations, ‘The Higuchi equation’ has become a prominent kinetic equation in its own right, as evidenced by employing drug dissolution studies that are recognized as an important element in drug delivery development. The Higuchi equation is considered one of the most widely used and most well-known controlled-release equations. The Higuchi equation can be represented in the simplified form Q=KH × t1/2; where, KH - Higuchi dissolution constant; Q – the cumulative amount of drug released in time t per unit area. Therefore the data obtained from the *in vitro* drug release study can be plotted as a cumulative percentage of drug release versus the square root of time. Hence if the correlation coefficient is higher for the above plot then we can interpret that the prime mechanism of drug release is a diffusion-controlled release mechanism.

Korsmeyer-Peppas model

To understand the dissolution mechanisms from the matrix, the release data were fitted using the well-known empirical equation proposed by Korsmeyer and Peppas. Korsmeyer and Peppas put forth a simple relationship described as the drug release from a polymeric system following which type of dissolution and represented by the following equation: log(Mt/M∞)=log Kkp+nlog t; Where Mt – the amount of drug released in time t; M∞ - the amount of drug released after time ∞; n- diffusional exponent or drug release exponent; Kkp - Korsmeyer release rate constant To study release kinetics, a graph is plotted between log cumulative % drug release vs. log time. Hence, the n value is used to characterize different release mechanisms.

Appendix 12

Constituents in the preparation of wound healing ointment loaded with pillar[5]arene-isatin inclusion complexes

(Belachew *et al*., 2020)

The process of wound healing is a very complex phenomenon where the skin or the affected organ after injury repairs itself. World Health Organization (WHO), as well as India, has been promoting the use of traditional medicine because they are less expensive, easily available and strong belief among the community in developing countries. In this regard, the active phytoconstituent of *Couroupita guianensis* was incorporated as a guest molecule into the host supramolecular system. This was further formulated as wound healing ointment and the base compositions are given as follows:

Formulation of ointment base

S. No.	Name of ingredient	Quantity
1.	Wool fat	0.5gm
2.	Cetostearyl alcohol	0.5gm
3.	Hard paraffin	0.5gm
4.	Yellow soft paraffin	8.5gm

Composition of developed wound healing ointment

S. No.	Name of ingredient	Quantity
1.	Pillar(5)arene	75mg
2.	Isatin	15mg
3.	Ointment base q.s.	10gm

The wound healing ointment was prepared by weighing all the constituents according to computation using the fusion method. Initially, the hard paraffin and cetostearyl alcohol were melted by placing them in an evaporating dish on a water

bath. To this melted form, add wool fat along with white soft paraffin and then stir effectively for complete melting of all components. After completion of the melting process, all the constituents strain the contents into another hot dish to remove impurities. Stir the mixtures completely, until they become cooled and a circumfluous base is attained. Then, the pillar[5]arene-isatin inclusion complex was mixed with the ointment base to prepare a smooth paste with 2 or 3 times its weight of base, gradually incorporating further bases until it forms a homogeneous ointment. After that, the prepared wound healing ointment with pillar[5]arene-isatin inclusion complex was transferred to a suitable vessel.

Appendix 13

Determination of cytotoxicity of pillar[5]arene-isatin inclusion complexes based ointment by MTT assay

(Igarashi and Miyazawa, 2001)

Principle

MTT is a water-soluble tetrazolium salt that is reduced by metabolically viable cells to a coloured water insoluble formazan salt. Live cells convert MTT into its formazan derivative, the number of surviving cells can be determined by the amount of MTT formazan produced, which is measured in a microtiter plate reader.

Reagent

1. PBS (Phosphate Buffer Saline) – pH-7.4
2. MTT-3mg/ml in PBS
3. Isopropanol in 0.04N HCl (acid-propanol)

Procedure

The pillar[5]arene-isatin inclusion complexes based wound healing ointment treated and untreated PBL cells were centrifuged. The supernatant was removed and then incubated with 50µl of MTT at 37ºC for 3 hours. After incubation, 200µl of PBS was added to all tests and the liquid was then carefully aspirated. Acid propanol of 200µl was added and left overnight in the dark. The absorbance was read at 650nm in a micro titre plate reader (Anthos 2020, Australia). The optical density of the control cells was fixed to be 100% viable and the percent viability of the cells in the treatment groups were calculated using the formula,

$$\% \text{ Viability} = \frac{(\text{Control OD} - \text{Sample OD})}{\text{Control OD}} \times 100$$

Annexure

भारत सरकार
विज्ञान और प्रौद्योगिकी मंत्रालय
जैव प्रौद्योगिकी विभाग
GOVERNMENT OF INDIA
MINISTRY OF SCIENCE & TECHNOLOGY
DEPARTMENT OF BIOTECHNOLOGY

सत्यमेव जयते

स्वच्छ भारत
एक कदम स्वच्छता की ओर

ब्लॉक-2, 7वां तल, सी0जी0ओ0 कॉम्पलैक्स
लोधी रोड, नई दिल्ली-110003
Block-2, 7th Floor, C.G.O. Complex
Lodhi Road, New Delhi-110003
Tele : 011-24365071 Fax : 011-24362884
Website : http://www.dbtindia.nic.in

No. BT/IBKP/684/2023 **Dated: 13.11.2024**

To

Dr. Kavitha Dhandapani
Assistant Professor (SS)
Avinashilingam Institute for Home Science and Higher Education for Women (Deemed to be University)
Department of Biochemistry, Biotechnology and Bioinformatics
Coimbatore - 641043, Tamil Nadu
Email: - kavitha_bio@avinuty.ac.in

Subject: Application submitted by Avinashilingam Institute for Home Science and Higher Education for Women, Coimbatore, for the information and records of Review Committee on Genetic Manipulation (RCGM) to carry out research and development work on inhibitory potential of Pillar[5]arene (P[5]A) derivatives and Isatin against clinical pathogens (*Staphylococcus aureus* and *Pseudomonas aeruginosa*). (BioRRAP ID: AVI26512024) (IBKP UAC No.: AVIRDIP50236)

Sir/Madam,

It is informed that the application to carry out research and development work on inhibitory potential of Pillar[5]arene (P[5]A) derivatives and Isatin against clinical pathogens (*Staphylococcus aureus* and *Pseudomonas aeruginosa*) was considered and noted by the Review Committee on Genetic Manipulation (RCGM) in its 296th meeting held on 30.10.2024.

2. You are required to comply with the '*Regulations and Guidelines for Recombinant DNA Research and Biocontainment, 2017*'.

Please acknowledge the receipt of the letter.

Yours faithfully,

(Dr. Nitin K. Jain)
Member Secretary, RCGM &
Scientist-'G', DBT

Publications

Avinashilingam Institute for HomeScience and Higher Education for Women

(Deemed to be University Estd. u/s 3 of UGC Act 1956, Category 'A' by MHRD
Re-accredited with A++ Grade by NAAC. CGPA 3.65/4, Category I by UGC
Coimbatore - 641 043, Tamil Nadu, India

Appendix L2
(Item No 5 of Check List)
Details of Research Publications

S.No	Article	Journal	Other Details Vol/No/Page No/ Year	Published in UGC CARE/ Scopus Indexed/ Web of Science
1	Antibacterial Potentials of Pillar[5]arene, pillar[4]arene[1]quinone derivative and their isatin inclusion complexes	Supramolecular Chemistry	33/12/ 701-708/ 2021	Scopus SCIE
2	Pillar[n]arenes in the fight against Biofilms: Current developments and future Perspectives	ACS Infectious Diseases	13/3/2024 Accepted	Scopus SCIE

*Proof of list of Journals from Internet to be attached along with copies of reprints.

Scholar : S. Jothinayaki

Supervisor : D. Kavitha

HoD

Checked By:

Dean of Respective School

The scholar miss. Jothinayaki, S (18PHBCP001) has published her articles in the following journals:

1. Supramolecular Chemistry - indexed & active in Scopus from 1992 to present,
2. ACS Infectious Diseases - indexed & active in Scopus from 2015 to present.

This may be considered.

J. Jothi
24.04.24

Both the journals are indexed and active in Scopus excel sheet.

This may be considered

24.06.2024

ACS Infectious Diseases

pubs.acs.org/journal/aidcbc

Review

Pillar[*n*]arenes in the Fight against Biofilms: Current Developments and Future Perspectives

Sekar Jothi Nayaki, Arivazhagan Roja, Ramya Ravindhiran, Karthiga Sivarajan, Murugan Arunachalam,* and Kavitha Dhandapani*

Cite This: https://doi.org/10.1021/acsinfecdis.3c00697

Read Online

ACCESS | Metrics & More | Article Recommendations

ABSTRACT: The global surge in bacterial infections, compounded by the alarming escalation of drug-resistant strains, has evolved into a critical public health crisis. Among the challenges posed, biofilms stand out due to their formidable resistance to conventional antibiotics. This review delves into the burgeoning potential of pillar[*n*]arenes, distinctive macrocyclic host molecules, as promising anti-biofilm agents. The review is structured into two main sections, each dedicated to exploring distinct facets of pillar[*n*]arene applications. The first section scrutinizes functionalized pillar[*n*]arenes with a particular emphasis on cationic derivatives. This analysis reveals their significant efficacy in inhibiting biofilm formation, underscoring the pivotal role of specific chemical attributes in combating microbial communities. The second section of the review shifts its focus to inclusion complexes, elucidating how pillar[*n*]arenes serve as encapsulation platforms for antibiotics. This encapsulation enhances the stability of antibiotics and enables a controlled release, thereby amplifying their antibacterial activity. The examination of inclusion complexes provides valuable insights into the potential synergy between pillar[*n*]arenes and traditional antibiotics, offering a novel avenue for overcoming biofilm resistance. This comprehensive review highlights the escalating global threat of bacterial infections and the urgent need for innovative strategies to counteract drug-resistant biofilms. The unique properties of pillar[*n*]arenes, both as functionalized molecules and as inclusion complex hosts, position them as promising candidates in the quest for effective anti-biofilm agents. The exploration of their distinct mechanisms opens new avenues for research and development in the ongoing battle against bacterial infections and biofilm-related health challenges.

KEYWORDS: *Biofilm inhibitors, Biofilm disruptors, Pillar[n]arenes, Host−Guest, Antimicrobial*

INTRODUCTION

A critical public health crisis has emerged from the worldwide increase in bacterial infections exacerbated by the alarming proliferation of drug-resistant strains. The ability of these pathogenic bacteria to cause harm and illness has necessitated an increased focus on research. Intensifying the intricacy of this situation is the worrisome trend of these bacteria developing resistance to well-established drugs and therapies.[1] Drug resistance has presented a daunting challenge for healthcare practitioners, as this situation has led to the declining efficacy of treatments that were once considered most effective and reliable.[2,3] The need to confront these two intertwined challenges of surging infections and drug resistance has become a pressing priority in the field of public health. Biofilms, structured communities of microorganisms enveloped within the matrix of extracellular polymeric substances (EPSs), have surfaced as a ubiquitous and complex challenge with wide-ranging consequences.[4−10] Biofilms are very difficult to eliminate with antibiotics because the extracellular matrix safeguards bacteria from conventional antibiotics. Pathogens associated with biofilms are notorious for developing antibiotic resistance. Despite being recognized as significant contributors to the onset of various human diseases, our understanding of biofilm-associated infections and effective treatment strategies is in early stages.[11−15] Conventional treatment methods often struggle to completely eradicate biofilms. Several treatment strategies have been explored apart from antibiotics to combat and eliminate biofilms, including the use of enzymes or antimicrobial peptides,[16−19] quorum sensing inhibitors,[20−23] and phage therapy.[24−27]

In recent years, one such promising avenue has been the use of pillar[*n*]arenes as anti-biofilm agents. Pillar[*n*]arenes, a class of macrocyclic host molecules with a distinctive pillar-shaped architecture, exhibit remarkable host−guest interactions, enabling them to complex with a diverse range of guest molecules.[28−34] Their significant properties stem from their unique structural features, rendering them promising candidates

Received: December 15, 2023
Revised: March 13, 2024
Accepted: March 13, 2024

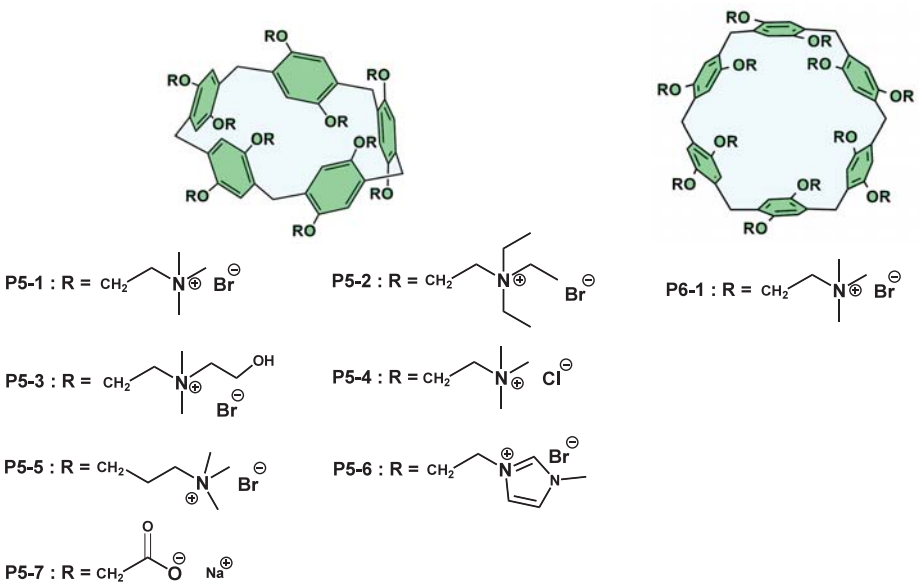

Figure 1. Molecular structures of cationic pillar[5]arene derivatives (**P5-1**–**P5-6**), anionic pillar[5]arene (**P5-7**), and pillar[6]arene (**P6-1**).

for various applications in supramolecular chemistry.[35−47] Modifiable functionalities and unique structural characteristics of pillar[*n*]arenes hold promise for developing materials specifically tailored for biological applications.[48−55] Pillar[*n*]-arenes have been shown to possess inherent antimicrobial properties against a broad range of planktonic bacteria, including both Gram-positive and Gram-negative strains.[51,56] Biocompatibility and safety are the essential aspects of any potential anti-biofilm agents for human use. Preliminary investigations suggest pillar[*n*]arenes and their derivatives as safe and biocompatible agents; hence they exhibit low cytotoxicity and minimal adverse effects.[57−62] The unique properties of pillar[*n*]arenes extend beyond their antimicrobial potential, encompassing artificial transmembrane transport capabilities.[63−67] Pillar[*n*]arene derivatives possess the capacity to facilitate the transport of specific molecules across cell membranes. This notable feature holds significant implications for drug delivery.

This comprehensive review explores the recent advances in developing anti-biofilm agents based on pillar[*n*]arenes. The ability of pillar[*n*]arene-based supramolecular materials to fight bacterial biofilms can be attributed to two main factors: either the modified structure of the macrocycles themselves or antibiotics and other antibacterial agents encapsulated within the cavities of pillar[*n*]arenes. As a result, this review categorizes the literature reports based on pillar[*n*]arenes and related macrocycles into two main sections: (1) Functionalized pillar[*n*]arenes as anti-biofilm agents: The first section of the review focuses on materials created by functionalizing the pillar[*n*]arenes to improve their anti-biofilm potentials. By introducing specific functional groups or modifications, researchers have tailored the pillar[*n*]arene macrocycles to directly exert biofilm inhibition and/or biofilm disruption effects. (2) Pillar[*n*]arene-based inclusion complexes to mitigate biofilms: The second section of this review highlights materials fabricated by forming inclusion complexes with antibiotics and other antibacterial drugs. The intrinsic hydrophobic cavities of pillar[*n*]arenes can encapsulate antibiotics and other antibacterial agents inside their cavities,[51,56,68−71] which improves the stability and controlled release of these therapeutic agents, leading to more effective antibacterial activity.

This review provides an overview of the fundamental concepts, innovative strategies, and recent advances in the use of pillar[*n*]arenes with a particular emphasis on cationic derivatives[72−76] as they have exhibited effective antibacterial potential. This review investigates how pillar[*n*]arenes can help to overcome bacterial resistance and biofilm-associated infections and also discusses the challenges and opportunities in designing biocompatible, stable, and effective antibacterial materials. The aim of this review is to provide a holistic overview of the progress made in this rapidly developing research area. By understanding the unique approaches of functionalized pillar-[*n*]arenes and inclusion complexes, we hope to stimulate further inquiries and innovations in the development of next-generation anti-biofilm agents with broader applications in medicine, materials science, and other related fields.

PILLAR[*N*]ARENE-BASED ANTI-BIOFILM AGENTS

Functionalized Pillar[*n*]arenes as Anti-biofilm Agents. In a notable contribution, Cohen and co-workers[77,78] highlighted the significant combination of chemical features required to mitigate biofilms and combat associated infections with a focus on cationic pillar[5]arenes as well as pillar[6]arenes. They assessed the capacity of pillar[*n*]arene derivatives **P5-1** to **P5-7** and **P6-1** (Figure 1) to inhibit the formation of biofilms caused by both Gram-positive (*Staphylococcus aureus* subsp. *aureus* Rosenbach ATCC 33592, *S. aureus* ATCC 29213, *S. aureus* BAA/043, *Enterococcus faecalis* ATCC 29212, *Staphylococcus epidermidis* RP62A, *Streptococcus mutans* ATCC 700610) and Gram-negative (*Escherichia coli* ATCC 25922, *Pseudomonas aeruginosa* PAO1) pathogens.

The Minimum Biofilm Inhibitory Concentration at which at least 50% inhibition of biofilm formation occurred ($MBIC_{50}$) was determined for the pillar[*n*]arenes **P5-1**–**P5-7** and **P6-1**. Inhibition of biofilm formation was selective for Gram-positive strains, and none of the cationic pillar[*n*]arenes tested inhibited biofilm formation by Gram-negative strains *E. coli* ATCC 25922

https://doi.org/10.1021/acsinfecdis.3c00697
ACS Infect. Dis. XXXX, XXX, XXX−XXX

Table 1. Biofilm Inhibitory Activity, $MBIC_{50}$ (μM), against Gram-Positive Strains

	bacterial strain					
compound	*S. aureus subsp. aureus* Rosenbach ATCC 33592	*S. aureus* ATCC 29213	*S. aureus* BAA/043	*E. faecalis* ATCC 29212	*S. epidermidis* RP62A	*S. mutans* ATCC 700610
P5-1	0.9	3.5	3.5	0.9	3.5	1.8
P5-2	1.5	5.9	5.9	1.5	5.9	5.9
P5-3	>12	>12	>12	>12	>12	>12
P5-4	1.1	4.4	8.8	1.1	2.2	8.8
P5-5	1.7	6.6	>13	1.7	1.7	6.6
P5-6	0.8	1.6	1.6	0.4	3.2	6.4
P5-7	>23	>23	>23	>23	>23	>23
P6-1	0.4	1.5	2.9	0.4	0.7	2.9
TMA-Cl	>292	>292	>292	>292	>292	>292
TMA-Br	>208	>208	>208	>208	>208	>208

Adapted with permission from ref 77. Copyright 2016 American Chemical Society.

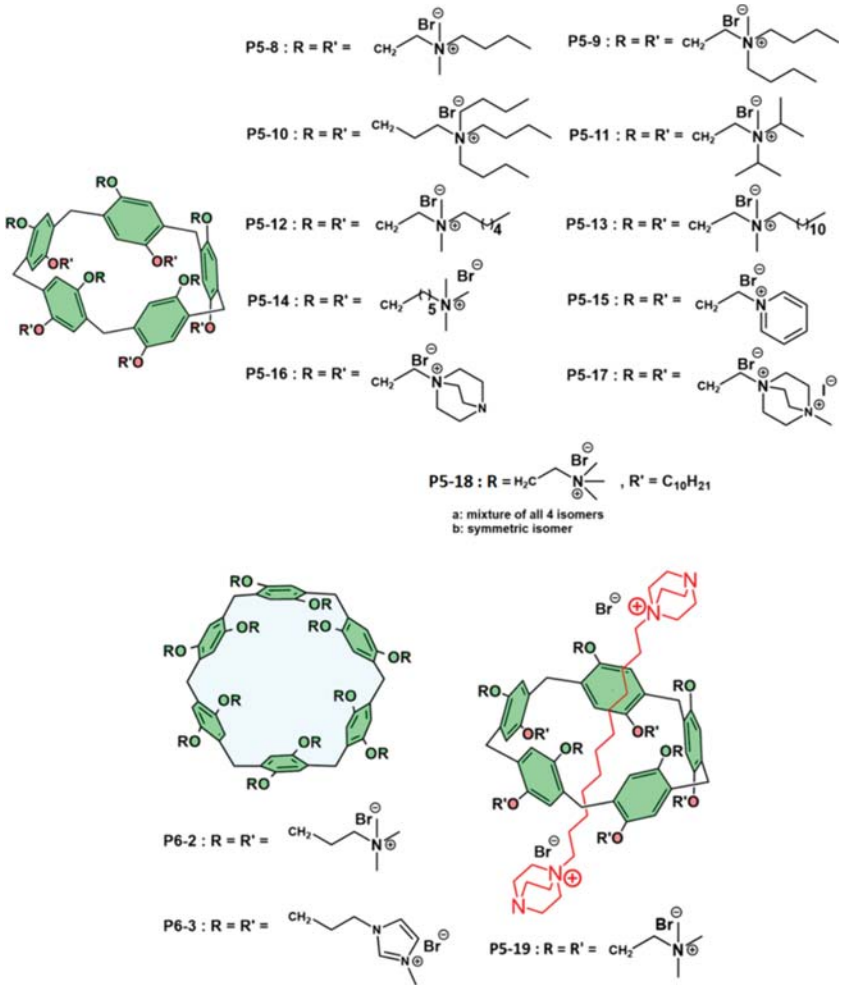

Figure 2. Molecular structures of cationic pillar[5]arene derivatives (**P5-8**–**P5-18**), pillar[6]arene derivatives **P6-2** and **P6-3**, and pillar[5]arene-based rotaxane **P5-19**.

and *P. aeruginosa* PAO1. The $MBIC_{50}$ values are listed in Table 1.

Notably, **P5-1** and **P5-6** displayed impressive biofilm inhibition, especially against clinically significant strains like methicillin-resistant *S. aureus* subsp. *aureus* Rosenbach ATCC 33592 and *E. faecalis* ATCC 29212. Structural modifications were evaluated, revealing that replacing the quaternary trimethylammonium head groups in **P5-1** with more hydrophobic triethyl quaternary ammonium groups in **P5-2** resulted in comparable biofilm inhibition. However, elevating hydro-

https://doi.org/10.1021/acsinfecdis.3c00697
ACS Infect. Dis. XXXX, XXX, XXX−XXX

philicity through hydroxyethyldimethyl quaternary ammonium groups in **P5-3** led to a pronounced loss of activity. The impact of halogen ions on biofilm inhibition was explored using the chloride analogue (**P5-4**) of **P5-1**, showing similar $MBIC_{50}$ values against certain strains but higher values against others, indicating the influence of the halogen ion type. The elongation of the aliphatic linker from an ethyl group in **P5-1** to a propyl chain in **P5-5** led to a meaningful decrease in biofilm inhibition. **P5-6** generally exhibited lower $MBIC_{50}$ values, except against *S. mutans* ATCC 700610, indicating a higher inhibitory activity. **P5-7** with negatively charged carboxylate head groups showed no biofilm inhibition, emphasizing the importance of a positive charge. Tetramethylammonium chloride (TMA-Cl) and tetramethylammonium bromide (TMA-Br) demonstrated no biofilm inhibition, suggesting that neither the quaternary ammonium head groups nor the halogen ions alone are responsible for the biofilm inhibitory effects observed in the pillar[*n*]arene derivatives. To explore the impact of quaternary ammonium cluster size and overall positive charge, **P6-1**, the pillar[6]arene analog of **P5-1**, was synthesized. **P6-1** demonstrated a notable 20% increase in overall positive charge compared to **P5-1**, coupled with a significant enlargement in cavity diameter (6.7 Å for **P6-1** vs 4.6 Å for **P5-1**). Compared to **P5-1**, the pillar[6]arene derivative **P6-1** exhibited 2−5-fold lower $MBIC_{50}$ values against four Gram-positive pathogens forming biofilms. No significant difference in biofilm inhibition was observed between **P5-1** and **P6-1** for *S. aureus* BAA/043, but for *S. mutans* ATCC 700610, **P5-1** showed slightly greater activity. These findings suggest that the structural modifications in **P6-1** generally enhance biofilm inhibition with some strain-specific variations compared to the pillar[5]arene counterpart. It was also observed that pillar[*n*]arenes **P5-1** and **P6-1**, despite being the most potent inhibitors of biofilm formation, were unable to completely eradicate mature biofilms. The Gram-positive strains exhibited MIC values over 16 times higher than the highest $MBIC_{50}$ value for **P6-1**. This suggests that the inhibition of biofilm formation is not due to a bactericidal effect. The testing on rat red blood cells demonstrated a lack of hemolysis, suggesting a favorable safety profile for membrane interactions. Additionally, **P6-1** showed no adverse effects on the viability of human monocytic THP1 cells (ATCC TIB 202) and cystic fibrosis human bronchial epithelial IB3-1 (ATCC CRL2777) cells which supported the potential use of **P6-1** as an antimicrobial agent with specific efficacy against Gram-positive strains and a low likelihood of adverse effects on mammalian cells.

Continuing their pursuit to establish the comprehensive Structure−Activity Relationship (SAR) for cationic pillar[*n*]-arene derivatives that can inhibit biofilm formation by clinically relevant Gram-positive pathogens, Cohen and colleagues have synthesized 15 additional cationic pillar[5,6]arene derivatives, as illustrated in Figure 2.[78] The $MBIC_{50}$ results (Table 2) obtained from the crystal violet assay revealed that most of the cationic pillar[5,6]arene derivatives effectively inhibited biofilm formation, with exceptions for specific compounds such as **P5-10**, **P5-13**, **P5-18a**, and **P5-18b**. Compound **P5-18a**, characterized by the presence of isomeric mixtures, and compound **P5-18b**, distinguished as the symmetric isomer, share a commonality of possessing 5 positive charges. Intriguingly, these two compounds demonstrated a noteworthy reduction in potency, roughly by an order of magnitude, in comparison to their counterparts each harboring 10 or more positive charges and exhibited significantly greater potency. This observation highlights the importance of the number and distribution of positive charges in influencing the biological activity of these compounds, with compounds featuring a higher positive charge content demonstrating enhanced effectiveness. Extending the length of one or two of the substituents had minimal impact, but a notable increase in hydrophobicity completely eliminated the activity. Altering cationic headgroup types or increasing the number of positive charges had minimal impact. Furthermore, to understand the role of pillar[5]arene cavity on anti-biofilm properties, they also successfully created a water-soluble rotaxane **P5-19** from **P5-1**, which sustained its anti-biofilm effectiveness. This suggests that the cavity within the pillar[5]-arene structure was not pivotal for hindering biofilm growth. Despite their cationic amphiphilic nature, pillar[*n*]arene derivatives **P5-1**, **P5-8**, **P5-9**, **P5-11**, **P5-12**, **P5-14**, **P5-15**, **P5-16**, **P5-17**, and **P5-19** exhibited no hemolysis even at concentrations exceeding 100-fold their $MBIC_{50}$ values. Noteworthy, the hydrophobic pillar[*n*]arene derivatives **P5-10**, **P5-13**, **P5-18a**, and **P5-18b** displayed hemolytic effects comparable to CTAB.

Table 2. Biofilm Inhibitory Activity, $MBIC_{50}$ (μM), against Gram-Positive Strains

	bacterial strain	
compound	*S. aureus subsp. aureus* Rosenbach ATCC 33592	*E. faecalis* ATCC 29212
P5-1	0.45 (1)	0.45 (1)
P5-8	0.37 (1)	0.19 (0.5)
P5-9	0.31 (1)	0.31 (1)
P5-10	>8.7 (>32)	>8.7 (>32)
P5-11	0.61 (2)	0.61 (2)
P5-12	0.32 (1)	0.32 (1)
P5-13	>7.72 (>32)	>7.72 (>32)
P5-14	0.35 (1)	0.35 (1)
P5-15	0.40 (1)	0.40 (1)
P5-16	0.71 (2)	0.36 (1)
P5-17	0.95 (4)	0.47 (2)
P5-18a	>14.94 (>32)	>14.94 (>32)
P5-18b	14.94 (32)	7.47 (16)
P6-2	0.69 (2)	0.69 (2)
P6-3	0.63 (2)	0.63 (2)
P5-19	0.35 (1)	0.18 (0.5)

The compounds that demonstrated proficiency in hindering biofilm formation exhibited nonhemolytic attributes (lack of harm to red blood cells) and showed no impact on bacterial proliferation. These findings yield valuable insights for the development of efficient materials targeting the prevention of biofilm establishment by Gram-positive bacteria.

Zhang and co-workers[79] also conducted a comprehensive investigation on the synthesis and characterization of quaternary ammonium (**P5-1**) and pyridinium (**P5-15**) functionalized pillar[5]arene derivatives and systematically studied their effects on bacterial growth, adhesion, and biofilm formation with a particular emphasis on activity against a drug-resistant Gram-negative pathogen, *P. aeruginosa* PAO1. During investigation of their effects on *P. aeruginosa* PAO1, macrocycles **P5-1** and **P5-15** were observed to exert a degree of inhibitory impact on bacterial growth. However, it is important to note that these effects were moderate in nature even at higher concentrations.

https://doi.org/10.1021/acsinfecdis.3c00697
ACS Infect. Dis. XXXX, XXX, XXX−XXX

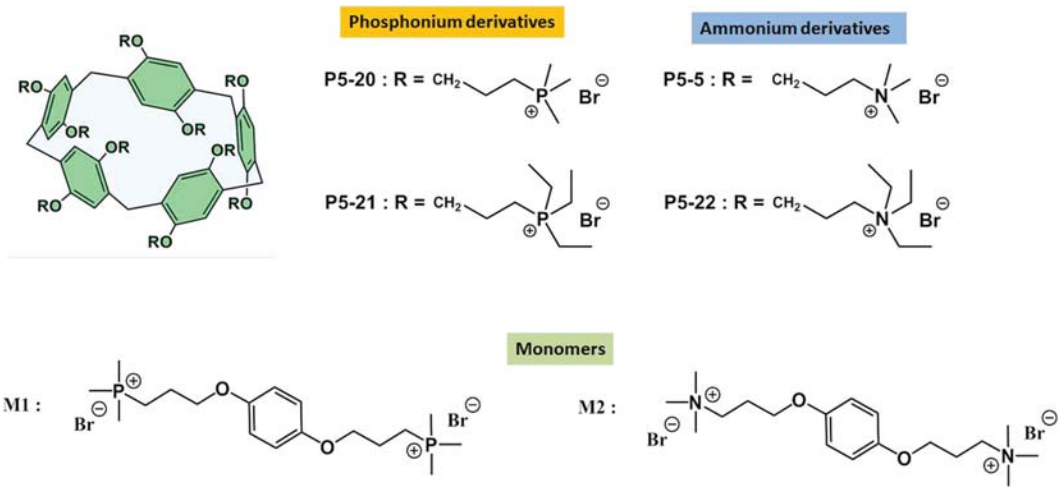

Figure 3. Molecular structures of pillar[5]arene derivatives **P5-5** and **P5-20**−**P5-22** and monomers **M1** and **M2**.

The results showed that pyridinium functionalized pillar[5]-arene (**P5-15**) exhibited stronger bactericidal and anti-biofilm formation activity against *P. aeruginosa* compared to tetraalkylammonium functionalized pillar[5]arene (**P5-1**) at 1/2 MIC concentration, i.e., 0.051 mmol L^{-1} which is approximately equivalent to 63 $\mu g \cdot mL^{-1}$. This notably high $MBIC_{50}$ concentration observed in **P5-15** aligns with observations made by Cohen and colleagues in their study against the Gram-negative *P. aeruginosa* PAO1 for cationic pillar[*n*]-arenes.[77] These findings emphasize the critical role played by different cation moieties on the pillar[5]arene rims. Importantly, **P5-15** demonstrated consistent antibacterial efficacy without developing resistance even after multiple passages.

To probe the influence of chemical identity of the cations on biofilm inhibition, Cohen and co-workers[80] have synthesized phosphonium-decorated pillar[5]arene derivatives **P5-20** and **P5-21** (Figure 3) and compared the biofilm inhibition properties with analogous quarternary ammonium derivatives of pillar[5]arene, **P5-5** (Figure 1) and **P5-22**, respectively. It is worth noting that **P5-5** had been previously studied by the same researchers in their earlier report.[77,78] The effects of cationic pillar[5]arene derivatives **P5-20**, **P5-21**, **P5-5**, and **P5-22**, were investigated for their impact on biofilm formation by two Gram-positive bacterial strains, *S. aureus* ATCC 33592 and *E. faecalis* ATCC 29212. The $MBIC_{50}$ values obtained from crystal violet assay showed that the phosphonium-derived pillar[5]arenes **P5-20** and **P5-21** and ammonium-derived pillar[5]arenes **P5-5** and **P5-22** effectively exhibited potent anti-biofilm activity as shown in Table 3.

The results also supported that while the positive charges were crucial for anti-biofilm activity, the nature of the charges (ammonium or phosphonium) had a marginal effect. The influence of hydrophobicity on biofilm inhibition was explored by comparing compounds **P5-21** and **P5-22** with compounds **P5-20** and **P5-5**. Despite differences in carbon atom counts, their $MBIC_{50}$ values did not significantly differ, indicating similar effectiveness in preventing biofilm formation. The $MBIC_{50}$ results also revealed that neither monomer **M1** nor **M2** caused measurable inhibition of biofilm formation, highlighting the crucial role of cumulative charge organization on the pillar[5]-arene scaffold for anti-biofilm activity, potentially attributed to a multivalency effect. To assess whether the inhibitory effect of

Table 3. Biofilm Inhibitory Activity, $MBIC_{50}$ ($\mu g\ mL^{-1}$), against Gram-Positive Strains

	bacterial strain	
compound	*S. aureus subsp. aureus* Rosenbach ATCC 33592	*E. faecalis* ATCC 29212
P5-20	1.55 (4)	1.55 (4)
P5-21	1.33 (4)	0.67 (2)
P5-5	1.66 (4)	1.66 (4)
P5-22	0.71 (2)	1.41 (4)
M1	>317 (160)	>317 (160)
M2	>340 (160)	>340 (160)

Adapted with permission from ref 80. Copyright 2016 Royal Society of Chemistry.

compounds **P5-20**, **P5-21**, **P5-5**, and **P5-22** on biofilm formation was due to potential antimicrobial activity, they also determined the minimal inhibitory concentrations (MICs) against the tested bacterial strains. These MIC values were more than 16 times higher than the highest $MBIC_{50}$ values measured for biofilm inhibition, indicating that the observed anti-biofilm effects were not solely attributed to antibacterial activity.

Gao and colleagues[81] focused on designing a zwitterionic pillar[5]arene (**P5-23**) and related model compounds (**P5-24**, **P5-2**, **M3**, and **M4**, Figure 4), exploring their self-assembly tendencies in aqueous solutions using transmission electron microscopy (TEM) and cryogenic transmission electron microscopy (Cryo-TEM) studies. The investigations confirmed the spontaneous formation of nearly spherical nanoaggregates (30 to 50 nm) for **P5-23**. Zeta potential measurements indicated a weakly positive charge (13.3 ± 1.22 mV) on the nanoaggregates, suggesting a prevalence of positive charges. NMR spectrum analysis revealed hexyl sulfate groups within the pillar[5]arene cavity, driven by hydrophobic and C−H···π interactions, influencing charge distribution. **P5-23** demonstrated stronger antibacterial effects compared to those of model compounds **P5-24**, **P5-2**, **M3**, and **M4** against Gram-negative *E. coli* (DH5α) and Gram-positive *S. aureus* (SH1000). This enhanced activity was attributed to the hydrophobic pillar[5]-arene skeleton, alkyl chains, sulfate, and ammonium groups in its structure. These positively charged nanoaggregates engaged bacterial biofilms through a combination of electrostatic and

https://doi.org/10.1021/acsinfecdis.3c00697
ACS Infect. Dis. XXXX, XXX, XXX−XXX

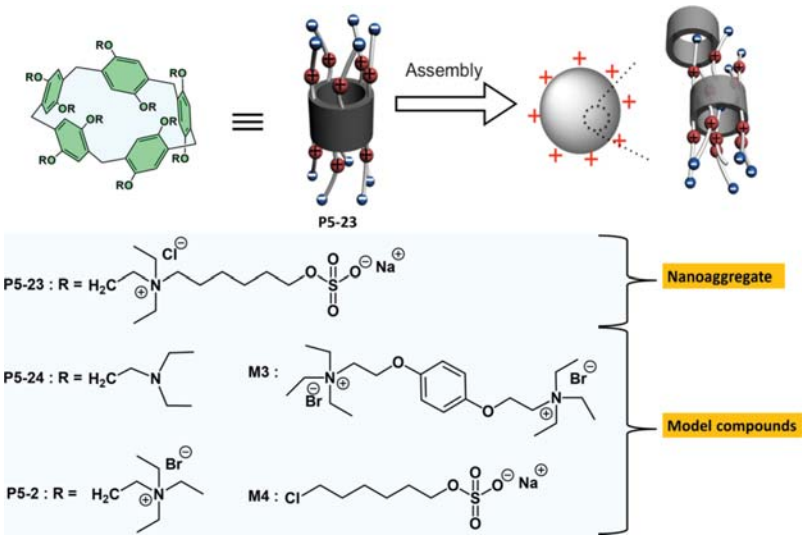

Figure 4. Molecular structures of **P5-2**, **P5-23**, **P5-24**, **M3**, and **M4** and schematic representations of the self-assembly of **P5-23** to positively charged nanoaggregates of **P5-23**. Adapted with permission from ref 81. Copyright 2019 John Wiley and Sons.

hydrophobic interactions, culminating in the disruption of bacterial cell membranes and, consequently, cell death. **P5-23** exhibited antibacterial activity against both *E. coli* (DH5α) and *S. aureus* (SH1000), and it can efficiently disrupt pre-established *E. coli* biofilms without leading to rapid resistance development with $MBIC_{50}$ and MBEC (minimum biofilm eradication concentration) values of 80 and 200 μM, respectively. The cytotoxicity of **P5-23** was evaluated by MTT assay with NIH/3T3 cells and MCF7 cells. The key findings are that the **P5-23** nanoaggregate exhibited lower toxicity to mammalian cells than to bacteria. Successful design of the zwitterionic **P5-23** with multifunctional properties opens up new avenues for exploring innovative approaches to combat antibiotic resistance and improve current strategies for managing biofilm-related infections. The findings not only broaden the understanding of anti-biofilm strategies but also lay the groundwork for future investigations on the combination of zwitterionic properties and the formation of positively charged nanoaggregates to fabricate the design of effective antibacterial compounds and enhance current biofilm-related infection management strategies.

Stoikov and co-workers[82] have developed a biocompatible supramolecular system based on a modified pillar[5]arene (**P5-25**, Figure 5A) that has the potential to inhibit the growth of pathogenic microorganisms, specifically *S. aureus* biofilms. The pillar[5]arene molecule **P5-25** was designed in such a way that it could interact with DNA via electrostatic as well as hydrogen bonding interactions. The modified macrocycle contains thioether and tertiary amino groups, making it capable of forming a stable self-association and nanosized complex with DNA as shown in Figure 5A. The binding stoichiometry of complexation between **P5-25** and DNA was estimated from UV−vis titration experiments which suggested the groove binding of one molecule of **P5-25** to the phosphate fragments of two pairs of nucleic bases as depicted in Figure 5B. Importantly, **P5-25** exhibited a remarkable characteristic of being nontoxic to human lung adenocarcinoma cells and bovine embryonic lung epithelial cells. Across the entire concentration range studied (0.5−100 μg/mL, corresponding to 1.7×10^{-8} to 3.4×10^{-5} M), the pillar[5]arene macrocycle **P5-25** did not exhibit reductions in the viability of both normal epithelial cells and A549 model cells. This suggests a promising therapeutic window, indicating a lack of significant cytotoxic effects of **P5-25** within the tested concentration range. This exceptional biocompatibility is a significant advantage, as it suggests the safety and potential utility of the cationic pillar[5]arene in biomedical applications. The capability of **P5-25** to effectively bind with DNA within biofilm matrices was utilized to reduce the thickness of *S. aureus* biofilms. Specifically, at a concentration of 10^{-5} M, it led to a significant 15% reduction in the thickness of these biofilms. As a synthetic, nontoxic DNA-binding agent, it has the potential to significantly enhance the effectiveness of combination therapy against infectious diseases.

Host−Guest Complexation of Pillar[*n*]arenes to Mitigate Biofilms. Pillar[*n*]arenes can act as hosts for various guest molecules through noncovalent interactions, such as hydrogen bonding and van der Waals forces.[83] The hydrophobic cavities of pillar[*n*]arenes can selectively accommodate certain guest molecules based on their size, shape, and chemical properties. The encapsulation of drugs/antibiotics within the pillar[*n*]arene cavities can provide protection against degradation.[84] This stabilization is particularly relevant for therapeutic agents aimed at disrupting biofilms. By shielding these molecules within the host−guest complex, pillar[*n*]arenes can enhance their bioavailability and effectiveness. The structure of pillararenes can be modified to tailor their host−guest interactions. Researchers can design pillar[*n*]arenes with specific functional groups or adjust the size of the cavities to optimize interactions with biofilm-related molecules. This tunability makes them versatile tools for targeted biofilm mitigation strategies. Pillar[*n*]arene-based inclusion complexes can also serve as drug delivery systems for antimicrobial agents.[56] The controlled release of drugs from the complexes, facilitated by noncovalent interactions, allows for sustained and targeted delivery to biofilm-associated microorganisms.

Selective recognition is crucial in the context of biofilms as it allows pillar[*n*]arenes to target specific molecules involved in biofilm formation or stability. Pillar[*n*]arene-based inclusion complexes can interfere with biofilm formation by interacting

https://doi.org/10.1021/acsinfecdis.3c00697
ACS Infect. Dis. XXXX, XXX, XXX−XXX

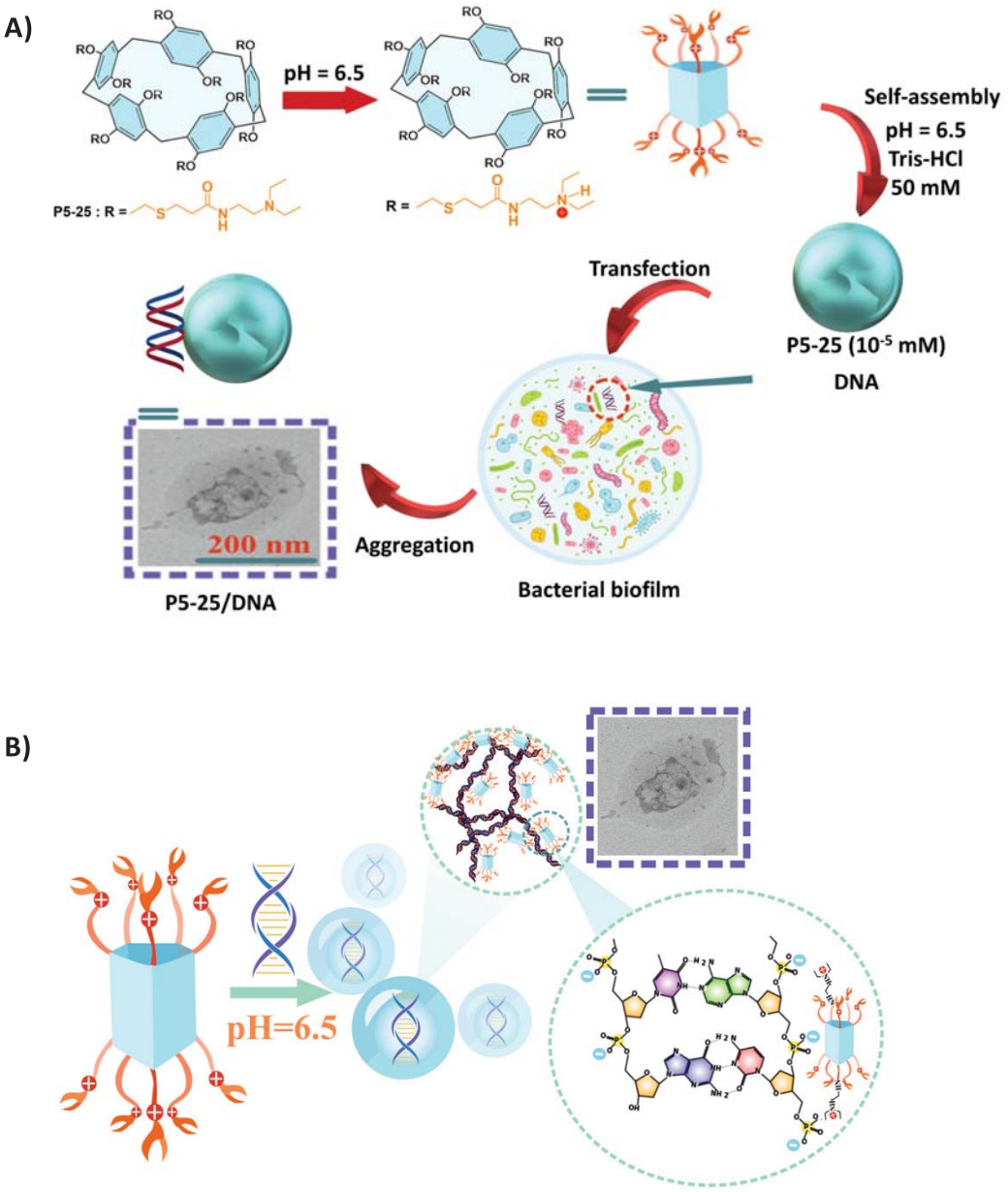

Figure 5. (A) Concept of using **P5-25** as a DNA-binding agent to suppress the development of pathogenic biofilms and (B) proposed mechanism of binding of **P5-25** to DNA. Adapted with permission from ref82, which is an open access article distributed under the Creative Commons Attribution License (CC-BY 4.0), MDPI.

with key molecules. For example, they may disrupt the signaling pathways involved in quorum sensing, a process by which bacteria coordinate their behavior in response to the population density. By inhibition of quorum sensing molecules through hydrogen bonding or other interactions, pillar[*n*]arenes can impede the formation of biofilms. Recently, Linder and their team conducted research with the objective of utilizing host–guest chemistry to combat bacterial virulence and eradicate biofilms, particularly in the context of multidrug-resistant *P. aeruginosa* and *Acinetobacter baumannii*.[85] To explore potential interactions between cavity-containing macrocycles and bacterial signaling molecules, the authors screened a diverse family of macrocycles such as crown ethers, calix[*n*]arenes, resorcin[*n*]-arenes, cucurbit[*n*]uril, cyclodextrins, and pillar[5]arene with varying inner cavity sizes (1.5−11.7 Å) and molecular weights (172−2260 g/mol). The screening aimed to understand the affinities, preferences, and determinants of these interactions with six different homoserine lactones (HSLs) that had diverse acyl chains, including branched carbon, carboxyl groups, and hydroxyl groups (Figure 6). This approach was undertaken to shed light on the link between cavity size and HSL affinity, considering the limited knowledge about these aspects in

https://doi.org/10.1021/acsinfecdis.3c00697
ACS Infect. Dis. XXXX, XXX, XXX−XXX

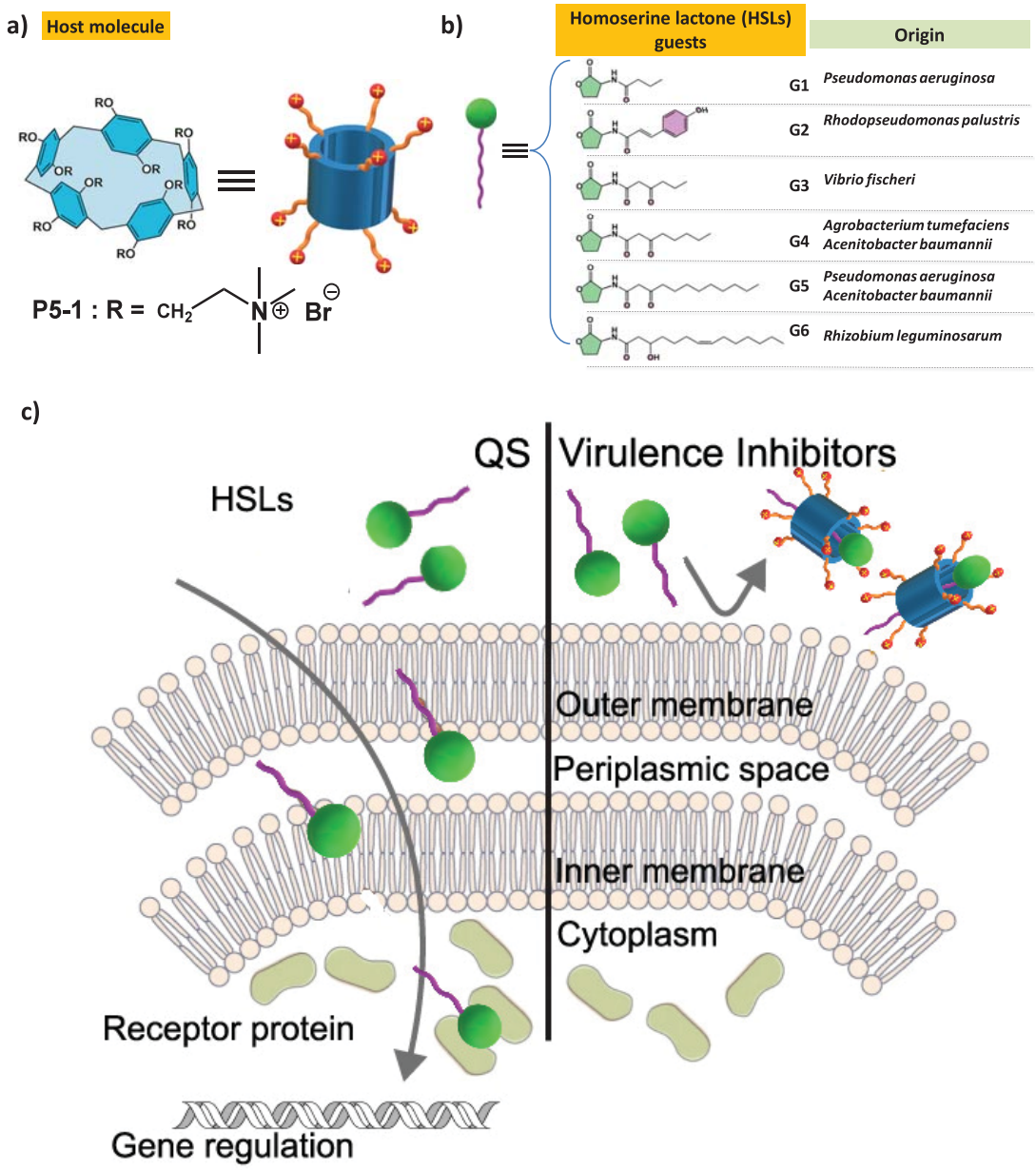

Figure 6. Host–guest interactions between macrocycle **P5-1** and bacterial homoserine lactones selective for HSLs with prolonged acyl chains. (a) Structure of **P5-1**. (b) Molecular structures and bacterial species of all QS HSLs used in the study. (c) Schematic representation of HSL quorum sensing in Gram-negative bacteria (left), along with a virulence inhibition approach (right). Adapted from ref 85, which is an open access article distributed under the Creative Commons Attribution License (CC-BY 4.0), Springer Nature.

previous efforts. To facilitate the screening, a fluorescent *E. coli* reporter system was developed capable of detecting the six different HSLs. Among the tested macrocycles, **P5-1** showed the highest concentration-dependent signal ratio, exhibiting varied binding strengths with different HSLs, indicating its potential as a versatile virulence inhibitor. Then, they focused their investigation particularly on interactions between a quaternary ammonium functionalized pillar[5]arene (**P5-1**, Figure 1) and critical bacterial virulence factors, specifically, N-acyl homoserine lactones (HSLs, Figure 6) and lipopolysaccharides (LPSs). Despite the fact that **P5-1** exhibited binding with all six HSLs, its binding varied. It ranged from minimal binding to **G1** (18%) with a very short acyl chain to strong binding to **G5** (64%) and **G6** (96%), both featuring longer acyl chains (Figure 6b). **P5-1** exhibited comparable effects on biofilm formation in *P. aeruginosa* isolate PAO1, which was associated with HSL-regulated quorum sensing. Pyocyanin, an exotoxin characterized by its vivid green color, is directly regulated by quorum sensing (QS) and serves as a surrogate indicator of virulence. The introduction of **P5-1** led to a concentration-dependent decrease

https://doi.org/10.1021/acsinfecdis.3c00697
ACS Infect. Dis. XXXX, XXX, XXX−XXX

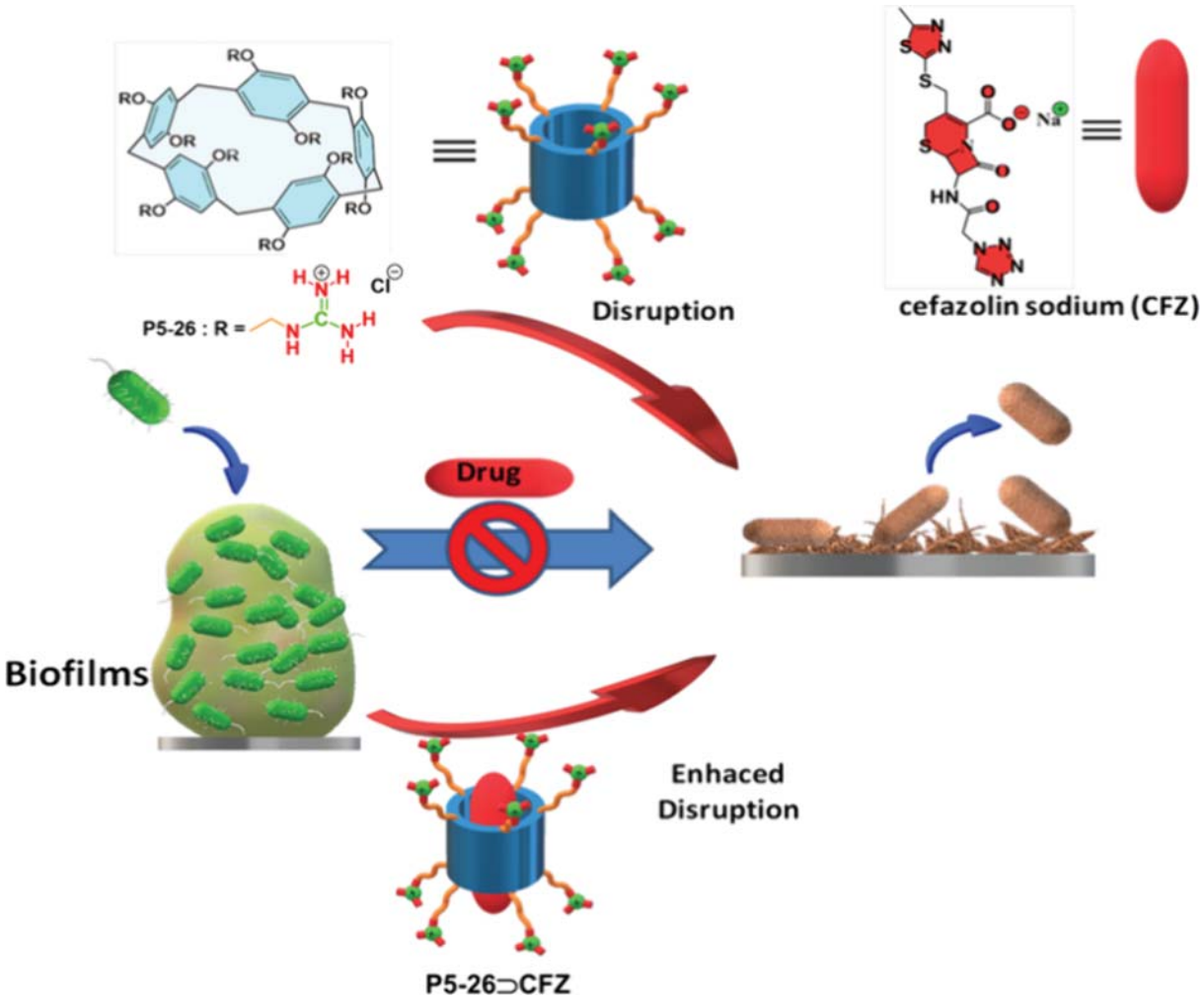

Figure 7. Structures of **P5-26** and CFZ, and disruption of biofilms by **P5-26** and **P5-26**⊃CFZ. Adapted with permission from ref 86. Copyright 2020 John Wiley and Sons.

in pyocyanin levels, with discernible effects starting at **P5-1** concentrations as low as 10 μM and complete suppression observed at 1 mM and higher concentrations. **P5-1** also demonstrated similar effects on biofilm formation in *P. aeruginosa* isolate PAO1, closely associated with HSL-regulated QS, as evidenced by the crystal violet assay, and displayed concentration dependence analogous to the observed trends in pyocyanin assessment. To address antibiotic resistance, the effectiveness of **P5-1** was tested against carbapenem- and cephalosporin-resistant strains of *P. aeruginosa* and *A. baumannii*, resulting in a statistically significant decrease in biofilm formation. Notably, **P5-1** showed efficacy against highly resistant strains, emphasizing its potential as a valuable treatment option for challenging "superbug" pathogens.

The design of quaternary ammonium functionalized **P5-1** is noteworthy, as it incorporates a lipophilic core along with hydrophilic quaternary ammonium functionalities. This unique molecular structure equips it with the ability to selectively bind to specific HSLs that possess hydrophobic long acyl chains. They explored the potential of this polycationic pillar[5]arene to form host−guest complexes with both HSLs and LPSs and hence inhibit biofilms in multidrug-resistant *P. aeruginosa* and *A. baumannii* as shown in Figure 6c.

Wang and co-workers[86] introduced a novel guanidinium-functionalized pillar[5]arene (**P5-26**, Figure 7) that demonstrated impressive antibacterial activity against both Gram-negative *E. coli* and Gram-positive *S. aureus* strains. **P5-26** exhibited remarkable ability to disrupt preformed *E. coli* biofilms with MBEC of 100 μM by penetrating through the biofilm barriers and destroying the biofilm-enclosed bacteria. Confocal laser scanning microscopy (CLSM) analysis of biofilms treated with **P5-26** showed significant structural disintegration and reduced cell viability, comparable to the positive control polymyxin B. Notably, **P5-26** exhibited biofilm-disrupting activity even in mature biofilms aged for 5 days, surpassing the effectiveness of polymyxin B. The exceptional biofilm disruption properties of **P5-26** can be attributed to its distinctive structure, characterized by densely preorganized guanidinium moieties integrated on the hydrophobic pillar[5]arene skeleton. These guanidinium groups engage bacterial cell walls and membranes through multiple electrostatic interactions, leading to membrane permeation followed by membrane rupture and cell lysis (Figure

https://doi.org/10.1021/acsinfecdis.3c00697
ACS Infect. Dis. XXXX, XXX, XXX−XXX

7). This mechanistic insight underscores the potential of **P5-26** as a promising biofilm disruptor. To enhance biofilm disruption, **P5-26** was conjugated with the broad-spectrum antibiotic cefazolin sodium (CFZ). An intriguing finding is that **P5-26** can form host−guest complexes with a conventional antibiotic, CFZ, which otherwise showed minimal activity against biofilms. The encapsulation of CFZ by **P5-26** was confirmed through various experiments, demonstrating a binding affinity of $(5.92 \pm 0.50) \times 10^4$ M^{-1}. While CFZ alone shows little activity against biofilms, **P5-26**⊃CFZ is significantly more effective than both free **P5-26** and free CFZ, with a median MBEC of 25 μM. Live/dead cell staining further confirmed the enhanced reduction in bacterial viability and density within the biofilm upon **P5-26**⊃CFZ treatment. The synergistic action of **P5-26** and CFZ within the biofilm matrix contributed to the improved biofilm disruption and antibacterial activities of **P5-26**⊃CFZ. The authors hypothesized that the increased effectiveness of disrupting biofilms attributed to CFZ encapsulated in **P5-26**, denoted as **P5-26**⊃CFZ, can be elucidated through several mechanisms. First, **P5-26**⊃CFZ exhibits notable penetrability through biofilms, facilitating its efficient access to bacterial membranes. Once inside the biofilm, **P5-26**⊃CFZ can more effectively breach bacterial membranes, reaching the periplasmic space. The localized presence of both **P5-26** and CFZ in this environment enables them to serve as potent antibiotic agents. The synergistic collaboration between **P5-26** and CFZ within the biofilm matrix amplified their combined antibacterial activities, leading to a more robust disruption of the biofilm. This synergistic strategy contributed to the overall efficacy of **P5-26**⊃CFZ in targeting bacteria within biofilms. This host−guest complex showcased a synergistic enhancement in disrupting *E. coli* biofilms, suggesting a promising supramolecular platform to effectively combat drug-resistant biofilms.

Recently, biphen[*n*]arenes (where n = 4, 5), a macrocyclic family related to pillar[*n*]arenes were synthesized with quaternary ammonium per-functionalization by Li and co-workers (Figure 8).[87] Biphen[*n*]arenes demonstrated a dual

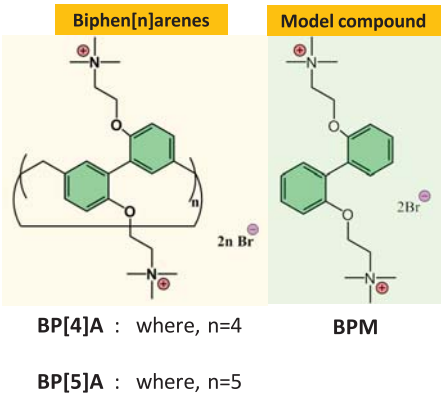

Figure 8. Structures of biphen[*n*]arenes (**BP**[4]**A** and **BP**[5]**A**) and the noncyclic monomer **BPM**.

capability, effectively inhibiting biofilm assembly and eliminating mature biofilms produced by both Gram-positive *S. aureus* (ATCC 25923) and Gram-negative *E. coli* (ATCC 25922) bacterial strains. Both biphen[*n*]arenes **BP**[4]**A** and **BP**[5]**A** demonstrated a dose-dependent inhibition effect, with $MBIC_{50}$ values ranging from 0.62 to 0.72 μM and an impressive biofilm inhibition concentration of 6.25 μM against both bacterial strains. However, no inhibition of biofilm formation was observed for the noncyclic monomer model compound **BPM**, even at a concentration of 125 μM. Both **BP**[4]**A** and **BP**[5]**A** also exhibited potent biofilm eradication capabilities, as evidenced by $MBEC_{50}$ values ranging from 4.94 to 6.82 μM against both *S. aureus* and *E. coli* biofilms. In this case also, the dicationic monomer, **BPM**, highlighted its ineffectiveness in disrupting mature biofilms of either bacterial strain, even at a 125 μM concentration. Moreover, CFZ was encapsulated within the cavities of biphen[*n*]arenes, and the resulting stable inclusion complexes played a crucial role in regulating the distribution, and site-specific concentration of the two bioactive components led to the synergistic healing efficiency. A $MBEC_{50}$ assay was conducted to assess the impact of host−guest complexation on the biofilm disruption efficacy. Remarkably, both the CFZ encapsulated biphen[*n*]arenes were significantly more effective than either individual macrocyclic hosts or CFZ alone in eradicating mature biofilms, with a $MBEC_{50}$ range of 1.15−1.51 μM. Moreover, the MBEC value was reduced to 6.25 μM. They also investigated the wound healing potential of the inclusion complex in an *E. coli*-infected Kunming mouse model. Treatments with CFZ encapsulated biphen[*n*]arenes accelerated the wound healing process compared to other treatments. Wounds treated with these complexes exhibited a significant reduction in size, nearly reaching the levels observed in uninfected mice within 9 days. These findings highlight the promising therapeutic implications of inclusion complexes in enhancing wound recovery and mitigating bacterial complications.

Zhang and co-workers[88] conducted an extensive investigation on the design and synthesis of a pillar[5]arene-based acid-triggered supramolecular photosensitizer utilizing the electrostatic interaction between carboxylato-pillar[5]arene (**P5-7**, Figure 9) and quaternary ammonium-functionalized tetrafluorophenyl porphyrin (TFPP-QA, Figure 9). The design of this supramolecular photosensitizer was intriguing, with the sensitizer tetrafluorophenyl porphyrin anchored to the ammonium cation through a long alkyl spacer. The cationic quarternary ammonium ions were strategically incorporated to attract negatively charged bacterial membranes, while the hydrophobic part aimed to disrupt bacterial cell membranes, potentially leading to bacterial cell death. However, a significant challenge in using quaternary ammonium compounds for antibacterial purposes is their broad cytotoxicity, which limits their application. To overcome this challenge, an acid-responsive carboxylato-pillar[5]arene (**P5-7**) was employed to complex with the quarternary ammonium cation, forming a supramolecular photosensitizer via host−guest inclusion and electrostatic interactions. This approach improved the biocompatibility of the quaternary ammonium compound. Under acidic conditions, the cationic quarternary ammonium group dissociated from **P5-7** due to the formation of neutral carboxylic acid, enhancing the binding of TFPP-QA to bacterial membranes. The design was strategically aligned with the acidic environment typically found at bacterial infection sites. Confocal laser scanning microscopy (CLSM) was used to examine the binding between TFPP-QA and the bacteria. Under normal physiological conditions (pH 7.4), TFPP hardly binds to bacteria. However, in an acidic environment (pH 5.5), TFPP-QA/**P5-7** nanoparticles exhibited strong fluorescence, indicating quaternary ammonium groups targeting bacteria. The antibacterial activity of pH-sensitive TFPP-QA/**P5-7** was

https://doi.org/10.1021/acsinfecdis.3c00697
ACS Infect. Dis. XXXX, XXX, XXX−XXX

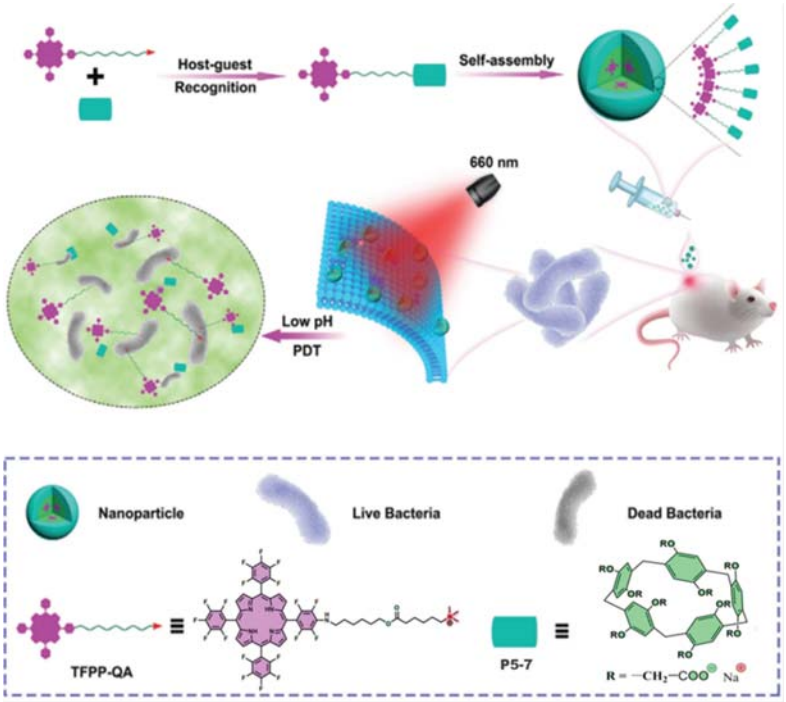

Figure 9. Schematic presentation of an acid-triggered supramolecular photosensitizer and its antibacterial activity under light irradiation. Adapted with permission from ref 88. Copyright 2021 John Wiley and Sons.

evaluated using minimum inhibitory concentration (MIC) assays against Gram-positive bacteria (MRSA) and Gram-negative bacteria (*E. coli*). Without light, treatments have minimal impact on bacterial viability, except for TFPP-QA, which shows weak bacterial cytotoxicity. With 660 nm light irradiation, TFPP-QA demonstrates pH-independent antibacterial efficacy, attributed to positively charged quaternary ammonium groups and generated reactive oxygen species (ROS). Notably, pH-responsive TFPP-QA/**P5-7** exhibited strong antibacterial effects, with the MIC_{90} for MRSA decreased from 40 to 20 $\mu g\ mL^{-1}$ and the MIC_{50} for *E. coli* decreased from 60 to 20 $\mu g\ mL^{-1}$ as the pH changes from 7.4 to 5.5. The difference in antibacterial ability between MRSA and *E. coli* is attributed to their distinct cell wall compositions. *In vitro* tests demonstrated effective antibacterial properties, with the supramolecular photosensitizer showing a remarkable dispersion of bacterial biofilms under light irradiation. Crystal violet assay was used to assess biofilm dispersion and quantify biofilm mass. In groups without light irradiation, the biofilm remained relatively intact, while under 660 nm light irradiation, TFPP-QA exhibited moderate dispersion and TFPP-QA/**P5-7** showed excellent dispersion, which was attributed to the ROS production damaging biofilm proteins and enzymes. In a MRSA-infected mouse wound model, the supramolecular photosensitizer exhibited substantial antibacterial effects and accelerated wound healing. *In vivo* evaluation using a mouse model with biofilm-colonized catheters demonstrated visible improvements in the TFPP-QA/**P5-7** under irradiation groups, showing minimal abscesses and a tendency to heal compared to the control groups. Agar plate experiments using leaching solutions from catheters confirmed the potent anti-biofilm infection capability of TFPP-QA/**P5-7** under light irradiation, as bacterial survival was significantly reduced. Overall, the supramolecular photosensitizer TFPP-QA/**P5-7** proved effective in attenuating pathogenic biofilms and demonstrated powerful anti-biofilm infection capabilities under light irradiation. This innovative strategy showcased the potential of using pillar[5]arene-based supramolecular photosensitizers for photodynamic antibacterial therapy with enhanced biocompatibility and targeted antibacterial action in acidic environments. This strategy not only enhances biocompatibility but also offers targeted antibacterial action in acidic environments, opening new avenues for the treatment of bacterial infections and biofilm-related challenges.

Stoikov and his team conducted a fascinating study where they synthesized polymers **P5-27** and **P5-28** (Figure 10) using mercapto-functionalized pillar[5]arene and demonstrated the remarkable self-healing properties of these materials.[89] The introduction of mercapto functional groups into the pillar[5]-arene enabled these polymers to exhibit self-healing characteristics through thiol−disulfide redox dynamic exchange reactions. Specifically, these reactions formed reversible disulfide bonds with mercapto-functionalized cross-linkers such as trimethylolpropane tris(3-mercaptopropionate) and pentaerythritol tetrakis(3-mercaptopropionate). The copolymers synthesized from mercapto-functionalized pillar[5]arene and cross-linkers resulted in the formation of films capable of self-healing through a dynamic disulfide exchange mechanism. The self-healing polymer materials were combined with the antibacterial drug moxifloxacin (MOXI, Figure 10), and the effectiveness of the MOXI/**P5-27** and MOXI/**P5-28** systems was evaluated against biofilm formation by Gram-negative and Gram-positive bacteria. The results were quite promising, demonstrating that surfaces modified with these systems had the capacity to reduce the biomass of biofilms formed by *S. aureus* and *Klebsiella pneumoniae* pathogens. Notably, the inclusion of MOXI in the polymer film helped maintain its antibacterial efficacy against

https://doi.org/10.1021/acsinfecdis.3c00697
ACS Infect. Dis. XXXX, XXX, XXX−XXX

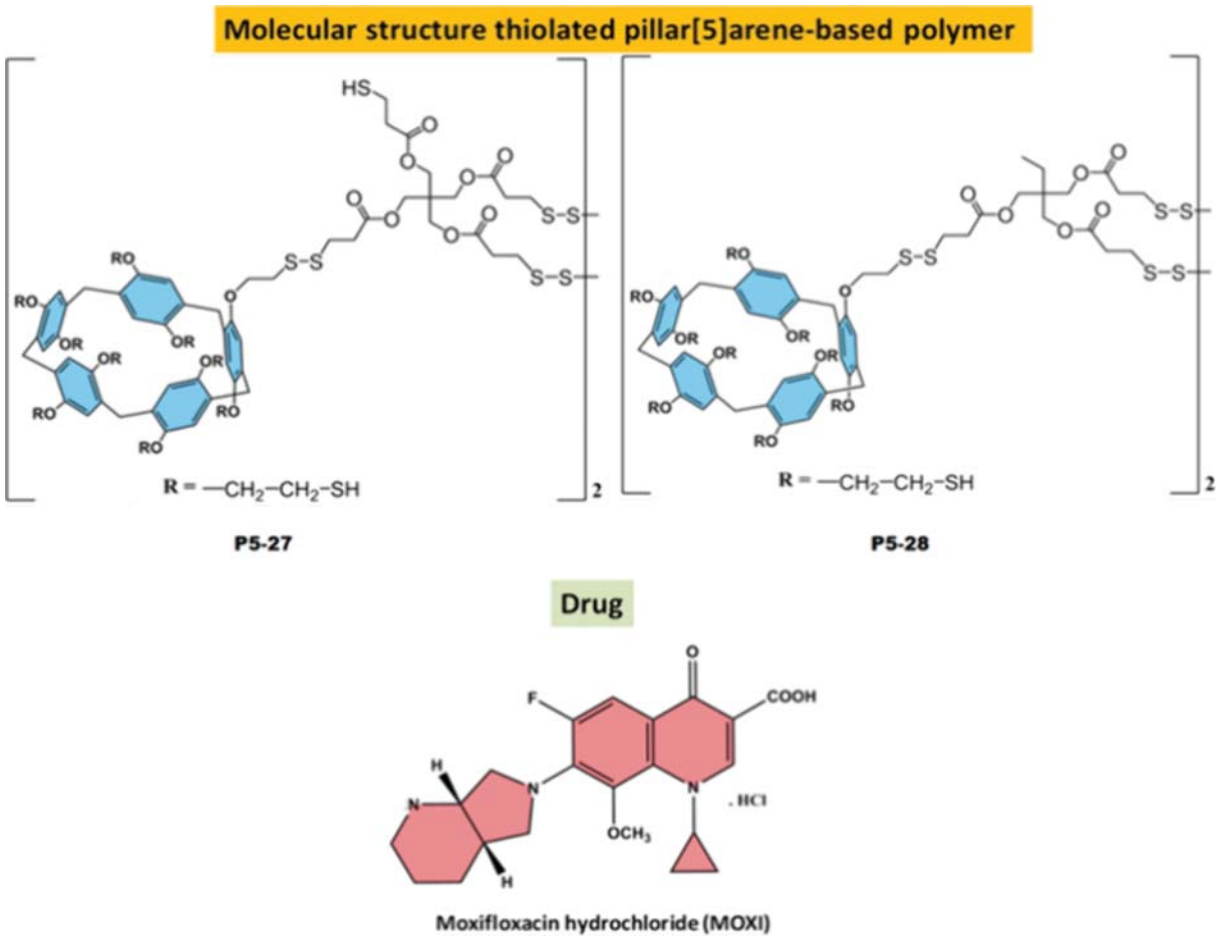

Figure 10. Molecular structures of **P5-27**, **P5-28**, and moxifloxacin hydrochloride (MOXI).[89]

biofilm formation, even in changing environmental conditions, thus preventing its easy washout from surfaces. Furthermore, the study proposed a mechanism for the gradual release of MOXI from the MOXI-loaded films. This mechanism utilized a guest exchange process, where amino acids like arginine and lysine were suggested as potential candidates due to their strong affinity for encapsulation within the cavity of the pillar[5]arene. This gradual release of moxifloxacin could ensure a sustained concentration of the active form of the drug within the biofilm matrix, enhancing its effectiveness against pathogenic microorganisms.

Mechanically interlocked molecules, such as rotaxanes, have also emerged as intriguing candidates for the inhibition of biofilms. In a notable development, a series of heterovalent glyco[2]rotaxanes (Figure 11) have been explored for their potential in this regard by Vincent et al.[90] These glyco[2]rotaxanes are composed of a central galactosylated pillar[5]arene, a tetrafucosylated dendron, and a tetraguanidinium tail, representing a sophisticated example of supramolecular self-assembly. In biofilm inhibition assays conducted on *P. aeruginosa*, it was found that glyco[2]rotaxanes **P5-29**–**P5-31**, which lack polycationic motifs, did not exhibit biofilm inhibition. It was observed that replacing the fucosidic subunits in the axle of **P5-30** and **P5-31** with the polyguanidinium groups in rotaxane **P5-32** led to a significant increase in biofilm inhibition, reaching 70% at a $MBIC_{50}$ of 37.5 μM. A comparable effect was also noted for **P5-33**. Extending the aliphatic monostoppered axle resulted in a comparable decrease in biofilm formation, but at a significantly lower $MBIC_{50}$ of 2.4 μM for rotaxane **P5-34**. These observations indicated that the presence of a polycationic motifs emerged as a crucial factor for achieving potent inhibition of biofilm formation, as evidenced by the effectiveness of rotaxanes **P5-32**–**P5-34**. The comparative analysis of glyco[2]rotaxanes **P5-32**–**P5-34** revealed that their anti-biofilm activity is only moderately influenced by the length and structure of the central axle of the rotaxanes. Importantly, their mechanism of action does not involve bactericidal effects, providing a distinct and innovative approach to combating *P. aeruginosa* infections. This research highlights the potential of mechanically interlocked molecules like glyco[2]rotaxanes as promising tools in the fight against biofilm-related challenges, offering a new avenue to address infections caused by bacteria such as *P. aeruginosa*.

CHALLENGES AND FUTURE PROSPECTS

Despite the exciting advancements in the field, challenges remain and continued research is required to improve their biocompatibility and efficacy in biological systems. Additionally, the design of multifunctional pillar[*n*]arenes, capable of integrating various functionalities, will open up new possibilities

https://doi.org/10.1021/acsinfecdis.3c00697
ACS Infect. Dis. XXXX, XXX, XXX−XXX

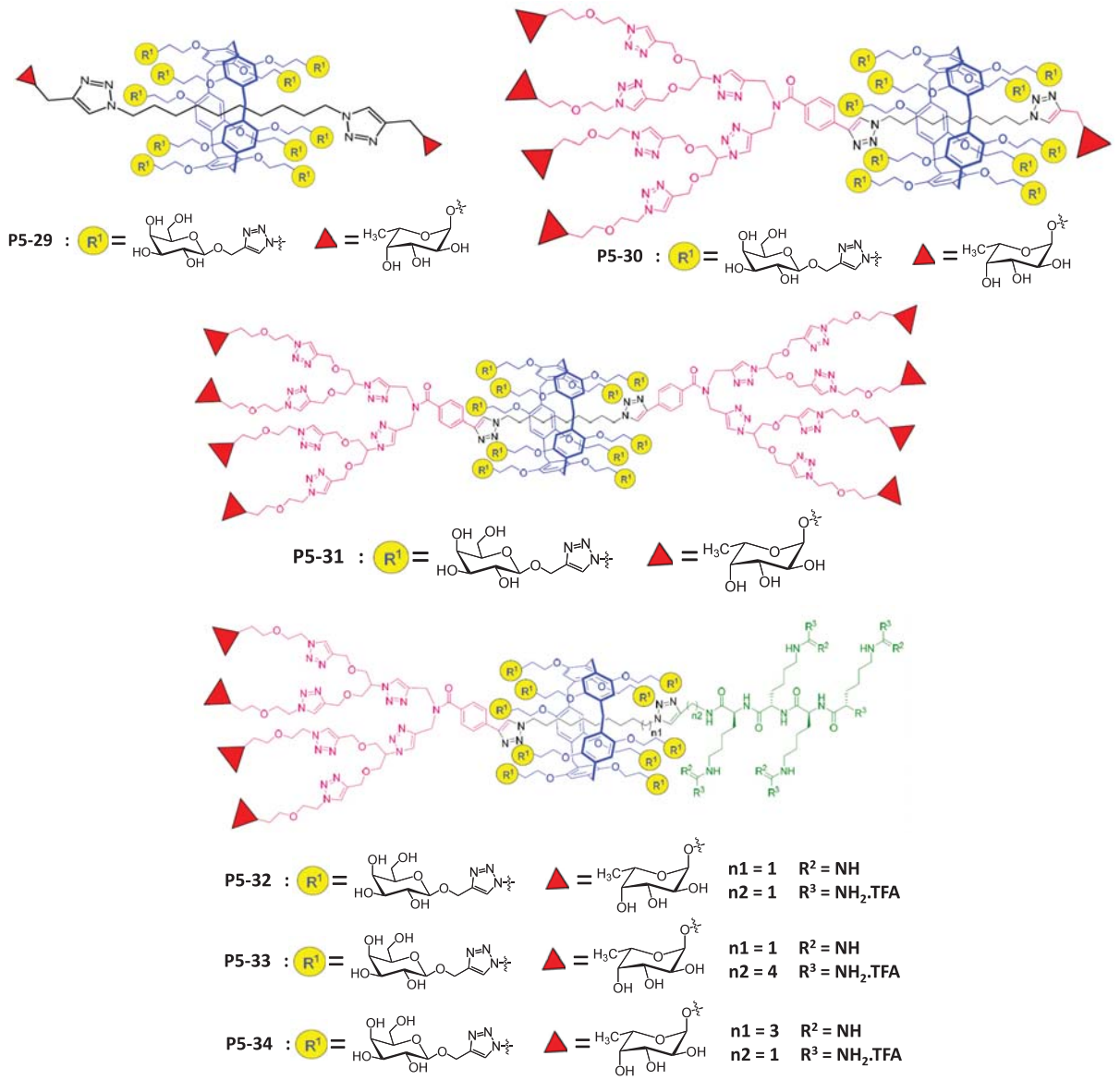

Figure 11. Molecular structures of **P5-29**−**P5-34**. Adapted with permission from ref 90. Copyright 2021 American Chemical Society.

for advanced applications. While current developments in using pillar[*n*]arenes against biofilms are promising, there are several challenges that need to be addressed: While studies have shown encouraging results *in vitro*, the effectiveness of pillar[*n*]arenes as biofilm disruptors *in vivo* remains to be fully elucidated. Further research is needed to evaluate their performance in animal models and eventually in clinical trials. The successful application of pillar[*n*]arenes as biofilm disruptors will depend on the development of suitable formulations and delivery methods. Ensuring the stability and controlled release of these molecules at the site of infection is crucial for their therapeutic potential. Biofilms are highly heterogeneous structures, and their response to treatment can vary significantly. Designing pillar[*n*]arenes that can target a wide range of biofilm types and adapt to the complexities of different biofilm environments will be essential for their widespread applicability.

Tackling infections associated with biofilms presents a complex challenge in the field of antibacterial research. One of the central challenges revolves around the development of anti-biofilm agents that can specifically target and disrupt biofilms without inadvertently affecting the growth and viability of the bacteria themselves.[91] Non-antimicrobial anti-biofilm agents offer a promising avenue as these agents aim to disrupt the formation, maintenance, or structural integrity of biofilms without necessarily exerting direct antimicrobial activity. By targeting the unique aspects of biofilm development, such agents may represent a breakthrough in combating biofilm-associated infections. Strategies may include interference with quorum sensing, disruption of extracellular polymeric substances, or the modulation of bacterial adhesion mechanisms. This level of selectivity is crucial, as it aims to spare beneficial bacteria and safeguard the well-being of human cells during treatment.

https://doi.org/10.1021/acsinfecdis.3c00697
ACS Infect. Dis. XXXX, XXX, XXX−XXX

Achieving precision in targeting biofilms while sparing other essential biological entities is of paramount importance. In pursuit of this selectivity, recent studies have delved into the intricate task of optimizing the chemical characteristics of cationic pillar[*n*]arenes. These investigations have underscored the critical need for a comprehensive understanding of the specific chemical attributes that are most conducive to effective anti-biofilm action. The challenge at hand lies in the meticulous identification of the precise combination of cationic functionalities, the level of hydrophobicity, and the appropriate arrangement of positive charges that collectively optimizes the potential of anti-biofilm agents. Additionally, a common hurdle in the field of antibacterial research pertains to the broad cytotoxicity associated with quaternary ammonium compounds. These compounds, while effective against bacteria, often exhibit a range of detrimental effects on various cells, including human cells. Addressing this issue presents a dual challenge: reducing the cytotoxicity of these compounds while preserving their antibacterial potency. Future research endeavors should be directed toward developing strategies that strike this delicate balance, allowing for effective antibacterial action without causing harm to other biological components. Biofilm resistance is yet another formidable challenge that confronts researchers in the battle against bacterial infections. Biofilms possess an inherent ability to develop resistance to conventional antibacterial agents, rendering many treatment approaches less effective over time. Overcoming this biofilm resistance is a pressing concern that calls for a deep understanding of the mechanisms that biofilms employ to thwart eradication efforts. Finding innovative strategies to circumvent these resistance mechanisms is pivotal in the pursuit of successful anti-biofilm treatments. Furthermore, a critical consideration in the development of anti-biofilm materials is their safety for use in biomedical applications. While these materials may exhibit promising anti-biofilm properties, it is imperative that they are biocompatible and do not pose any harm to normal cells. Ensuring the biocompatibility of anti-biofilm materials is a significant challenge that must be addressed to pave the way for their application in medical contexts.

The concept of selective toxicity, particularly in the context of pathogenic biofilms, offers a promising avenue for the development of more targeted antibacterial approaches. This selectivity is rooted in the ability of anti-biofilm agents to specifically target and harm the biofilms formed by pathogenic bacteria while sparing mammalian cells. The significance of this approach lies in its potential to minimize harm to human tissues and cells during treatment, making antibacterial therapies safer and more precise. Future developments in this direction are poised to revolutionize antibacterial treatments by further enhancing their safety and efficacy. A comprehensive understanding of these interactions is vital for designing anti-biofilm agents that can more effectively disrupt and eradicate biofilms. This knowledge will enable the development of anti-biofilm agents that are highly specific in their action, targeting the structural and molecular components of biofilms with precision.

Furthermore, studies in this field should emphasize the importance of combining anti-biofilm agents with traditional antibiotics. The rationale behind this approach is that the synergy between anti-biofilm agents and antibiotics can potentially lead to a more robust and effective antibacterial strategy. While supramolecular anti-biofilm agents target the biofilms themselves, traditional antibiotics can focus on planktonic bacteria within the biofilm matrix. This dual-pronged approach has the potential to offer a synergistic enhancement to disrupting biofilms and eradicating bacterial infections. These endeavors aim to make antibacterial therapies safer, more targeted, and more potent in their ability to combat biofilm-associated infections.

In conclusion, pillar[*n*]arenes hold significant promise as biofilm disruptors due to their unique structural features and inherent antimicrobial activity. However, further research and development are needed to fully harness their potential as effective and safe agents in the fight against biofilms. With continued advancements and innovative strategies, we envisage that pillar[*n*]arenes may pave the way for more efficient and targeted biofilm control in various industrial, medical, and environmental applications.

AUTHOR INFORMATION

Corresponding Authors

Murugan Arunachalam − *Department of Chemistry, The Gandhigram Rural Institute (Deemed to be University), Dindigul, Tamil Nadu 624 302, India;* orcid.org/0000-0002-6573-7797; Email: chemarun81@gmail.com, m.arunachalam@ruraluniv.ac.in

Kavitha Dhandapani − *Department of Biochemistry, Biotechnology and Bioinformatics, Avinashilingam Institute for Home Science and Higher Education for Women, Coimbatore, Tamil Nadu 641 043, India;* orcid.org/0000-0002-7498-6082; Email: kavitha_bio@avinuty.ac.in

Authors

Sekar Jothi Nayaki − *Department of Biochemistry, Biotechnology and Bioinformatics, Avinashilingam Institute for Home Science and Higher Education for Women, Coimbatore, Tamil Nadu 641 043, India*

Arivazhagan Roja − *Department of Chemistry, The Gandhigram Rural Institute (Deemed to be University), Dindigul, Tamil Nadu 624 302, India*

Ramya Ravindhiran − *Department of Biochemistry, Biotechnology and Bioinformatics, Avinashilingam Institute for Home Science and Higher Education for Women, Coimbatore, Tamil Nadu 641 043, India*

Karthiga Sivarajan − *Department of Biochemistry, Biotechnology and Bioinformatics, Avinashilingam Institute for Home Science and Higher Education for Women, Coimbatore, Tamil Nadu 641 043, India*

Complete contact information is available at: https://pubs.acs.org/10.1021/acsinfecdis.3c00697

Notes

The authors declare no competing financial interest.

ACKNOWLEDGMENTS

The authors acknowledge the Council of Scientific and Industrial Research [01(3001)/19/EMR-II] for financial assistance.

REFERENCES

(1) Chinemerem Nwobodo, D.; Ugwu, M. C.; Oliseloke Anie, C.; Al-Ouqaili, M. T. S.; Chinedu Ikem, J.; Victor Chigozie, U.; Saki, M. Antibiotic resistance: The challenges and some emerging strategies for tackling a global menace. *J. Clin. Lab. Anal.* **2022**, *36* (9), e24655.

(2) Salam, M. A.; Al-Amin, M. Y.; Salam, M. T.; Pawar, J. S.; Akhter, N.; Rabaan, A. A.; Alqumber, M. A. A. Antimicrobial Resistance: A

Growing Serious Threat for Global Public Health. *Healthcare* **2023**, *11* (13), 1946.
(3) Petchiappan, A.; Chatterji, D. Antibiotic Resistance: Current Perspectives. *ACS Omega* **2017**, *2* (10), 7400−7409.
(4) Sauer, K.; Stoodley, P.; Goeres, D. M.; Hall-Stoodley, L.; Burmølle, M.; Stewart, P. S.; Bjarnsholt, T. The biofilm life cycle: expanding the conceptual model of biofilm formation. *Nat. Rev. Microbiol.* **2022**, *20* (10), 608−620.
(5) Flemming, H.-C.; Neu, T. R.; Wozniak, D. J. The EPS Matrix: The "House of Biofilm Cells. *J. Bacteriol.* **2007**, *189* (22), 7945−7947.
(6) Penesyan, A.; Paulsen, I. T.; Kjelleberg, S.; Gillings, M. R. Three faces of biofilms: a microbial lifestyle, a nascent multicellular organism, and an incubator for diversity. *npj Biofilms Microbiomes* **2021**, *7* (1), 80.
(7) Prakash, B.; Veeregowda, B. M.; Krishnappa, G. Biofilms: A survival strategy of bacteria. *Curr. Sci.* **2003**, *85* (9), 1299−1307.
(8) Sharma, D.; Misba, L.; Khan, A. U. Antibiotics versus biofilm: an emerging battleground in microbial communities. *Antimicrob. Resist. Infect. Control* **2019**, *8* (1), 76.
(9) Bjarnsholt, T. The role of bacterial biofilms in chronic infections. *APMIS* **2013**, *121* (s136), 1−58.
(10) Siva, N. Understanding biofilms—are we getting closer? *Lancet Infect. Dis.* **2009**, *9* (4), 216.
(11) Wang, S.; Zhao, Y.; Breslawec, A. P.; Liang, T.; Deng, Z.; Kuperman, L. L.; Yu, Q. Strategy to combat biofilms: a focus on biofilm dispersal enzymes. *npj Biofilms Microbiomes* **2023**, *9* (1), 63.
(12) Joo, H.-S.; Otto, M. Molecular Basis of In Vivo Biofilm Formation by Bacterial Pathogens. *Chem. Biol.* **2012**, *19* (12), 1503−1513.
(13) Davies, D. Understanding biofilm resistance to antibacterial agents. *Nat. Rev. Drug Discovery* **2003**, *2* (2), 114−122.
(14) Stewart, P. S.; William Costerton, J. Antibiotic resistance of bacteria in biofilms. *Lancet* **2001**, *358* (9276), 135−138.
(15) Sharma, S.; Mohler, J.; Mahajan, S. D.; Schwartz, S. A.; Bruggemann, L.; Aalinkeel, R. Microbial Biofilm: A Review on Formation, Infection, Antibiotic Resistance, Control Measures, and Innovative Treatment. *Microorganisms* **2023**, *11* (6), 1614.
(16) Thorn, C. R.; Howell, P. L.; Wozniak, D. J.; Prestidge, C. A.; Thomas, N. Enhancing the therapeutic use of biofilm-dispersing enzymes with smart drug delivery systems. *Adv. Drug Delivery Rev.* **2021**, *179*, 113916.
(17) Borges, A.; Meireles, A.; Mergulhão, F.; Melo, L.; Simões, M. Biofilm control with enzymes. In *Recent Trends in Biofilm Science and Technology*, Simoes, M., Borges, A., Chaves Simoes, L., Eds.; Academic Press: 2020; Chapter 11, pp 249−271.
(18) Ramakrishnan, R.; Singh, A. K.; Singh, S.; Chakravortty, D.; Das, D. Enzymatic dispersion of biofilms: An emerging biocatalytic avenue to combat biofilm-mediated microbial infections. *J. Biol. Chem.* **2022**, *298* (9), 102352.
(19) Jee, S.-C.; Kim, M.; Sung, J.-S.; Kadam, A. A. Efficient Biofilms Eradication by Enzymatic-Cocktail of Pancreatic Protease Type-I and Bacterial α-Amylase. *Polymers* **2020**, *12* (12), 3032.
(20) Soukarieh, F.; Gurnani, P.; Romero, M.; Halliday, N.; Stocks, M.; Alexander, C.; Cámara, M. Design of Quorum Sensing Inhibitor−Polymer Conjugates to Penetrate Pseudomonas aeruginosa Biofilms. *ACS Macro Lett.* **2023**, *12* (3), 314−319.
(21) Vadakkan, K. Molecular Mechanism of Bacterial Quorum Sensing and Its Inhibition by Target Specific Approaches. In *Quorum Sensing: Microbial Rules of Life*; Dhiman, S. S., Ed.; ACS Symposium Series; American Chemical Society: 2020; Vol. *1374*, pp 221−234.
(22) Chen, Y.; Gao, Y.; Huang, Y.; Jin, Q.; Ji, J. Inhibiting Quorum Sensing by Active Targeted pH-Sensitive Nanoparticles for Enhanced Antibiotic Therapy of Biofilm-Associated Bacterial Infections. *ACS Nano* **2023**, *17* (11), 10019−10032.
(23) Solano, C.; Echeverz, M.; Lasa, I. Biofilm dispersion and quorum sensing. *Curr. Opin. Microbiol.* **2014**, *18*, 96−104.
(24) Khan, A.; Wahl, L. M.; Yu, P. In Phage Therapy and Antibiotics for Biofilm Eradication: A Predictive Model. In *Recent Advances in Mathematical and Statistical Methods*; Kilgour, D. M., Kunze, H., Makarov, R., Melnik, R., Wang, X., Eds.; Springer International Publishing: Cham, 2018; pp 375−383.
(25) Pires, D. P.; Meneses, L.; Brandão, A. C.; Azeredo, J. An overview of the current state of phage therapy for the treatment of biofilm-related infections. *Curr. Opin. Virol.* **2022**, *53*, 101209.
(26) Liu, S.; Lu, H.; Zhang, S.; Shi, Y.; Chen, Q. Phages against Pathogenic Bacterial Biofilms and Biofilm-Based Infections: A Review. *Pharmaceutics* **2022**, *14* (2), 427.
(27) Chang, C.; Yu, X.; Guo, W.; Guo, C.; Guo, X.; Li, Q.; Zhu, Y. Bacteriophage-Mediated Control of Biofilm: A Promising New Dawn for the Future. *Front. Microbiol.* **2022**, *13*, 825828.
(28) Wang, Y.; Ping, G.; Li, C. Efficient complexation between pillar[5]arenes and neutral guests: from host−guest chemistry to functional materials. *Chem. Commun.* **2016**, *52* (64), 9858−9872.
(29) Tuo, W.; Sun, Y.; Lu, S.; Li, X.; Sun, Y.; Stang, P. J. Pillar[5]arene-Containing Metallacycles and Host−Guest Interaction Caused Aggregation-Induced Emission Enhancement Platforms. *J. Am. Chem. Soc.* **2020**, *142* (40), 16930−16934.
(30) Strutt, N. L.; Forgan, R. S.; Spruell, J. M.; Botros, Y. Y.; Stoddart, J. F. Monofunctionalized Pillar[5]arene as a Host for Alkanediamines. *J. Am. Chem. Soc.* **2011**, *133* (15), 5668−5671.
(31) Ogoshi, T.; Yamagishi, T. -a.; Nakamoto, Y. Pillar-Shaped Macrocyclic Hosts Pillar[n]arenes: New Key Players for Supramolecular Chemistry. *Chem. Rev.* **2016**, *116* (14), 7937−8002.
(32) Kiruthika, J.; Boominathan, M.; Srividhya, S.; Ajitha, V.; Arunachalam, M. Pillar[4]arene[1]quinone-based pseudo[3]rotaxanes by cooperative Host-Guest binding. *Supramol. Chem.* **2021**, *33* (7), 390−399.
(33) Guo, F.; Sun, Y.; Xi, B.; Diao, G. Recent progress in the research on the host-guest chemistry of pillar[n]arenes. *Supramol. Chem.* **2018**, *30* (2), 81−92.
(34) Boominathan, M.; Kiruthika, J.; Arunachalam, M. Construction of anion-responsive crosslinked polypseudorotaxane based on molecular recognition of pillar[5]arene. *J. Polym. Sci., Part A: Polym. Chem.* **2019**, *57* (14), 1508−1515.
(35) Kato, K.; Fa, S.; Ohtani, S.; Shi, T. -h.; Brouwer, A. M.; Ogoshi, T. Noncovalently bound and mechanically interlocked systems using pillar[n]arenes. *Chem. Soc. Rev.* **2022**, *51* (9), 3648−3687.
(36) Song, N.; Kakuta, T.; Yamagishi, T. -a.; Yang, Y.-W.; Ogoshi, T. Molecular-Scale Porous Materials Based on Pillar[n]arenes. *Chem.* **2018**, *4* (9), 2029−2053.
(37) Song, N.; Lou, X.-Y.; Ma, L.; Gao, H.; Yang, Y.-W. Supramolecular nanotheranostics based on pillarenes. *Theranostics* **2019**, *9* (11), 3075−3093.
(38) Qi, X.-N.; Lin, Q.; Wei, T.-B.; Tian, W.; Li, Z.-L. Pillar[5]arene-based supramolecular gel: construction and applications. *Polym. Chem.* **2023**, *14* (13), 1414−1446.
(39) Wang, Y.; Pei, Z.; Feng, W.; Pei, Y. Stimuli-responsive supramolecular nano-systems based on pillar[n]arenes and their related applications. *J. Mater. Chem. B* **2019**, *7* (48), 7656−7675.
(40) Zhang, H.; Liu, Z.; Zhao, Y. Pillararene-based self-assembled amphiphiles. *Chem. Soc. Rev.* **2018**, *47* (14), 5491−5528.
(41) Xiao, T.; Qi, L.; Zhong, W.; Lin, C.; Wang, R.; Wang, L. Stimuli-responsive nanocarriers constructed from pillar[n]arene-based supra-amphiphiles. *Mater. Chem. Fron.* **2019**, *3* (10), 1973−1993.
(42) Chen, Y.-Y.; Jiang, X.-M.; Gong, G.-F.; Yao, H.; Zhang, Y.-M.; Wei, T.-B.; Lin, Q. Pillararene-based AIEgens: research progress and appealing applications. *Chem. Commun.* **2021**, *57* (3), 284−301.
(43) Chen, J.-F.; Lin, Q.; Zhang, Y.-M.; Yao, H.; Wei, T.-B. Pillararene-based fluorescent chemosensors: recent advances and perspectives. *Chem. Commun.* **2017**, *53* (100), 13296−311.
(44) Xiao, T.; Zhong, W.; Xu, L.; Sun, X.-Q.; Hu, X.-Y.; Wang, L. Supramolecular vesicles based on pillar[n]arenes: design, construction, and applications. *Org. Biomol. Chem.* **2019**, *17* (6), 1336−1350.
(45) Khalil-Cruz, L. E.; Liu, P.; Huang, F.; Khashab, N. M. Multifunctional Pillar[n]arene-Based Smart Nanomaterials. *ACS Appl. Mater. Interfaces* **2021**, *13* (27), 31337−31354.

https://doi.org/10.1021/acsinfecdis.3c00697
ACS Infect. Dis. XXXX, XXX, XXX−XXX

(46) Kiruthika, J.; Arunachalam, M. Pillar[5]arene-based cross-linked polymer for the rapid adsorption of iodine from water and vapor phases. *Polymer* **2022**, *259*, 125322.
(47) Boominathan, M.; Arunachalam, M. Formation of Supramolecular Polymer Network and Single-Chain Polymer Nanoparticles via Host−Guest Complexation from Pillar[5]arene Pendant Polymer. *ACS Appl. Polym. Mater.* **2020**, *2* (11), 4368−4372.
(48) Yang, K.; Yang, K.; Chao, S.; Wen, J.; Pei, Y.; Pei, Z. A supramolecular hybrid material constructed from pillar[6]arene-based host−guest complexation and ZIF-8 for targeted drug delivery. *Chem. Commun.* **2018**, *54* (70), 9817−9820.
(49) Wu, D.; Li, Y.; Shen, J.; Tong, Z.; Hu, Q.; Li, L.; Yu, G. Supramolecular chemotherapeutic drug constructed from pillararene-based supramolecular amphiphile. *Chem. Commun.* **2018**, *54* (59), 8198−8201.
(50) Cao, S.; Zhou, L.; Liu, C.; Zhang, H.; Zhao, Y.; Zhao, Y. Pillararene-based self-assemblies for electrochemical biosensors. *Biosens. Bioelectron.* **2021**, *181*, 113164.
(51) Ping, G.; Wang, Y.; Shen, L.; Wang, Y.; Hu, X.; Chen, J.; Hu, B.; Cui, L.; Meng, Q.; Li, C. Highly efficient complexation of sanguinarine alkaloid by carboxylatopillar[6]arene: pKa shift, increased solubility and enhanced antibacterial activity. *Chem. Commun.* **2017**, *53* (53), 7381−7384.
(52) Peng, H.; Xie, B.; Yang, X.; Dai, J.; Wei, G.; He, Y. Pillar[5]arene-based, dual pH and enzyme responsive supramolecular vesicles for targeted antibiotic delivery against intracellular MRSA. *Chem. Commun.* **2020**, *56* (58), 8115−8118.
(53) Shu, X.; Xu, K.; Hou, D.; Li, C. Molecular Recognition of Water-soluble Pillar[n]arenes Towards Biomolecules and Drugs. *Isr. J. Chem.* **2018**, *58* (11), 1230−1240.
(54) Peng, H.; Xie, B.; Cen, X.; Dai, J.; Dai, Y.; Yang, X.; He, Y. Glutathione-responsive multifunctional nanoparticles based on mannose-modified pillar[5]arene for targeted antibiotic delivery against intracellular methicillin-resistant S. aureus. *Mater. Chem. Front.* **2022**, *6* (3), 360−367.
(55) Liu, L.; Zhou, Q.; He, Q.; Duan, W.; Huang, Y. A pH-Responsive Supramolecular Drug Delivery System Constructed by Cationic Pillar[5]arene for Enhancing Antitumor Activity. *Front. Chem.* **2021**, *9*, 661143.
(56) JothiNayaki, S.; Ramya, R.; Srividhya, S.; Kiruthika, J.; Ramya, K.; Karthiga, S.; Arunachalam, M.; Kavitha, D. Antibacterial potentials of pillar[5]arene, pillar[4]arene[1]quinone derivative and their isatin inclusion complexes. *Supramol. Chem.* **2021**, *33* (12), 701−708.
(57) Sathiyajith, C.; Shaikh, R. R.; Han, Q.; Zhang, Y.; Meguellati, K.; Yang, Y.-W. Biological and related applications of pillar[n]arenes. *Chem. Commun.* **2017**, *53* (4), 677−696.
(58) Feng, W.; Jin, M.; Yang, K.; Pei, Y.; Pei, Z. Supramolecular delivery systems based on pillararenes. *Chem. Commun.* **2018**, *54* (97), 13626−13640.
(59) Zhang, H.; Ma, X.; Nguyen, K. T.; Zhao, Y. Biocompatible Pillararene-Assembly-Based Carriers for Dual Bioimaging. *ACS Nano* **2013**, *7* (9), 7853−7863.
(60) Zhou, L.; Cao, S.; Liu, C.; Zhang, H.; Zhao, Y. Pillar[n]arene-based polymeric systems for biomedical applications. *Coord. Chem. Rev.* **2023**, *491*, 215260.
(61) Shurpik, D. N.; Aleksandrova, Y. I.; Mostovaya, O. A.; Nazmutdinova, V. A.; Zelenikhin, P. V.; Subakaeva, E. V.; Mukhametzyanov, T. A.; Cragg, P. J.; Stoikov, I. I. Water-soluble pillar[5]arene sulfo-derivatives self-assemble into biocompatible nanosystems to stabilize therapeutic proteins. *Bioorg. Chem.* **2021**, *117*, 105415.
(62) Cragg, P. J. Pillar[n]arenes at the Chemistry-Biology Interface. *Isr. J. Chem.* **2018**, *58* (11), 1194−1208.
(63) Feng, W.-X.; Sun, Z.; Barboiu, M. Pillar[n]arenes for Construction of Artificial Transmembrane Channels. *Isr. J. Chem.* **2018**, *58* (11), 1209−1218.
(64) Chen, L.; Si, W.; Zhang, L.; Tang, G.; Li, Z.-T.; Hou, J.-L. Chiral Selective Transmembrane Transport of Amino Acids through Artificial Channels. *J. Am. Chem. Soc.* **2013**, *135* (6), 2152−2155.
(65) Xin, P.; Sun, Y.; Kong, H.; Wang, Y.; Tan, S.; Guo, J.; Jiang, T.; Dong, W.; Chen, C.-P. A unimolecular channel formed by dual helical peptide modified pillar[5]arene: correlating transmembrane transport properties with antimicrobial activity and haemolytic toxicity. *Chem. Commun.* **2017**, *53* (83), 11492−11495.
(66) Xin, P.; Zhao, L.; Mao, L.; Xu, L.; Hou, S.; Kong, H.; Fang, H.; Zhu, H.; Jiang, T.; Chen, C.-P. Effect of charge status on the ion transport and antimicrobial activity of synthetic channels. *Chem. Commun.* **2020**, *56* (89), 13796−13799.
(67) Andrei, I. M.; Chen, W.; Baaden, M.; Vincent, S. P.; Barboiu, M. Proton- versus Cation-Selective Transport of Saccharide Rim-Appended Pillar[5]arene Artificial Water Channels. *J. Am. Chem. Soc.* **2023**, *145* (40), 21904−21914.
(68) Barbera, L.; De Plano, L. M.; Franco, D.; Gattuso, G.; Guglielmino, S. P. P.; Lando, G.; Notti, A.; Parisi, M. F.; Pisagatti, I. Antiadhesive and antibacterial properties of pillar[5]arene-based multilayers. *Chem. Commun.* **2018**, *54* (72), 10203−10206.
(69) Qi, Z.; Achazi, K.; Haag, R.; Dong, S.; Schalley, C. A. Supramolecular hydrophobic guest transport system based on pillar[5]arene. *Chem. Commun.* **2015**, *51* (51), 10326−10329.
(70) Yao, Y.; Wang, Y.; Zhao, R.; Shao, L.; Tang, R.; Huang, F. Improved in vivo tumor therapy via host−guest complexation. *J. Mater. Chem. B* **2016**, *4* (15), 2691−2696.
(71) Wheate, N. J.; Dickson, K.-A.; Kim, R. R.; Nematollahi, A.; Macquart, R. B.; Kayser, V.; Yu, G.; Church, W. B.; Marsh, D. J. Host-Guest Complexes of Carboxylated Pillar[n]arenes With Drugs. *J. Pharm. Sci.* **2016**, *105* (12), 3615−3625.
(72) Dey, R.; De, K.; Mukherjee, R.; Ghosh, S.; Haldar, J. Small antibacterial molecules highly active against drug-resistant Staphylococcus aureus. *MedChemComm* **2019**, *10* (11), 1907−1915.
(73) Hoque, J.; Konai, M. M.; Sequeira, S. S.; Samaddar, S.; Haldar, J. Antibacterial and Antibiofilm Activity of Cationic Small Molecules with Spatial Positioning of Hydrophobicity: An in Vitro and in Vivo Evaluation. *J. Med. Chem.* **2016**, *59* (23), 10750−10762.
(74) Seferyan, M. A.; Saverina, E. A.; Frolov, N. A.; Detusheva, E. V.; Kamanina, O. A.; Arlyapov, V. A.; Ostashevskaya, I. I.; Ananikov, V. P.; Vereshchagin, A. N. Multicationic Quaternary Ammonium Compounds: A Framework for Combating Bacterial Resistance. *ACS Infect. Dis.* **2023**, *9* (6), 1206−1220.
(75) Jennings, M. C.; Minbiole, K. P. C.; Wuest, W. M. Quaternary Ammonium Compounds: An Antimicrobial Mainstay and Platform for Innovation to Address Bacterial Resistance. *ACS Infect. Dis.* **2015**, *1* (7), 288−303.
(76) Saverina, E. A.; Frolov, N. A.; Kamanina, O. A.; Arlyapov, V. A.; Vereshchagin, A. N.; Ananikov, V. P. From Antibacterial to Antibiofilm Targeting: An Emerging Paradigm Shift in the Development of Quaternary Ammonium Compounds (QACs). *ACS Infect. Dis.* **2023**, *9* (3), 394−422.
(77) Joseph, R.; Naugolny, A.; Feldman, M.; Herzog, I. M.; Fridman, M.; Cohen, Y. Cationic Pillararenes Potently Inhibit Biofilm Formation without Affecting Bacterial Growth and Viability. *J. Am. Chem. Soc.* **2016**, *138* (3), 754−757.
(78) Kaizerman-Kane, D.; Hadar, M.; Joseph, R.; Logviniuk, D.; Zafrani, Y.; Fridman, M.; Cohen, Y. Design Guidelines for Cationic Pillar[n]arenes that Prevent Biofilm Formation by Gram-Positive Pathogens. *ACS Infect. Dis.* **2021**, *7* (3), 579−585.
(79) Yang, H.; Jin, L.; Zhao, D.; Lian, Z.; Appu, M.; Huang, J.; Zhang, Z. Antibacterial and Antibiofilm Formation Activities of Pyridinium-Based Cationic Pillar[5]arene Against Pseudomonas aeruginosa. *J. Agric. Food Chem.* **2021**, *69* (14), 4276−4283.
(80) Joseph, R.; Kaizerman, D.; Herzog, I. M.; Hadar, M.; Feldman, M.; Fridman, M.; Cohen, Y. Phosphonium pillar[5]arenes as a new class of efficient biofilm inhibitors: importance of charge cooperativity and the pillar platform. *Chem. Commun.* **2016**, *52* (70), 10656−10659.
(81) Gao, L.; Li, M.; Ehrmann, S.; Tu, Z.; Haag, R. Positively Charged Nanoaggregates Based on Zwitterionic Pillar[5]arene that Combat Planktonic Bacteria and Disrupt Biofilms. *Angew. Chem., Int. Ed.* **2019**, *58* (11), 3645−3649.

https://doi.org/10.1021/acsinfecdis.3c00697
ACS Infect. Dis. XXXX, XXX, XXX−XXX

(82) Aleksandrova, Y. I.; Shurpik, D. N.; Nazmutdinova, V. A.; Mostovaya, O. A.; Subakaeva, E. V.; Sokolova, E. A.; Zelenikhin, P. V.; Stoikov, I. I. Toward Pathogenic Biofilm Suppressors: Synthesis of Amino Derivatives of Pillar[5]arene and Supramolecular Assembly with DNA. *Pharmaceutics* **2023**, *15* (2), 476.
(83) Li, Y.; Wen, J.; Li, J.; Wu, Z.; Li, W.; Yang, K. Recent Applications of Pillar[n]arene-Based Host−Guest Recognition in Chemosensing and Imaging. *ACS Sens.* **2021**, *6* (11), 3882−3897.
(84) Li, W.; Xu, W.; Zhang, S.; Li, J.; Zhou, J.; Tian, D.; Cheng, J.; Li, H. Supramolecular Biopharmaceutical Carriers Based on Host−Guest Interactions. *J. Agric. Food Chem.* **2022**, *70* (40), 12746−12759.
(85) Jonkergouw, C.; Beyeh, N. K.; Osmekhina, E.; Leskinen, K.; Taimoory, S. M.; Fedorov, D.; Anaya-Plaza, E.; Kostiainen, M. A.; Trant, J. F.; Ras, R. H. A.; Saavalainen, P.; Linder, M. B. Repurposing host-guest chemistry to sequester virulence and eradicate biofilms in multidrug resistant Pseudomonas aeruginosa and Acinetobacter baumannii. *Nat. Commun.* **2023**, *14* (1), 2141.
(86) Guo, S.; Huang, Q.; Chen, Y.; Wei, J.; Zheng, J.; Wang, L.; Wang, Y.; Wang, R. Synthesis and Bioactivity of Guanidinium-Functionalized Pillar[5]arene as a Biofilm Disruptor. *Angew. Chem., Int. Ed.* **2021**, *60* (2), 618−623.
(87) Du, X.; Ma, M.; Zhang, Y.; Yu, X.; Chen, L.; Zhang, H.; Meng, Z.; Jia, X.; Chen, J.; Meng, Q.; Li, C. Synthesis of Cationic Biphen[4,5]arenes as Biofilm Disruptors. *Angew. Chem., Int. Ed.* **2023**, *62* (21), e202301857.
(88) Xia, L.; Tian, J.; Yue, T.; Cao, H.; Chu, J.; Cai, H.; Zhang, W. Pillar[5]arene-Based Acid-Triggered Supramolecular Porphyrin Photosensitizer for Combating Bacterial Infections and Biofilm Dispersion. *Adv. Healthc. Mater.* **2022**, *11* (4), 2102015.
(89) Shurpik, D. N.; Aleksandrova, Y. I.; Mostovaya, O. A.; Nazmutdinova, V. A.; Tazieva, R. E.; Murzakhanov, F. F.; Gafurov, M. R.; Zelenikhin, P. V.; Subakaeva, E. V.; Sokolova, E. A.; Gerasimov, A. V.; Gorodov, V. V.; Islamov, D. R.; Cragg, P. J.; Stoikov, I. I. Self-Healing Thiolated Pillar[5]arene Films Containing Moxifloxacin Suppress the Development of Bacterial Biofilms. *Nanomaterials* **2022**, *12* (9), 1604.
(90) Mohy El Dine, T.; Jimmidi, R.; Diaconu, A.; Fransolet, M.; Michiels, C.; De Winter, J.; Gillon, E.; Imberty, A.; Coenye, T.; Vincent, S. P. Pillar[5]arene-Based Polycationic Glyco[2]rotaxanes Designed as Pseudomonas aeruginosa Antibiofilm Agents. *J. Med. Chem.* **2021**, *64* (19), 14728−14744.
(91) Worthington, R. J.; Richards, J. J.; Melander, C. Small molecule control of bacterial biofilms. *Org. Biomol. Chem.* **2012**, *10* (37), 7457−7474.

https://doi.org/10.1021/acsinfecdis.3c00697
ACS Infect. Dis. XXXX, XXX, XXX−XXX

Supramolecular Chemistry

ISSN: (Print) (Online) Journal homepage: www.tandfonline.com/journals/gsch20

Antibacterial potentials of pillar[5]arene, pillar[4]arene[1]quinone derivative and their isatin inclusion complexes

Sekar JothiNayaki, Ravindhiran Ramya, Sankar Srividhya, Jeyavelraman Kiruthika, Krishnamurthy Ramya, Sivarajan Karthiga, Murugan Arunachalam & Dhandapani Kavitha

To cite this article: Sekar JothiNayaki, Ravindhiran Ramya, Sankar Srividhya, Jeyavelraman Kiruthika, Krishnamurthy Ramya, Sivarajan Karthiga, Murugan Arunachalam & Dhandapani Kavitha (2021) Antibacterial potentials of pillar[5]arene, pillar[4]arene[1]quinone derivative and their isatin inclusion complexes, Supramolecular Chemistry, 33:12, 701-708, DOI: 10.1080/10610278.2023.2173072

To link to this article: https://doi.org/10.1080/10610278.2023.2173072

SUPRAMOLECULAR CHEMISTRY
2021, VOL. 33, NO. 12, 701–708
https://doi.org/10.1080/10610278.2023.2173072

Taylor & Francis
Taylor & Francis Group

Antibacterial potentials of pillar[5]arene, pillar[4]arene[1]quinone derivative and their isatin inclusion complexes

Sekar JothiNayaki[a], Ravindhiran Ramya[a], Sankar Srividhya[b], Jeyavelraman Kiruthika[b], Krishnamurthy Ramya[a], Sivarajan Karthiga[a], Murugan Arunachalam[b] and Dhandapani Kavitha[a]

[a]Department of Biochemistry, Biotechnology and Bioinformatics, Avinashilingam Institute for Home Science and Higher Education for Women, Coimbatore, India; [b]Department of Chemistry, the Gandhigram Rural Institute (Deemed to Be University), Dindigul, India

ABSTRACT

Host–guest complexation of decamethoxypillar[5]arene and difunctionalized pillar[4]arene[1]quinone with isatin were demonstrated by ^{1}H NMR titration experiments. The antibacterial potentials of isatin, decamethoxypillar[5]arene, difunctionalized pillar[4]arene[1]quinone and their isatin inclusion complexes were evaluated against both Gram-positive and Gram-negative bacteria by the well-diffusion method. The results of the antibacterial assay revealed that decamethoxypillar[5]arene displayed very good antibacterial activity than the difunctionalized pillar[4]arene[1]quinone. Isatin inclusion complex of decamethoxypillar[5]arene showed very good antibacterial activity as that of chloramphenicol with *S. aureus, P. aeruginosa, K. pneumoniae* and *E. coli*. Checkerboard assay revealed synergic effects of P[5]A and isatin combinations against selected microorganisms. In silico toxicity predictions suggested the potential of isatin, decamethoxypillar[5]arene and the difunctionalized pillar[4]arene[1]quinone as prospective drug candidates.

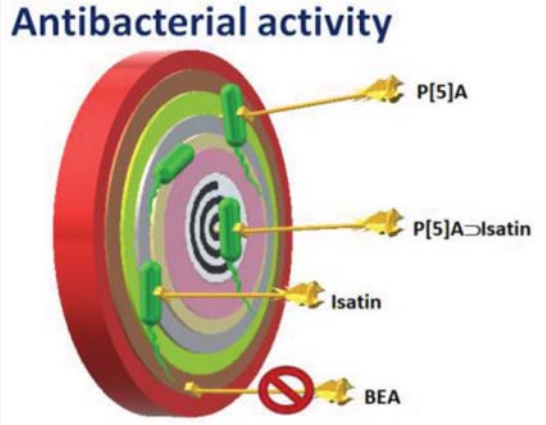

ARTICLE HISTORY
Received 29 March 2022
Accepted 22 January 2023

KEYWORDS
Pillar[5]arene; isatin; antibacterial activity; Host-guest; macrocycle

Introduction

Classical prodrugs mainly consist of covalently linked drug molecules onto molecular systems that impart efficient pharmacokinetic properties than the drug molecule [1]. The main disadvantage of covalent prodrugs is their inefficient release at the target cells. Supramolecular host–guest–based drug delivery systems [2][3] attracted much attention in recent years owing to their control over the encapsulation and delivery of drug molecules depending on the microenvironment. The dynamic and reversible nature of supramolecular interactions imparts salient stimuli-responsive characteristics to supramolecular prodrugs [4]. Several reports are available in the literature demonstrating the use of macrocyclic hosts for encapsulation and stimuli-responsive delivery of drugs [5]. Among various supramolecular hosts, pillar[5]arenes and their derivatives attracted burgeoning interest in the recent past due to their rigid, symmetric and tubular architecture with electron-rich interior cavities capable of encapsulating small molecules *via*

CONTACT Murugan Arunachalam m.arunachalam@ruraluniv.ac.in Department of Chemistry, the Gandhigram Rural Institute (Deemed to Be University), Dindigul, India; Dhandapani Kavitha kavitha_bio@avinuty.ac.in Department of Biochemistry, Biotechnology and Bioinformatics, Avinashilingam Institute for Home Science and Higher Education for Women, Coimbatore, India
Supplemental data for this article can be accessed online at https://doi.org/10.1080/10610278.2023.2173072

supramolecular interactions [6]7,8 [9]. Recent reports revealed the possibility of using pillar[n]arenes for biological and related applications [10] such as artificial transmembrane transporters [11][12],13, cell adhesives [14], DNA binders [15], drug delivery systems [16] and sensors for biologically relevant molecules [17][18]. A very limited number of reports based on pillar[n]arenes and related materials were shown to demonstrate antibacterial activities [19][20] 21–23[24]. For instance, Gao and co-workers demonstrated the antibacterial activity against *E. coli* and *S. aureus* and the biofilm-disrupting property of pillar[5]arene-based zwitterion molecule.[12c] Cohen and co-workers demonstrated the inhibition of biofilm formed by Gram-positive pathogens by cationic pillar[5]arenes [25]. Very recently, Wang et al. showed the synthesis and biofilm disruptor characteristics of guanidinium-functionalised pillar[5]arene against both Gram-positive and Gram-negative pathogens.[12a]

Isatin is one of the high-profile indole-based natural alkaloids abundantly present in plants, and its derivatives reported to show biological activities like antimicrobial, anticonvulsant, anticancer, etc [26]. It is also found as a metabolite derivative of the adrenaline hormone [27]. Herein, we report the host–guest complexation studies of decamethoxypillar[5]arene (**P[5]A**) and difunctionalized pillar[4]arene[1]quinine derivative (**BEA**) with isatin and explored the antibacterial activities of **P[5]A** and its inclusion complex with isatin (**P[5]A⊃isatin**) against Gram-positive and Gram-negative bacteria. We have also studied the antibacterial activities for ethanolamine-functionalised pillar[4]arene[1]quinone derivative (**BEA**) and its isatin inclusion complex, **BEA⊃isatin**. Molecular structures of **P[5]A** [28], **BEA** [29] and **isatin** are shown in Chart 1. Initial investigation by ^{1}H NMR titration experiments suggested the formation of inclusion complexation between **P[5]A** and **isatin** and the stoichiometry of host–guest complexation was probed by ^{1}H NMR titration experiments. ^{1}H NMR titration experiments of **isatin** with **BEA** showed weak complexation with 1:1 host–guest binding stoichiometry. The Well-diffusion method was used to reveal the antimicrobial potentials of **P[5]A, BEA** and their isatin inclusion complexes against both Gram-positive and Gram-negative bacteria. The antibacterial assay showed that **P[5]A** and **P[5]A⊃isatin** exhibited very good antibacterial activity against *S. aureus, P. aeruginosa, K. pneumoniae* and *E. coli* as that of chloramphenicol than **BEA** and **BEA⊃isatin**. In-silico toxicity predictions revealed the potential of isatin, decamethoxypillar[5]arene and the difunctionalized pillar[4]arene[1]quinone as a possible drug candidates against Gram-positive and Gram-negative bacteria.

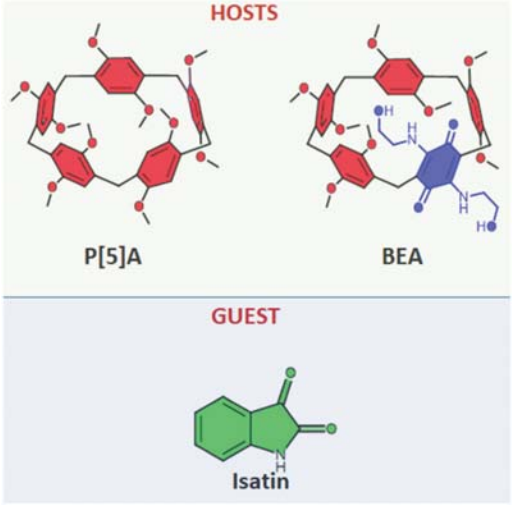

Chart 1. Molecular structures of **P[5]A, BEA** and **isatin**.

Results and discussion

Host–guest complexation studies in solution

The binding affinity of **P[5]A** towards **Isatin** was first tested by ^{1}H NMR titration experiments. Upon mixing the equimolar mixture of **P[5]A** and **Isatin** in $CDCl_3$-acetone-d_6, significant changes in the chemical shift values of both **P[5]A** and **Isatin** were observed (Figure 1). All the aryl–CH protons in isatin have experienced

inclusion-induced deshielding effect upon host–guest complexation. Chemical shifts of H_a, H_b, H_c and H_d of isatin were shifted from 9.95, 7.02, 7.60 and 7.10 to

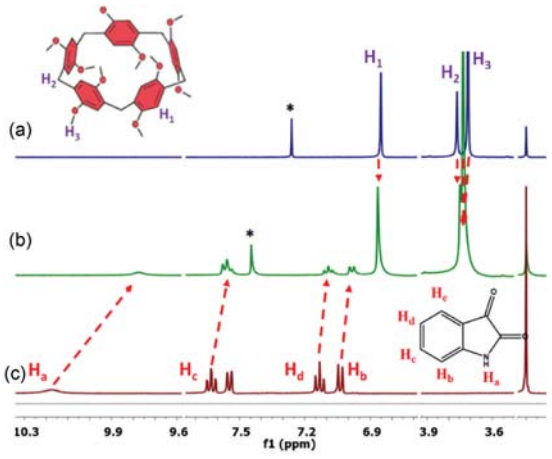

Figure 1. Partial ^{1}H NMR (400 MHz) spectrum of (A) P[5]A, (B) a mixture of P[5]A and isatin and (c) only isatin. *Residual solvent signals.

9.78, 6.99, 7.57 and 7.09 ppm; chemical shifts of aryl –C-H protons of **P[5]A** labelled as H_1 and methoxy protons labelled as H_3 were shifted from 6.87 and 3.72 to 6.86 and 3.74 ppm, respectively (Figure 1). These NMR spectral observations supported the inclusion complex (**P[5]A⊃Isatin**) formation between **P[5]A** and **Isatin**. ^{1}H NMR titration experiments were performed to estimate the binding constants and host–guest binding stoichiometry between **P[5]A** and **Isatin**. Isatin is soluble in acetone and insoluble in chloroform. On the other hand, **P[5]A** is soluble in chloroform and insoluble in acetone. We have attempted to perform ^{1}H NMR experiments in 1:1 v/v mixture of $CDCl_3$/acetone-d_6. Unfortunately, the samples precipitated in NMR tube, which restricted us to perform ^{1}H NMR experiments in a mixed solvent system. Hence, titration experiments (Figure 2A) were performed by adding aliquots of isatin in *acetone-d_6* (81.6 mM) with the constant concentration of $CDCl_3$ solution of **P[5]A** (8 mM) in the NMR tube. Job's plot analysis of the ^{1}H NMR titration data showed 1:1 host–guest binding stoichiometry between **P[5]A** and **Isatin** (Figure S1, see Supporting Information). ^{1}H NMR titration data were fitted for 1:1 host–guest stoichiometry using WINEQNMR2 (Figure S3, see SI) [30]. Association constant log *K* estimated for the binding of **P[5]A** and **isatin** is 3.3 ± 0.4. The plots of mole fraction against equivalents of **isatin** (Figure 2B) show that the equimolar mixture of **P[5]A** and **Isatin** resulted in the formation of almost 80% complexation in solution. The observed binding constant does not solely reflect the host–guest complexation because the ^{1}H NMR titration experiments were performed with varying ratios of $CDCl_3$ and acetone-d_6, and the solvent polarity might also have affected the binding affinity. UV–vis spectroscopic analysis was performed to get further insight on the host–guest complexation between **P[5]A** and **isatin**. UV–Vis spectrum of isatin in 1:1 $CHCl_3$-acetone (v/v) medium displayed a characteristic strong band with maxima at 296 nm and a broad band at 417 nm (Figure 3). Job's plot analysis of the UV–Vis titration data confirmed 1:1 host–guest binding stoichiometry between **P[5]A** and **isatin** (Figure S5).

We also performed host–guest complexation studies between **BEA** and **isatin** by ^{1}H NMR titration experiments. Unlike **P[5]A**, the complexation between **isatin** with **BEA** is very weak and very little changes in chemical shifts were observed in ^{1}H NMR titration experiments (Figure S2) even after the addition of four equivalents of **Isatin** to **BEA**. The weak binding between **Isatin** and **BEA** is reflected in the binding constant value (log K = 2.0 ± 0.6) calculated from ^{1}H NMR titration experiments

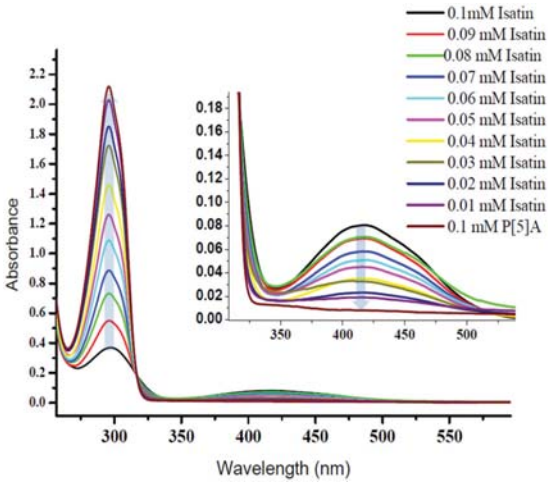

Figure 3. UV-Vis titrations of **P[5]A** (0.1 mM) with varying concentrations of **Isatin** in 1:1 chloroform-acetone mixture.

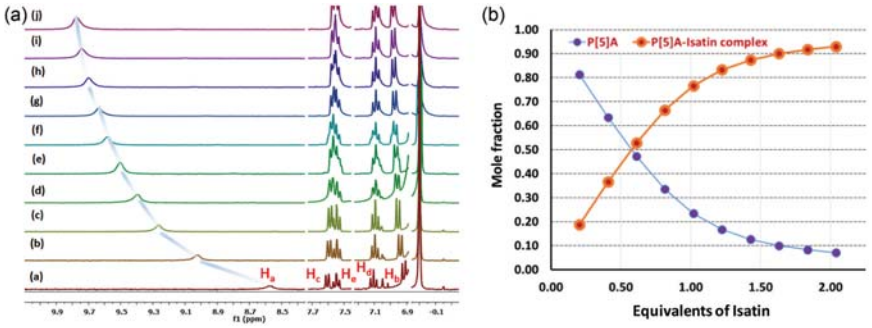

Figure 2. (A) Partial ^{1}H NMR (400 MHz) titration spectra of **P[5]A** (8 mM) with various equivalents of **Isatin** in $CDCl_3$: acetone-d_6 at 25°C. Ratios of [**P[5]A**]/[**Isatin**]: (a) 0.2, (b) 0.4, (c) 0.6, (d) 0.8, (e) 1.0, (f) 1.2, (g) 1.4, (h) 1.6, (i) 1.8 and (j) 2.0. (B) Plots of mole fractions of **P[5]A** (blue) and **P[5]A⊃Isatin** (Orange) versus equivalents of **Isatin.**

plotted against 1:1 stoichiometry using WINEQNMR2. We also probed the host–guest binding of BEA with Isatin by UV–Vis spectroscopic analysis. BEA showed

characteristic absorbance maxima 294 nm and 353 nm in acetone. The addition of aliquots of Isatin to the 10 μM acetone solution of BEA showed a decrease in absorbance intensity at 353 nm and an increase in intensity at 294 nm and 450 nm with clear isobestic points at 328 nm and 304 nm. Job's plot analysis of the UV–Vis titration data showed 1:1 **BEA-Isatin** binding stoichiometry in solution (Figure S6, see Supporting Information).

Antibacterial activities of P[5]A, BEA and their isatin inclusion complexes

The antibacterial activities of P[5]A and P[5]A⊃isatin complex were screened against Gram-positive bacteria (*S. aureus* and *B. subtilis*) and Gram-negative bacteria (*P. aeruginosa, K. pneumoniae, E. coli* and *S. paratyphi A)* using well-diffusion method (Figure 4). Chloramphenicol was used as positive control, and DMSO is monitored as a negative control. The diameter of the zone of inhibition for the **Isatin, P[5]A, P[5]A⊃Isatin, BEA** and **BEA⊃Isatin** against the selected microorganisms are listed in Table 1. It is observed from the zone of inhibition results (Figure 4) that **P[5]A** (7.3 ± 1 mm) and **isatin** (7.7 ± 0.6 mm) alone have good antibacterial activity (Figure S7A, see Supporting Information) against a Gram-positive bacteria *S. aureus* comparable to that of chloramphenicol (6.7 ± 0.6 mm). **P[5]A⊃Isatin** displayed significantly increased antimicrobial inhibition (12.3 ± 0.6 mm) against *S. aureus,* which is almost double the zone of inhibition shown by chloramphenicol. On the other hand, the structurally similar macrocyclic host **BEA** showed poor antibacterial activity (1.7 ± 0.6 mm) against *S. aureus* (Figure S7B). **BEA⊃Isatin** displayed a comparable zone of inhibition as that of isatin and chloramphenicol, which might be due to the presence of isatin in the complex. For another Gram-positive bacteria *B. subtilis*, **Isatin, P[5]A, BEA** and **BEA⊃isatin** complex showed comparatively lesser antibacterial activity than the positive control (Figure S8, see Supporting Information). **P[5]A⊃Isatin** showed comparable antibacterial potential with that of positive control against *B. subtilis* (Figure S8, see Supporting Information). Antibacterial potentials of **Isatin, P[5]A, P[5]A⊃Isatin, BEA** and **BEA⊃Isatin** were also studied for Gram-negative bacteria *P. aeruginosa* (Figure S9, see Supporting Information), *K. pneumoniae* (Figure S10, see Supporting Information), *E.coli* (Figure S11, see Supporting Information) and *S. paratyphi A* (Figure S12, see Supporting Information). The zone of inhibition results suggested that **P[5]A⊃Isatin** showed enhanced antibacterial activity against *P. aeruginosa* (8.7 ± 0.6 mm), *K. pneumoniae* (12.0 ± 0.6 mm) and *E. coli* (11.7 ± 1.2 mm) than positive control and comparable bacterial inhibition against *S. paratyphi A* (7.7 ± 1.2 mm).

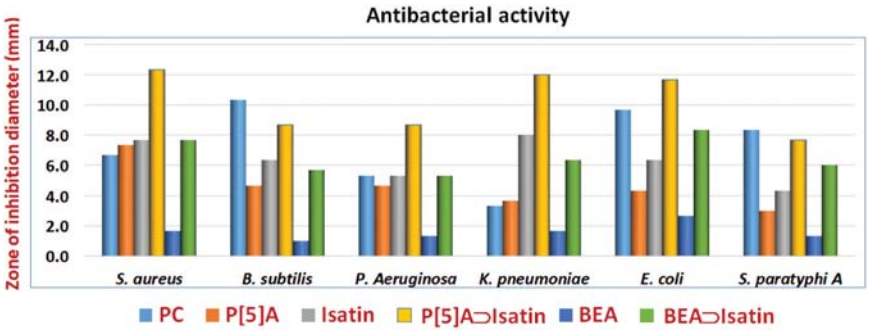

Figure 4. Antibacterial of DMSO solution of chloramphenicol, **P[5]A, Isatin, P[5]A⊃Isatin, BEA** and **BEA⊃Isatin.**

Table 1. Antibacterial activity of DMSO solutions of P[5]A, BEA, Isatin, P[5]A⊃isatin and BEA⊃isatin[#].

		Diameter of zone of inhibition (mm)					
Microorganism		Chloramphenicol	P[5]A	BEA	Isatin	P[5]A⊃Isatin	BEA⊃Isatin
Gram-positive bacteria	*S. aureus*	6.7 ± 0.6	7.3± 1.2	1.7 ± 0.6	7.7 ± 0.6	12.3 ± 0.6	7.7 ± 0.6
	B. subtilis	10.0 ± 0.6	4.7± 0.6	1.0 ± 0	6.3 ± 0.6	8.7 ± 0.6	5.7 ± 0.6
Gram-negative bacteria	*P. aeruginosa*	5.3 ± 1.0	4.7± 0.6	1.3 ± 0.6	5.3 ± 0.6	11.7 ± 0.6	5.3 ± 0.6
	K. pneumoniae	3.3 ± 0.6	3.7± 1.2	1.7 ± 0.6	8 ± 1.0	8.7 ± 0.6	6.3 ± 0.6
	E. coli	9.7 ± 0.6	4.3± 0.6	2.7 ± 0.6	6.3 ± 0.6	11.7 ± 1.2	8.3 ± 0.6
	S. paratyphi A	8.3 ± 0.6	3.0± 1.0	1.3 ± 0.6	4.3 ± 0.6	7.7 ± 1.2	6 ± 1.0

[#]Values are mean ± standard deviation of at least 3 independent experiments.

Table 2. MIC values (mg/ml) of P[5]A⊃Isatin.

Category of pathogen	Pathogenic Bacteria	MIC values (mg/ml)
Gram-negative bacteria	*E. coli*	2.5
	K. pneumoniae	5
	S. paratyphi A	10
	P. aeruginosa	10
Gram-positive bacteria	*S. aureus*	5
	B. subtilis	5

Table 3. MIC of combination of P[5]A and Isatin against selected microorganisms.

Microorganisms	MIC (mg/ml) P[5]A/Isatin	FIC of P[5]A (A)	FIC of Isatin (B)	FICI (A+B)	FICI interpretation
E. coli	1.88/0.19	0.25	0.25	0.5	Synergistic
K. pneumonia	3.75/0.38	0.5	0.25	0.75	Additive
S. paratyphi A	1.88/0.09	0.125	0.0625	0.1875	Synergistic
P. aeruginosa	3.75/0.75	1.0	0.5	1.5	Indifferent
S. aureus	1.88/0.38	0.5	0.5	1.0	Indifferent
B. subtilis	0.94/0.18	0.125	0.125	0.25	Synergistic

Table 4. *In-silico* toxicity predicted values of **Isatin, P[5]A** and **BEA** using pkCSM online server.

	Predictions		
Predicted parameters	Isatin	P[5]A	BEA
AMES toxicity	No	NO	NO
Max. tolerated dose (log mg/Kg/day)	0.139	0.378	0.26
hERG I inhibitor	No	No	No
hERG II inhibitor	No	Yes	Yes
Oral rat acute toxicity (LD50) (mol/Kg)	2.158	2.352	2.745
Oral rat acute toxicity (LOAEL) (log mg/Kg-bw/day)	1.641	0.096	3.041
Hepatotoxicity	No	No	Yes
Skin sensitisation	Yes	No	No
T.Pyriformis toxicity (log µg/L)	0.497	0.285	0.285
Minnow toxicity (log mM)	2.068	−9.563	−1.661

Moreover, zone of inhibition results suggested that **isatin** alone displayed good antibacterial activity against *P. aeruginosa* and *K. pneumoniae*. The minimum inhibitory concentration (MIC) was assessed by microdilution method using series of diluted test samples of **P[5]A, Isatin** and **P[5]A⊃Isatin** complex in sterile nutrient broth. MIC values of **P[5]A⊃Isatin** against Gram-positive and Gram-negative bacteria are listed in Table 2. MIC results of **P[5]A⊃Isatin** complex against Gram-positive and Gram-negative bacteria showed that **P[5]A⊃Isatin** complex exhibited the lowest MIC against *E. coli,* describing the potency of the isatin-drug conjugate as a potential drug candidate.

Synergistic effects of P[5]A and Isatin

To explore the synergistic antibacterial effects between **P[5]A** and **Isatin**, we have performed checkerboard assay against the microorganisms. The MICs of different combinations are summarised in Table 3.

The MICs of combinations of **P[5]A** and Isatin depicted in Table 3 are reduced compared with the MICs of **P[5]A** and Isatin alone against all the microorganisms studied. The fractional inhibitory concentration index (FICI) values suggest synergistic effect for the combination of **P[5]A** and **isatin** against *E. Coli, S. paratyphi A* and *B. subtilis*.

In-silico toxicity prediction of Isatin, P[5]A and P[5]A⊃isatin complex

In-silico toxicity studies to predict the drug-likeness of **Isatin, P[5]A** and **BEA** were performed using pkCSM online server (Table 4).

Both **P[5]A** and **BEA** proposed to have hERG II inhibition potentials. According to the predicted toxicity results, **isatin, P[5]A** and **BEA** are found to be non-carcinogenic. Hepatotoxicity predictions suggested that **Isatin** and **P[5]A** are non-toxic, and maximum tolerated doses of **P[5]A, isatin** and **BEA** suggested that they are safe.

Conclusion

The synergic combination of pillar[5]arene (**P[5]A**) and isatin enables increased efficacy against both Gram-positive and Gram-negative bacteria. The results observed in this study suggest the use of pillar[5]arene-isatin complexes as a promising drug candidate to combat various infections caused by pathogens. Efforts are underway for the synthesis of bio-compatible pillar[5]arene-based drug inclusion complexes for practical applications to combat the infections and mechanism of their antimicrobial potential and biofilm inhibition abilities.

Experimental section

Materials

All solvents and reagents were purchased from commercial sources and used without further purification. **P[5]A** [28] and **BEA** [29] were synthesised according to previously published procedures.

Physical methods

^{1}H NMR spectroscopic analyses were performed on a Avance III HD Nanobay 400 MHz NMR spectrometer operating at 400 MHz with TMS or residual undeuterated solvent as an internal standard. Chemical shifts are reported as δ in parts per million (ppm). NMR data were processed from MestReNova NMR software, and binding constants were calculated from ^{1}H NMR titration data using the WINEQNMR2 program.

HOST–guest complexation studies in solution

NMR spectra were recorded at room temperature in $CDCl_3$/acetone-d_6. Chemical shifts are reported as δ in parts per million (ppm). ^{1}H NMR titration experiments were performed to establish the formation of host–guest complexation between **P[5]A** and **Isatin**. Isatin solution was prepared by dissolving it (5.5 mM) in 0.5 mL of acetone-d_6, and the **P[5]A** solution was prepared by dissolving it (60 mM) in 0.5 mL of $CDCl_3$. ^{1}H NMR titrations were performed by the addition of 10 µL aliquots of **isatin** to **P[5]A** solution in the NMR tube. The sample was shaken carefully after each addition, and ^{1}H-NMR spectra were recorded at 25°C. NMR data were processed from MestReNova NMR software, and binding constants were calculated from ^{1}H NMR titration data using the WINEQNMR2 program [30].

UV–vis titration experiments

Host–guest complexation of isatin was probed by UV–Vis spectroscopy by adding varying concentrations of isatin with P[5]A and BEA. A series of solutions of P[5]A and Isatin were prepared in DMSO. The volume of host and guest solutions varied from 0.5:4.5 to 4.5:0.5, respectively, with the constant total concentration of P[5]A and Isatin to be 1×10^{-4} M. To the 1×10^{-4} M solution of BEA, aliquots of Isatin were added with varying equivalents from 0.2 to 5, and UV–Vis spectra were recorded.

Antibacterial experiments

Test microorganisms

Test microorganisms used in the present study were the clinical isolates collected from PSG Hospitals, Coimbatore. Microorganisms used in this study are *Staphylococcus aureus, Bacillus subtilis, Pseudomonas aeruginosa, Klebsiella pneumoniae, Escherichia coli* and *Salmonella paratyphi A.*

Agar well-diffusion method

Inoculums of the test pathogens were prepared from the culture grown overnight in nutrient broth. Agar plates were inoculated by spreading microbial inoculum over the entire agar plate surface. By using the sterile tip, a hole with a diameter of 6–8 mm was punched aseptically. 20 mM stock solutions of **P[5]A** (15 mg ml^{-1}), **BEA** (17 mg ml^{-1}), Isatin (3 mg ml^{-1}), **P[5]A⊃Isatin** (18 mg ml^{-1}), **BEA⊃Isatin** (20 mg ml^{-1}) were prepared by dissolving the compounds in DMSO. 20 **µ**l of the antimicrobial agent was introduced into the well. The plates were covered and placed in an incubator at 37°C for 24 hrs. The plates were then removed, and the zone of inhibition for each sample was measured and reported in millimetres.

MIC study

The minimum inhibitory concentration (MIC) was determined by microdilution method using a serially diluted test sample. The test sample was diluted to get a series of concentrations in a sterile nutrient broth. The microorganism suspension of 50 µl was added to the broth dilutions. These were incubated for 18 hours at 37°C. MIC of each test sample was taken as the lowest concentration that did not give any visible bacterial growth.

Evaluation of synergistic effect by checkerboard assay

The protocol reported by Bellio et al. was followed for the evaluation of checkerboard assay [31,32]. The concentrations of **P[5]A** was varied from 7.5 mg/ml to 7 µg/ml and isatin was varied from 3 mg/ml to 50 µg/ml. **P[5]A** and **isatin** alone were monitored as control. The fractional inhibitory concentration index (FICI) values were calculated by comparing the MIC of P[5]A and isatin with the MICC values of P[5]A and isatin in combination as follows:

$$FICI = FIC\ of\ P[5]A + FIC\ of\ isatin$$

where, FIC of P[5]A = (MIC_{50} of P[5]A in combination)/(MIC_{50} of P[5]A alone) and FIC of isatin = (MIC_{50} of isatin in combination)/(MIC_{50} of isatin alone). FICI ≤ 0.5 was interpreted as synergy, 0.5 < FICI ≤ 1 as additive, 1 < FICI ≤ 4 as indifferent and 4 < FICI as anatogonistic.

In-silico toxicity studies

The molecular structures of Isatin, P[5]A and BEA were drawn using the Chemdraw drawing tool and were converted into SMILES molecular file format for in-silico prediction studies using pkCSM platform[19] (pkCSM (unimelb.edu.au)) which uses graph-based signatures. AMES toxicity, hERG I, II inhibitor potentials, oral rat acute toxicity, hepatotoxicity, skin sensitisation, T.Pyriformis toxicity and Minnow toxicity were analysed using pkCSM platform.

Acknowledgments

The authors acknowledge the Council of Scientific and Industrial Research [01(3001)/19/EMR-II] for financial assistance. The authors also sincerely acknowledge the NMR facility created under DST-FIST program (SR/FST/CSI-255/2013(C)) in the Department of Chemistry, The Gandhigram Rural Institute (Deemed to be University).

Disclosure statement

No potential conflict of interest was reported by the author(s).

Funding

This work was supported by the Council of Scientific and Industrial Research [01(3001)/19/EMR-II].

References

[1] Walther R, Rautio J, Zelikin AN. Prodrugs in medicinal chemistry and enzyme prodrug therapies. Adv Drug Deliv Rev. **2017**;118:65–77.
[2] Webber MJ, Langer R. Drug delivery by supramolecular design. Chem Soc Rev. **2017**;46:6600–6620.
[3] Zhou J, Yu G, Huang F. Supramolecular chemotherapy based on host–guest molecular recognition: a novel strategy in the battle against cancer with a bright future. Chem. Soc. Rev. 2017;46:7021–7053.
[4] Geng W-C, Sessler JL, Guo D-S. Supramolecular prodrugs based on host–guest interactions. Chem Soc Rev.**2020**;49:2303–2315.
[5] Yu G, Chen X. Host-Guest Chemistry in Supramolecular Theranostics. Theranostics.**2019**;9:3041–3074.
[6] Yang K, Pei Y, Wen J, et al. Recent advances in pillar[n]arenes: synthesis and applications based on host–guest interactions. Chem Commun. **2016**;52:9316–9326.
[7] Boominathan M, Kiruthika J, Arunachalam M. Construction of anion-responsive crosslinked polypseudorotaxane based on molecular recognition of pillar[5]arene. J. Polym. Sci. Part A: Polym. Chem. 2019;57:1508–1515.
[8] Han C, Zhao D, Lü Z,et al. Synthesis of a Difunctionalized Pillar[5]arene with Hydroxyl and Amino Groups at A1/A2 Positions. Eur. J. Org. Chem. 2019;14:2508–2512.
[9] Han C, Zhao D, Li H, et al. Effective Binding of Neutral Dinitriles by Pillar[4]arene[1]quinone both in Solution and in Solid State. ChemistrySelect. 2018;3:11–14.
[10] Cragg PJ. Recent advances in pillar[n]arenes: synthesis and applications based on host–guest interactions. Isr J Chem. **2018**;58:1194–1208.
[11] Si W, Li Z-T, Hou J-L. Voltage-Driven Reversible Insertion into and Leaving from a Lipid Bilayer: Tuning Transmembrane Transport of Artificial Channels. Angew Chem Int Ed. **2014**;53:4578–4581.
[12] Barboiu M. Artificial Water Channels. Angew. Chem. Int. Ed. 2012;51:11674–11676.
[13] Si W, Chen L, Hu X, et al. Selective Artificial Transmembrane Channels for Protons by Formation of Water Wires. Angew. Chem. Int. Ed. 2011;50:12564–12568.
[14] Buffet K, Nierengarten I, Galanos N,et al.Pillar[5]arene-Based Glycoclusters: Synthesis and Multivalent Binding to Pathogenic Bacterial Lectins Chem Eur J. **2016**;22:2955–2963.
[15] Nierengarten I, Nothisen M, Sigwalt D, et al. Polycationic Pillar[5]arene Derivatives: Interaction with DNA and Biological Applications. Chem Eur J. **2013**;19:17552–17558.
[16] Shu X, Xu K, Hou D, et al. Molecular Recognition of Water-soluble Pillar[n]arenes Towards Biomolecules and Drugs. *Isr. J. Chem.* **2018**;58:1230–1240.
[17] Sathiyajith C, Shaikh RR, Han Q, et al. Biological and related applications of pillar[n]arenes. Chem Commun. **2017**;53:677–696.
[18] Joseph R. Pillar[n]arene Derivatives as Sensors for Amino Acids. ChemistrySelect. 2021;6:3519–3533.
[19] Guo S, Huang Q, Chen Y,et al. Synthesis and Bioactivity of Guanidinium-Functionalized Pillar[5]arene as a Biofilm Disruptor. Angew Chem Int Ed. **2021**;60:618–623.
[20] Yang H, Jin L, Zhao D, et al. Antibacterial and Antibiofilm Formation Activities of Pyridinium-Based Cationic Pillar[5]arene Against Pseudomonas aeruginosa Antibacterial and Antibiofilm Formation Activities of Pyridinium-Based Cationic Pillar[5]arene Against Pseudomonas aeruginosa.J. Agric. Food Chem. 2021;69:4276–4283.

[21] Gao L, Li M, Ehrmann S, et al. Positively Charged Nanoaggregates Based on Zwitterionic Pillar[5]arene that Combat Planktonic Bacteria and Disrupt Biofilms. Angew. Chem. Int. Ed. 2019;58:3645–3649.
[22] Kaizerman-Kane D, Hadar M, Joseph R, et al. Design Guidelines for Cationic Pillar[n]arenes that Prevent Biofilm Formation by Gram-Positive PathogensDesign Guidelines for Cationic Pillar[n]arenes that Prevent Biofilm Formation by Gram-Positive Pathogens. ACS Infect. Dis. 2021;7:579–585.
[23] Peng H, Xie B, Yang X, et al. Pillar[5]arene-based, dual pH and enzyme responsive supramolecular vesicles for targeted antibiotic delivery against intracellular MRSA. Chem. Commun. **2020**;56(58):8115–8118. DOI:10.1039/D0CC02522D
[24] Nierengarten I, Buffet K, Holler M, et al. A mannosylated pillar[5]arene derivative: chiral information transfer and antiadhesive properties against uropathogenic bacteria. Tetrahedron Letters. **2013**;54(19):2398–2402. DOI:10.1016/j.tetlet.2013.02.100
[25] Joseph R, Naugolny A, Feldman M, et al. Cationic Pillararenes Potently Inhibit Biofilm Formation without Affecting Bacterial Growth and Viability. J Am Chem Soc. **2016**;138:754–757.
[26] Varun S, Kakkar R. Isatin and its derivatives: a survey of recent syntheses, reactions, and applications. Med Chem Comm. **2019**;10:351–368.
[27] d'ischia M, Palumbo A, Prota G. Adrenalin oxidation revisited. New products beyond the adrenochrome stage. Tetrahedron. **1988**;44:6441–6446.
[28] Boinski T, Szumna A. A facile, moisture-insensitive method for synthesis of pillar[5]arenes—the solvent templation by halogen bonds. Tetrahedron. **2012**;68:9419–9422.
[29] Kiruthika J, Srividhya S, Arunachalam M. Anion-Responsive Pseudo[3]rotaxane from a Difunctionalized Pillar[4]arene[1]quinone and a Bis-Imidazolium Cation. *Org. Letters*. **2020**;22:7831–7836.
[30] Hynes MJ. EQNMR: a computer program for the calculation of stability constants from nuclear magnetic resonance chemical shift data. J.Chem. Soc., Dalton Trans. **1993**;311–312.
[31] Pires DEV, Blundell TL, Ascher DB. pkCSM: Predicting Small-Molecule Pharmacokinetic and Toxicity Properties Using Graph-Based Signatures. J Med Chem. **2015**;58:4066–4072.
[32] Bellio P, Fagnani L, Nazzicone L, et al. New and simplified method for drug combination studies by checkerboard assay. MethodsX. **2021**;8:101543.